

## PERSPECTIVES

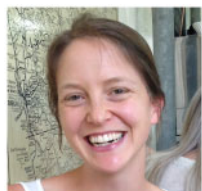
# Strongly Peraluminous Granites across the Archean–Proterozoic Transition

Claire E. Bucholz<sup>1\*</sup> and Christopher J. Spencer<sup>2</sup>

<sup>1</sup>Division of Geological and Planetary Sciences, California Institute of Technology, 1200 E California Blvd, Pasadena, CA 91125, USA; <sup>2</sup>Earth Dynamics Research Group, The Institute of Geoscience Research (TIGeR), School of Earth and Planetary Sciences, Curtin University, Perth, WA 6845, Australia

\*Corresponding author. Telephone: 626-395-1315. E-mail: cbucholz@caltech.edu

Received February 11, 2019; Accepted June 3, 2019



**Claire Bucholz** is an assistant professor in the Division of Geological and Planetary Sciences at the California Institute of Technology. She earned her BS from Yale University before pursuing a PhD in Geochemistry from the Massachusetts Institute of Technology–Woods Hole Oceanographic Institution Joint Program in 2016. Her research focuses on the formation and evolution of the continental crust with a particular emphasis on subduction-zone magmatism and strongly peraluminous granites. She approaches her work through field-based studies, numerous analytical techniques, and geochemical modeling.



**Christopher Spencer** is a senior research fellow in The Institute of Geoscience Research (TIGeR) and School of Earth and Planetary Sciences at Curtin University. He earned his BS and MS from Brigham Young University and a PhD from the University of St Andrews in 2014. Using field work, mass spectrometry, and isotope geochemistry, his research foci include isotopic characteristics of plate tectonics and the secular change of orogenesis and crustal growth through time.

## ABSTRACT

Strongly peraluminous granites (SPGs) form through the partial melting of metasedimentary rocks and therefore represent archives of the influence of assimilation of sedimentary rocks on the petrology and chemistry of igneous rocks. With the aim of understanding how variations in sedimentary rock characteristics across the Archean–Proterozoic transition might have influenced the igneous rock record, we compiled and compared whole-rock chemistry, mineral chemistry, and isotope data from Archean and Paleo- to Mesoproterozoic SPGs. This time period was chosen as the Archean–Proterozoic transition broadly coincides with the stabilization of continents, the rise of subaerial weathering, and the Great Oxidation Event (GOE), all of which left an imprint on the sedimentary rock record. Our compilation of SPGs is founded on a detailed literature review of the regional geology, geochronology, and inferred origins of the SPGs, which suggest derivation from metasedimentary source material. Although Archean and Proterozoic SPGs are similar in terms of mineralogy or major-element composition owing to their compositions as near-minimum melts in the peraluminous haplogranite system, we discuss several features of their mineral and whole-rock chemistry. First, we review a previous analysis of Archean and Proterozoic SPGs biotite and whole-rock compositions indicating that Archean SPGs, on average, are more reduced than Proterozoic SPGs. This observation suggests that Proterozoic SPGs were derived from metasedimentary sources that on average had more oxidized bulk redox states relative to their Archean counterparts, which could reflect an increase in atmospheric O<sub>2</sub> levels and more oxidized sedimentary source rocks after the GOE. Second, based on an analysis of Al<sub>2</sub>O<sub>3</sub>/TiO<sub>2</sub> whole-rock ratios

and zircon saturation temperatures, we conclude that Archean and Proterozoic SPGs formed through partial melting of metasedimentary rocks over a similar range of melting temperatures, with both 'high-' and 'low-'temperature SPGs being observed across all ages. This observation suggests that the thermo-tectonic processes resulting in the heating and melting of metasedimentary rocks (e.g. crustal thickening or underplating of mafic magmas) occurred during generation of both the Archean and Proterozoic SPGs. Third, bulk-rock CaO/Na<sub>2</sub>O, Rb/Sr, and Rb/Ba ratios indicate that Archean and Proterozoic SPGs were derived from partial melting of both clay-rich (i.e. pelites) and clay-poor (i.e. greywackes) source regions that are locality specific, but not defined by age. This observation, although based on a relatively limited dataset, indicates that the source regions of Archean and Proterozoic SPGs were similar in terms of sediment maturity (i.e. clay component). Last, existing oxygen isotope data for quartz, zircon, and whole-rocks from Proterozoic SPGs show higher values than those of Archean SPGs, suggesting that bulk sedimentary <sup>18</sup>O/<sup>16</sup>O ratios increased across the Archean–Proterozoic boundary. The existing geochemical datasets for Archean and Proterozoic SPGs, however, are limited in size and further work on these rocks is required. Future work must include detailed field studies, petrology, geochronology, and constraints on sedimentary source ages to fully interpret the chemistry of this uniquely useful suite of granites.

**Key Words:** Archean–Proterozoic transition; Great Oxidation Event; peraluminous granites; partial melting; metasedimentary rock; assimilation

## INTRODUCTION

The igneous rock record across the Archean–Proterozoic transition is characterized by dramatic changes in lithology and chemistry (Condle, 1989; Condie & O'Neill, 2010; Keller & Schoene, 2012; Keller & Schoene, 2018). The continental crust in the early Archean (>2.8 Ga) was dominated by Na-rich tonalite–trondjemite–granodiorite (TTG) suites (as well as less abundant ultramafic to mafic greenstone terranes), but underwent a transition to being characterized by a more K-rich granite–granodiorite series in the Neoproterozoic (2.5–2.8 Ga) and Proterozoic (Barker, 1979; Hill *et al.*, 1992; Smithies & Champion, 2000; Champion & Smithies, 2001; Moyen 2003; Martin *et al.*, 2009; Condie & O'Neill, 2010; Laurent *et al.*, 2014; Halla *et al.*, 2017; Joshi *et al.*, 2017). Simultaneously, komatiites decreased in abundance in the volcanic rock record, being replaced by lower-MgO basalts typical of those erupted at the present day (Grove & Parman, 2004; Arndt *et al.*, 2009; Condie & O'Neill, 2010). In terms of chemistry, trace element ratios, which are sensitive to degree of mantle melting and depth of source region or differentiation, changed dramatically in basalts across this time period, suggesting lower degrees of mantle melting and shallower depths of magma generation on average in the Proterozoic (Condle, 1989; Herzberg *et al.*, 2010; Keller & Schoene, 2012). Additionally, maximum values of oxygen isotope ratios (as expressed as  $\delta^{18}\text{O} = [({}^{18}\text{O}/{}^{16}\text{O})_{\text{sample}}/({}^{18}\text{O}/{}^{16}\text{O})_{\text{VSMOW}} - 1] \times 1000$ ), where VSMOW is the Vienna Standard Mean Ocean Water) in igneous and detrital zircon remained relatively low and uniform in the Archean ( $\delta^{18}\text{O} = \sim 7.5\text{‰}$ ), but dramatically increased in the Proterozoic (>10‰ by

$\sim 2.0$  Ga; Valley *et al.*, 2005; Dhuime *et al.*, 2012; Spencer *et al.*, 2014, 2019; Payne *et al.*, 2015).

Understanding how these lithological and geochemical changes in igneous rocks record global transformations across the Archean–Proterozoic transition has been the focus of extensive and long-standing research. This task is complicated, however, as the Archean–Proterozoic transition was one of the most dynamic times in Earth's history, with fundamental changes occurring across geophysical, tectonic, and atmospheric realms. Although still debated, a large number of researchers agree that something akin to modern-style plate tectonics developed between  $\sim 3.0$  and 2.6 Ga, resulting in collisional orogens, an increase in continental crust volume, and the stabilization of cratonic cores by the end of the Archean (McCulloch & Bennett, 1994; Taylor & McLennan, 1995; Condie, 1998; Condie & O'Neill, 2010; Campbell & Davies, 2017). In addition, the continental crust changed from being dominantly below sea level to subaerial, as evidenced by the ubiquitous occurrence of pillow basalts in Archean greenstone belts in contrast to thick sequences of clastic sediments in the early Proterozoic (Windley, 1977; Thurston, 1990; Condie, 1994; Arndt, 1999; Kump & Barley, 2007; Flament *et al.*, 2008; Campbell & Davies, 2017). Concurrently the late Archean mantle began to cool significantly (Korenaga, 2008; Condie & O'Neill, 2010; Herzberg *et al.*, 2010) and the earliest Paleoproterozoic was heralded with a decrease in the volume of the preserved continental crust, a time referred to as the Rhyacian tectono-magmatic lull (Condle *et al.*, 2009; Spencer *et al.*, 2017). Superimposed on and potentially related to these massive changes in continental growth, tectonics, and mantle

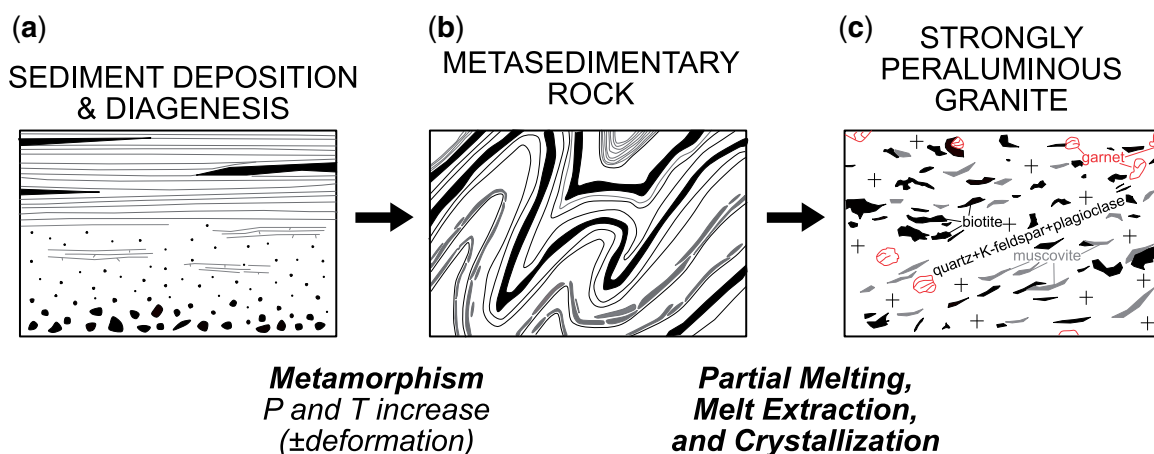


**Fig. 1.** Branch of the rock cycle showing how strongly peraluminous granites (SPGs) are formed. (a) Sediments are deposited and transformed into sedimentary rocks through diagenesis. (b) Metamorphism of sediments and formation of metasedimentary rocks is caused by an increase in pressure and temperature during burial or heating by an external magma source. This is sometimes, but not always, accompanied by deformation. (c) If metamorphism progresses to sufficiently high temperatures ( $>650^{\circ}\text{C}$ ), metasedimentary rocks may melt. Partial melts segregate and cool to form SPGs with minerals indicative of the peraluminous composition of the melt (e.g. garnet or muscovite).

dynamics, the Earth's atmosphere experienced an increase in oxygen concentrations by about five orders of magnitude at c. 2.3–2.4 Ga [i.e. the Great Oxidation Event (GOE); Holland, 1984, 2002, 2006; Canfield *et al.*, 2000; Kasting, 2001; Kump *et al.*, 2001; Bekker *et al.*, 2004; Catling & Claire, 2005; Guo *et al.*, 2009; Lyons *et al.*, 2014; Gumsley *et al.*, 2017]. The dramatic increase in atmospheric oxygen profoundly affected speciation of redox-sensitive elements at the surface of the Earth (e.g. Fe, S, Mo, U; Scott *et al.*, 2008; Partin *et al.*, 2013; Reinhard *et al.*, 2013; Planavsky *et al.*, 2014), which in turn destabilized some minerals during weathering (e.g. pyrite, uraninite, molybdenite; Rasmussen & Buick, 1999), while stabilizing new classes of  $\text{Fe}^{3+}$ -bearing clays, phosphorites/ates, and sulfates (Hazen *et al.*, 2008, 2013; Sverjensky & Lee, 2010).

All of these global transitions certainly affected the igneous rock record. Most directly, a change in plate-tectonic regime and mantle cooling would have shifted the location, depth of melting, and chemistry of magmatism. In addition, a change in sedimentary compositions owing to oxidation of the near-surface could be imprinted on the chemistry of igneous rocks through partial melting or assimilation of sediments. However, pinpointing the relationship between these global transformations during the Archean–Proterozoic transition and the major changes observed in the chemistry and lithologies of igneous rocks is difficult, as igneous rocks often record complicated, multi-faceted origins that are incompletely understood. For example, the chemistry of a felsic igneous rock may reflect its initial source, assimilation of crustal material, and differentiation processes, as well as late-stage alteration and metamorphism. Therefore, it can be hard to disentangle the source of petrological or chemical features when multiple potential causes are at play. Here we focus on a specific igneous rock type that can shed light on one

piece of this complicated puzzle: strongly peraluminous granites (SPGs). SPGs are formed when sedimentary rocks (Fig. 1a) are metamorphosed (Fig. 1b) and heated to sufficiently high temperatures to partially melt. These melts may then be extracted from their source sediments and cooled, forming SPG plutons (Fig. 1c). Although SPGs are several steps removed from sedimentary rocks (e.g. metamorphism, partial melting, and crystallization), they have the potential to record variations in sedimentary compositions and thus the input of supracrustal material into magmas. Therefore, if the chemical influence of sedimentary incorporation into magmas varied across the Archean–Proterozoic transition, SPGs should record this signature, but not be influenced by other global transitions (e.g. secular cooling of the mantle). SPGs can provide a valuable tool in this puzzle to understand the relationship between changing surface conditions (such as the rise of atmospheric oxygen or onset of subaerial weathering) and the chemistry of igneous rocks across the Archean–Proterozoic transition.

The goal of this study is to catalogue and describe known localities of SPGs in the Archean and Paleo- to Mesoproterozoic, synthesize existing petrology, mineralogy, chemistry, and isotopic data from these localities, discuss these data in the context of what is known about changing surface conditions, and highlight potential avenues for future research. Although SPGs of this age range have been recognized and described (see following detailed locality descriptions), there has not been a synthesis of a global dataset of Archean and Proterozoic SPGs. The most extensive prior treatment of this subject that we are aware of comprises studies focused on the broader topic of Archean granites (Sylvester, 1994; Moyen, 2003). By compiling and analyzing existing geological, petrological, and chemical

data for these important rocks, we hope to provide the groundwork for future studies.

## DEFINITION

Before proceeding with a discussion of SPGs across the Archean–Proterozoic transition, it is necessary to define these granites. Peraluminous granites are those that include corundum in their CIPW norms (Shand, 1927). This translates into excess  $\text{Al}_2\text{O}_3$  in their bulk composition that cannot be accommodated in feldspar by coordinating with Ca, Na, and K. Here we define strongly peraluminous granites as granites with an aluminum saturation index (ASI) or molar  $\text{Al}/(\text{Ca} - 1.78\text{P} + \text{Na} + \text{K}) > 1.1$  (note reduction of Ca by the amount necessary to combine with  $\text{P}_2\text{O}_5$  to make apatite). In terms of mineralogy, the peraluminous nature is manifest by the presence of an aluminous mineral (other than biotite) such as muscovite, garnet, tourmaline, cordierite, kyanite, sillimanite, or andalusite (e.g. Fig. 1c). For all samples considered in this study, there is at least one of these aluminous phases present (generally, but not always in addition to biotite) in the rock.

Strongly peraluminous granites are often considered synonymous with ‘S-type’ granites, or those derived through the partial melting of metasedimentary rocks. In their original definition of ‘S-type’ granites, Chappell & White (1974) used a variety of criteria to distinguish granitoids of the Lachlan fold belt (Australia) in addition to ASI. These included other geochemical indices, such as initial whole-rock  $^{87}\text{Sr}/^{86}\text{Sr} > 0.708$  and  $\delta^{18}\text{O} \geq 10\text{‰}$ , strongly suggesting derivation from weathered sedimentary material. However, since the initial studies of the Lachlan fold belt, other studies have demonstrated that many S-type granites from the Lachlan fold belt have a significant mantle contribution and thus are not pure melts of sediments (Gray, 1984; Collins, 1996; Healy *et al.*, 2004; Kemp *et al.*, 2006, 2007). For this reason, we do not label the granites discussed within this study as ‘S-type’, as most have not been rigorously scrutinized using modern geochemical techniques to confirm a purely sedimentary source (e.g. Hopkinson *et al.*, 2017; Spencer *et al.*, 2017). However, with careful review of the existing data we include only localities with sufficient geological and chemical information to suggest that they were derived predominantly, if not wholly, from a metasedimentary source region. The data we consider include geological setting, field relationships, mineralogy, and oxygen isotope data (when available).

## OCCURRENCES AND GEOLOGICAL SETTINGS

SPGs of all ages typically form in collisional tectonic settings where quartzo-feldspathic sedimentary material is buried and heated to sufficient temperatures to partially melt (e.g. Sylvester, 1998; Nabelek, 2019) or syn- to post-collisional mafic magmas heat basinal (e.g. fore-arc or back-arc) sedimentary rocks (e.g. Lalonde,

1989). Archean and Proterozoic SPGs are no exception, generally being located within or associated with meta-sedimentary rocks of old orogenic belts. Here we briefly describe the different localities considered in this review by craton or orogenic belt, emphasizing the inferred tectonic setting, source material, and the petrogenesis of the granites. Table 1 provides further details and references on individual localities and Fig. 2 illustrates their global distribution.

We note here that we undertook an extensive review of all localities where SPGs were present, but include only those where there is clear evidence for derivation from a sedimentary source rock and significant volumes of *sensu stricto* granitic melt (i.e. not migmatites nor pegmatites). For example, localities that are not included in our compilation or our description here, but are worth noting, are ~2.7 Ga migmatites associated with metasedimentary rocks from the Karelia craton (Mikkola *et al.*, 2012), the ~2.9 Ga Mata Surrao biotite ± garnet-bearing monzogranite of the Amazonia craton (Duarte *et al.*, 1991; Althoff *et al.*, 2000), ~2.8 Ga peraluminous pegmatites from the Pilbara craton (Blockley, 1980; Sweetapple & Collins, 2002), numerous Neoarchean pegmatite localities associated with anatexis of clastic metasedimentary rocks in the Canadian Shield (Černý, 1990, 1991a; Breaks *et al.*, 2003), ~2.6 Ga migmatites of the Opinaca subprovince of the Superior craton (Morfin *et al.*, 2013), ~2.7 Ga migmatites of the Mkhondo Valley Metamorphic Suite (Swaziland; Taylor & Stevens, 2010), and of the Southern Marginal Zone of the Limpopo Belt (South Africa; Nicoli *et al.*, 2014, 2017), and 1.6–1.7 Ga peraluminous granites of the Durlacher supersuite of the Mangaroon Orogen (Australia; Sheppard *et al.*, 2005). In addition, we do not exclude the possibility that other localities exist that either we have missed in our literature review or have not been described or examined sufficiently to determine whether they are SPGs. Lastly, we have attempted to be thorough in our citation of existing work on the SPGs; however, there were instances where references were available only in non-English languages and we did not feel comfortable citing these references without being able to read them first-hand. These references are listed within other sources cited here and we encourage the reader to explore them.

## Archean localities

### Superior Craton, Canada and USA

Traditionally the Superior Craton has been subdivided into sub-provinces based on lithological characteristics (Card, 1990), with more recent efforts being focused on distinction of tectonic terranes that were juxtaposed during the Neoarchean assembly of the craton (Percival *et al.*, 2006; Stott *et al.*, 2010). The terranes can be broadly divided into two kinds: those dominated by (1) plutonic or orthogneissic rocks and greenstones and (2) metasedimentary rocks. The former (e.g. Uchi, Winnipeg River, Wabigoon, Wawa–Abitibi subprovinces) are considered



**Table 1:** Archean and Proterozoic SPG locality details

No.	Locality	Detailed location	Age (Ma)*	Lithologies*	Petrogenesis	Notes	Selected References
<b>Archean Superior Craton</b>							
1	Preissac-Lacorne-Lamotte-Moly Hill granites + Pontiac garnet-muscovite granites (GMG)	Abitibi (Lacorne block) and Pontiac subprovinces (Quebec, Canada)	'GMG' granites from Lacorne block and Pontiac subprovince: $2644 \pm 13$ (av. U-Pb zrc); Lamotte: $2647 \pm 2$ , U-Pb mnz-ttn; Preissac: $2681 \pm 2660$ , U-Pb mnz-ttn	ms+bt monzogranite; ms±grt monzogranite	syncollisional, partial melting of mature Pontiac basin meta-sediments (max. depositional age ~2690 Ma) during continent-arc collision	associated with migmatites in metasedimentary rocks and Mo, Li, and Be mineralization in pegmatites	Dawson, 1966; Bourne & Danis, 1987; Feng & Kerrich, 1991, 1992a, 1992b; Feng <i>et al.</i> , 1993; Mulja <i>et al.</i> , 1995a, 1995b; Ducharme <i>et al.</i> , 1997; Breaks <i>et al.</i> , 2003
2	Allison Lake batholith	Boundary of English River and Uchi subprovinces (Ontario, Canada)	no precise age (Neoproterozoic)	bt+ms granite, grt+ms granite, bt+ms potassic pegmatite. Locally tur- and F-ap-bearing.	partial melting of English River meta-sedimentary rocks	~16 km × 40 km intrusion	Breaks <i>et al.</i> , 2003
3	Wenasaga Lake batholith	Boundary of English River and Uchi subprovinces (Ontario, Canada)	no precise age (Neoproterozoic)	bt+ms (leuco-)granite to pegmatite with rare crd+qtz symplectites and scarce garnet	partial melting of English River meta-sedimentary rocks	~7 km × 26 km intrusion, local enclaves of metasedimentary migmatite	Breaks <i>et al.</i> , 2003
4	Root Bay pluton	Boundary of English River and Uchi subprovinces (Ontario, Canada)	no precise age (Neoproterozoic)	ms+tur granite	partial melting of English River meta-sedimentary rocks	associated with Li mineralization in pegmatites	Breaks <i>et al.</i> , 2003
5	Sharpe Lake batholith	Boundary of English River and Uchi subprovinces (Ontario, Canada)	no precise age (Neoproterozoic)	bt+ms±grt granite, accessory tur and F-ap	partial melting of English River meta-sedimentary rocks	abundant pegmatitic segregations and metasedimentary restitic material	This study
6	Twinn Lake stock and Caron Lake pluton	Boundary of English River and Uchi subprovinces (Ontario, Canada)	no precise age (Neoproterozoic)	bt+ms leucogranite with local grt and tur	partial melting of English River meta-sedimentary rocks	65–145 km <sup>2</sup> plutons	Kay & Stott, 1985; Stott, 1996; Breaks <i>et al.</i> , 2003
7	Ghost Lake batholith (and Zealand stock)	Boundary of Winnipeg River and Wabigoon subprovinces (Ontario, Canada)	c. 2885, U-Pb mnz	bt+crd granite to evolved ms+grt+tur leucogranite	syncollisional, melting of basinal wackes and mudstones of the Sioux Lookout terrane	metasedimentary xenoliths abundant in parts of batholith. Associated with Li and Ta mineralization	Breaks & Moore, 1992; Larbi <i>et al.</i> , 1999; Breaks <i>et al.</i> , 2003, 2005; Bucholz <i>et al.</i> , 2018
8	Medicine Lake pluton	Boundary of Winnipeg River and Wabigoon subprovinces (Ontario, Canada)	no precise age (Neoproterozoic)	ms+bt granite to leucogranite, ms+grt leucogranite. Accessory brl and tur	partial melting of metasediments	0.5 km × 1.5 km	Breaks <i>et al.</i> , 2003

(continued)

Table 1: Continued

No.	Locality	Detailed location	Age (Ma)*	Lithologies*	Petrogenesis	Notes	Selected References
9	Separation Rapids pluton + Treeline Lake complex	English River subprovince (Ontario, Canada)	Sep. Rap.: 2646 ± 2, U-Pb mnz	bt ± grt ± cord granite (Treeline Lake complex), grt + bt and ms + bt granite to pegmatite	partial melting of clastic metasedimentary rocks of English River subprovince, heat source from intrusion of older tonalite–granodiorite plutons	metasedimentary enclave-rich zones	Pan & Breaks, 1997; Pan <i>et al.</i> , 1997; Larbi <i>et al.</i> , 1999
10	Cat Lake–Winnipeg River pegmatite field (associated leucogranites)	Bird River greenstone belt (boundary of Winnipeg River and English River subprovince) (Manitoba, Canada)	2549 (Rb–Sr isochron; see Černý, 1991)	bt + ms ± grt to ms + grt leucogranite	partial melts of greenstone metasedimentary rocks (e.g. metatubidites). Some leucogranites may have some tonalitic component in source.	associated with pegmatites with Li–Cs–Ta mineralization	Černý <i>et al.</i> , 1981, 2005; Longstaffe <i>et al.</i> , 1981; Goad & Černý, 1981; Černý, 1989, 1991a
11	Georgia Lake granites (e.g. Glacier Lake batholith, Barbara Lake stock)	Quetico subprovince, (Ontario, Canada)	no precise age (Neoproterozoic)	bt + ms granite. Occasional crd + qtz symplectites	partial melting of clastic metasedimentary rocks of Quetico subprovince	metasedimentary enclaves common	Breaks <i>et al.</i> , 2003
12	Armstrong Highway area	Quetico subprovince, (Ontario, Canada)	no precise age (Neoproterozoic)	bt + ms granite, grt + bt ± crd granite, ms + bt ± grt pegmatite, local tur	partial melting of clastic metasedimentary rocks of Quetico subprovince	metasedimentary enclaves common	Breaks <i>et al.</i> , 2003
13	Sturgeon Lake and Vermillion granites	Quetico subprovince, (Ontario, Canada & Minnesota, USA)	2671 ± 2, U–Pb mnz	bt + ms leucogranite, local grt, tur, crd, and als	partial melting of greywackes of Quetico subprovince	Abundant metasedimentary enclaves. Associated migmatites	Southwick & Sims, 1979; Percival <i>et al.</i> , 1985; Day & Weiblen, 1986; Sawyer & Barnes, 1988; Percival & Williams, 1989; Southwick, 1991
14	Shannon Lake granite	Wawa subprovince, (Minnesota, USA)	2674 ± 5, U–Pb zrc	bt + ms granite, local tur and grt	partial melting of metasedimentary rock	Metasedimentary xenoliths locally abundant. Associated with pegmatites	Boerboom & Zartman, 1993
<i>Wyoming Craton</i>							
15	Mt Owen batholith	Beartooth–Bighorn magmatic zone (Wyoming, USA)	2547 ± 3, U–Pb zrc	pegmatitic to fine-grained bt + ms leucogranite with local grt	partial melting of pelitic or intermediate to felsic crustal source	post-deformational	Reed & Zartman, 1973; Zartman & Reed, 1998; Frost <i>et al.</i> , 2006, 2018
16	South Pass granites (South Pass and Sweetwater plutons)	Beartooth–Bighorn magmatic zone (Wyoming, USA)	2504 ± 40 to 2575 ± 50, Pb–Pb zrc (ages reported for 'Bears Ear pluton' of	bt + ms granite with local grt	partial melting or significant incorporation of host rock, the Miners Delight formation	—	Bayley <i>et al.</i> , 1973; Stuckless <i>et al.</i> , 1985; Stuckless, 1989; Hausel

(continued)

Table 1: Continued

No.	Locality	Detailed location	Age (Ma)*	Lithologies*	Petrogenesis	Notes	Selected References
17	Tin Cup Spring granite	Beartooth-Bighorn magmatic zone (Wyoming, USA)	<a href="#">Stuckless et al., 1985</a> ~2630 (minimum age based on cross-cutting relationships)	bt+ms±grt±tur granite	(dominantly meta-greywacke) of the South Pass supra-crustal belt petrogenesis not clearly established. Unpublished Sr–Nd isotopic work strongly suggests crustal source	occurs as dikes up to several meters in apparent thickness, as well as massive bodies up to tens of meters	<a href="#">1991; Frost et al., 1998</a>  <a href="#">Ludwig &amp; Stuckless, 1978; Stuckless &amp; Miesch, 1981; Meredith 2005; Bagdonas, 2014; Bagdonas et al., 2016</a>
18	Bear Mountain granite	Black Hills terrane (South Dakota, USA)	2592±10, U–Pb zrc	ms±bt±grt granite	partial melting of metasedimentary rocks	associated with pegmatite sills	<a href="#">Gosselin et al., 1988, 1990; McCombs et al., 2004</a>
<i>Slave Craton</i> 19	Yellowknife granite–pegmatite field (e.g. Prosperous Lake, Sparrow Lake, and Prestige plutons)	Northwest Territories, Canada	Sparrow Lake: 2596 ± 2 (U–Pb mnz); Prestige: 2608±4 (U–Pb ap)	bt+ms granite, with local grt and rare tur. Local pegmatites with tur, brl, and spd	partial melting of metasedimentary rocks of Burwash formation	consists of numerous plutons from 1 to 380 km <sup>2</sup> . xenoliths of schist common	<a href="#">Green et al., 1968; Kretz, 1968, 1982, 1985; Green &amp; Baadsgaard, 1971; Drury, 1979; Meintzer et al., 1984; Meintzer, 1987; Davis &amp; Bleeker, 1999; Palmer et al., 2016; Palmer, 2018</a>
20	Contwoyto plutonic suite	Northwest Territories, Canada	2581–2585 (U–Pb mnz)	ms±bt tonalite to monzogranite, locally tur- and sil-bearing.	partial melting of turbiditic metagreywackes, potentially of the Yellowknife Supergroup	post-deformational. metasedimentary xenoliths common	<a href="#">Davis, 1992; Davis &amp; Hegner, 1992; King et al., 1992; van Breemen et al., 1992a; Davis et al., 1994</a>
<i>Yilgarn Craton</i> 21	'post-tectonic, low-Ti' peraluminous granites	Western gneiss terrane (Western Australia, Australia)	2630–2640 (U–Pb zrc)	grt+ms+tur granite	post-tectonic partial melting of sedimentary rocks owing to lithospheric delamination	spatially associated with metasedimentary rocks	<a href="#">Qui, 1997; Qui &amp; Groves, 1999</a>
<i>Kaapvaal Craton</i> 22	'low-Ca' granites (Sinceni, Mooihoek, Mhlosheni, Godlwayo,	Barberton greenstone belt, (South Africa and Swaziland)	Sinceni: 3074±4 (Pb–Pb zrc); Mooihoek: 2824±6; Mhlosheni: 2822±5; Godlwayo: 2863±8; Kwetta:	bt+ms granite. Sinceni pluton: bt+ms+tur granite	partial melting of metasedimentary rocks in crust at depths > 15 km	intrude the Pongola Supergroup. Sinceni pluton associated	<a href="#">Blamart et al., 1993; Maphalala &amp; Kröner, 1993; Trumbull, 1993; Meyer et al.,</a>

(continued)

Table 1: Continued

No.	Locality	Detailed location	Age (Ma)*	Lithologies*	Petrogenesis	Notes	Selected References
	Spekboom, and Kwetta plutons)		2722±6; Spekboom: 2807±8 (all Rb–Sr whole-rock)			pegmatites with Sn mineralization. Spekboom and Godlwayo plutons contain xenoliths of quartzite and pelitic hornfels on margins	1994; Robb <i>et al.</i> , 2006
23	Lekkersmaak suite granites (including Willie granite and Discovery pluton)	Murchison greenstone belt, (South Africa)	Willie Granite: 2820±38 (Pb–Pb upper intercept zrc)	bt±ms±grt±tur leucogranite	partial melting of Murchison belt metapelites (similar to La France domain schists)	ms-bearing pegmatites abundant in area	Poujol, 2001; 2003; Zeh <i>et al.</i> , 2009; Jaguin <i>et al.</i> , 2010, 2012
<i>Grunehogna Craton</i>							
24	Annandagstoppane granite	East Antarctica	3067±8 (U–Pb zrc)	bt+ms granite, cross-cut by grt-bearing pegmatite dikes	deep burial of clastic sediments (deposited after ~3175 Ma) followed by melting during cratonization process	exposed only in 3–4 small nunataks (outcrop area <0.1 km <sup>2</sup> ); presence of inherited zircons with ages up to 3433±7 Ma	Barton <i>et al.</i> , 1987; Marschall <i>et al.</i> , 2010
<i>Proterozoic Wopmay Orogen</i>							
25	Hepburn intrusive suite	Northwest Territories, Canada	1885 (U–Pb zrc)	bt+ms±grt±sill monzogranite and syenogranite	mantle-derived basalt generated in a back-arc setting that subsequently assimilated and/or partially melted significant amounts of the sedimentary basin host rocks	abundant metamorphic enclaves and inherited zircons; mafic plutons (e.g. gabbro, norite, and diorite) present in small volumes, suggesting contribution of heat from a mantle source	Lalonde, 1986; Lalonde, 1989; Lalonde & Bernard, 1993
<i>Talston magmatic zone</i>							
26	Arch Lake, Slave, and Konth intrusive suites	Northwest Territories, Canada	Arch Lake granite: 1938±3 (U–Pb zrc), 1935±3 (U–Pb mnz); Slave granite: 1955±2 (U–Pb mnz); Konth granite: 1940, (U–Pb mnz)	Slave and Konth: bt±grt±cord±sp granite, locally opx	burial and melting of metasedimentary rocks during continental collision of the Talston–Thelon Orogeny	pelitic enclaves common in Slave granite	Bostock <i>et al.</i> , 1987, 1991; Bostock & Loveridge, 1988; Thériault, 1992; van Breemen <i>et al.</i> , 1992b; (continued)



Table 1: Continued

No.	Locality	Detailed location	Age (Ma)*	Lithologies*	Petrogenesis	Notes	Selected References
<i>Trans-Hudson Orogen</i>							
27	Cree Lake granites	Wollaston domain (Saskatchewan, Canada)	associated pegmatites: 1803±3, 1819±6 (U–Pb zrc); Sue Lake pegmatite: 1810±3, (U–Pb mnz)	bt±ms±grt±sill±tur leucogranite; associated pegmatite sills and dikes	partial melting of Wollaston Group metasedimentary rocks during crustal thickening and increased lower crustal heat flow during Trans-Hudson Orogeny	form syn- to late-orogenic plutons, sheets, and dikes intruding the Paleoproterozoic Wollaston Group metasedimentary rocks	McNicoll <i>et al.</i> , 1993; Chacko <i>et al.</i> , 1994; Chacko & Creaser, 1995; Grover <i>et al.</i> , 1997; De <i>et al.</i> , 2000
28	Harney Peak granite (+ satellite intrusions; e.g. Calamity Peak pluton)	South Dakota, USA	1715±3 (U–Pb mnz)	bt±ms±grt granite; ms±tur±grt granite; associated pegmatite sills	partial melting of Archean and/or Paleoproterozoic metasedimentary rocks through crustal thickening by sediment underthrusting during culmination of Trans-Hudson Orogeny	bt and tur occurrence in granites are mutually exclusive	Annesley <i>et al.</i> , 1997, 2005; McKechnie <i>et al.</i> , 2012a, 2012b, 2013
<i>Mesoproterozoic SW USA</i>							
29	Silver Plume and St Vrain batholiths	Colorado, USA	1420–1450 (Rb–Sr whole-rock and min isochrons)	bt±ms±sill granite	anorogenic(?) crustal melting, peraluminous quartzofeldspathic source	—	Redden <i>et al.</i> , 1982, 1990; Duke <i>et al.</i> , 1992; Nabelek <i>et al.</i> , 1992a, 1992b, 1999, 2001
30	Ak-Chin, Maricopa, Oracle, Sierra Estrella, Dells, and Lawler Peak granites	Arizona, USA	Lawler Peak granite: 1411±3 (U–Pb zrc); Dells granite: 1400±15 (U–Pb zrc); Ruin and Oracle granites: 1440±20 (U–Pb zrc)	bt±ms±grt±tur granite	anorogenic crustal melting, dominantly Proterozoic metasedimentary source	—	Peterman <i>et al.</i> , 1968; DePaolo, 1981; Anderson & Thomas, 1985; Anderson & Cullers, 1999
<i>Svecofennian Orogen</i>							
31	Turku area (Varsinais-Suomi, Finland)	Turku area (Varsinais-Suomi, Finland)	1814±3 (U–Pb zrc)	bt+grt granite	partial melting of Proterozoic pelitic to	associated with bt+grt+crd	Silver <i>et al.</i> , 1981; Anderson & Bender, 1989; Anderson & Morrison, 2005
							Ehlers <i>et al.</i> , 1993; Väisänen <i>et al.</i> , (continued)

Table 1: Continued

No.	Locality	Detailed location	Age (Ma)*	Lithologies*	Petrogenesis	Notes	Selected References
Late Svecofennian granite-migmatite zone							
<i>North China Craton</i>							
32	Liangcheng complex	Fengzhen belt in Khondalite belt (North China)	1930–1920 (U–Pb zrc)	grt±bt±crd granite	partial melting of Fengzhen belt UHT metapelites (khondalites)	sedimentary protoliths to khondalites deposited at 2000–1960 Ma	2000; Johannes <i>et al.</i> , 2003
33	Helanshan complex	Helanshan complex in Khondalite belt (North China)	1902±22 (U–Pb zrc)	Bt-ms and grt±bt granite	partial melting of Fengzhen belt UHT metapelites (khondalites)	sedimentary protoliths to khondalites deposited at 2000–1960 Ma	Guo <i>et al.</i> , 2001; Zhong <i>et al.</i> , 2007; Peng <i>et al.</i> , 2012; Wang <i>et al.</i> , 2018
34	Peraluminous granites associated with Jungsan and Machollyong sediments	Nangrim massif/Imjingang belt (North Korea)	1908±12; 1903±49 (U–Pb zrc)	grt±sil granite	partial melting of Paleoproterozoic Jungsan and Machollyong Group metasedimentary rocks	intrude into and are in gradational contact with Jungsan and Machollyong sediments	Dan <i>et al.</i> , 2014; Zhang <i>et al.</i> , 2017a
35	Nonggeori and Naedeokri granites and grt-bearing leucogranites	Yeongnam massif (South Korea)	1926±41 (Sm–Nd whole-rock-grt isochron)	bt+ms±tur±grt±crd sil granite, associated pegmatites	remelting of gneissic basement rocks of the Sino-Korean craton (although source rock not definitively known)	occur as dikes, sills, and stocks, as well as larger plutons (5–20 km <sup>2</sup> )	Zhao <i>et al.</i> , 2006
<i>Guyana Shield</i>							
36	Serra Dourada granite	Uatumã-Anauá domain (Amazonas, Brazil)	1969±4 and 1962±2 (U–Pb zrc)	bt+ms+crd granite	partial melting of metagreywackes	maximum depositional age of source rocks is earliest	Kim & Cho, 2003; Lee <i>et al.</i> , 2005; Kim <i>et al.</i> , 2012
37	Curuxuim, Taiano, and Amajari granites	Central Guyana domain (Amazonas, Brazil)	Taiano granite: 1969±3.5 (U–Pb zrc)	bt+ms+grt granite	partial melting of metagreywackes	Paleoproterozoic maximum depositional age of source rocks is earliest	Almeida <i>et al.</i> , 2008; CPRM, 2003; Almeida <i>et al.</i> , 2007
<i>São Francisco Craton</i>							
38	Gemeleira Massif, Riacho das Pedras,		Carnaíba: 1883±87; Riacho de Pedras:	ms±bt±grt granite associated with	syntectonic to post-tectonic partial	mica+grt-rich	Almeida <i>et al.</i> , 2007

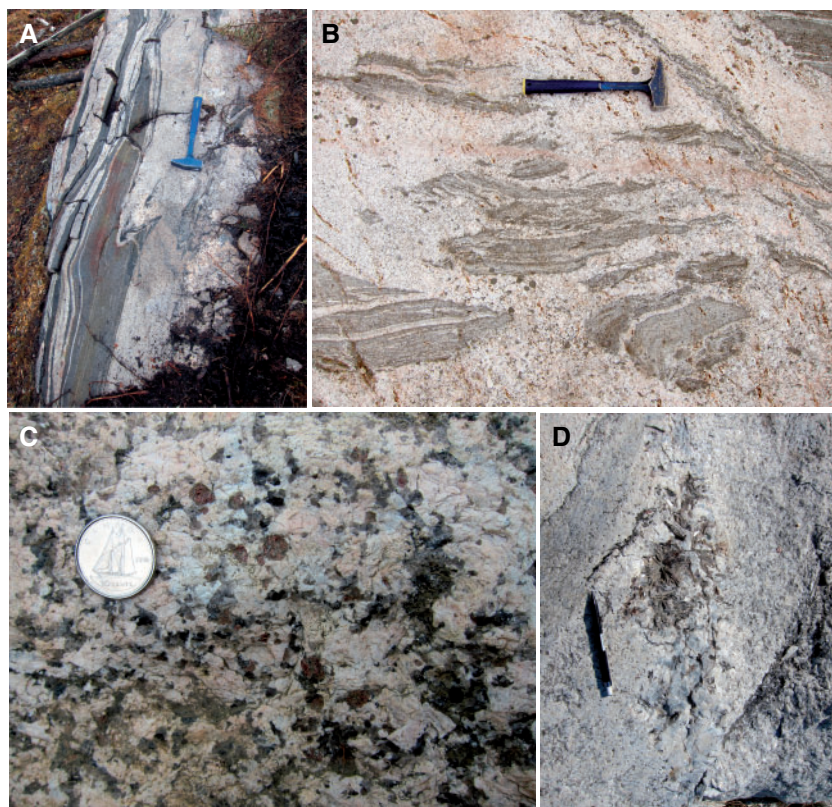
(continued)

Table 1: Continued

No.	Locality	Detailed location	Age (Ma)*	Lithologies*	Petrogenesis	Notes	Selected References
39	Caetano, Lagoa Grande, Aliança, Lagoinha plutons; Campo Formoso Massif and Carnaíba plutons	Jacobina–Contendas Mirante belt, (Bahia, Brazil)	1929 ± 16; Gameleira Massif: 1947 ± 54; Campo Formoso: 1969 ± 29; Lagoinha & Lagoa Grande: 1974 ± 36 (all Rb/Sr whole-rock)	tur+grt+brl-bearing pegmatites	melting of metasedimentary rocks during crustal thickening associated with continental collision	metasedimentary/restititic xenoliths common in Gameleira Massif	1990; <a href="#">Marinho et al., 1993</a>
	Cape Coast granites	Baoulé Mossi domain (Ghana and Côte d'Ivoire)	2125 ± 18 and 2093 ± 2 Ma (U–Pb zrc)	bt+ms and ms-granite	not definitive, possibly assimilation or partial-melting of host metasedimentary lithologies (from Birman Supergroup) during intrusion of granites into crust	meter-scale metasedimentary xenoliths in granites	<a href="#">Leube et al., 1990</a> ; <a href="#">Pettersson et al., 2016</a>

bt, biotite; ms, muscovite; grt, garnet; crd, cordierite; tur, tourmaline; sil, sillimanite; F-ap, fluorapatite; brl, beryl; spd, spodumene; zrc, zircon; mnz, monazite; ttn, titanite.





**Fig. 3.** Field photographs of Archean SPGs from Ontario, Canada. (a) and (b) show inclusion-rich zones of (a) the Ghost Lake batholith (location of photograph: 49°48'53.7"N, 092°57'4.7"W) and (b) migmatite zone of the English River subprovince (location of photograph: 50°5'56.9"N, 093°16'7.7"W). (c) Biotite + garnet granite of Treelined Lake complex (location of photograph: 50°16'56.1"N, 094°29'40.2"W). (d) Pegmatitic pod with muscovite rosettes hosted within biotite + muscovite granite of the Ghost Lake batholith (location of photograph: 49°48'53.7"N, 092°57'4.7"W). Hammer is 36 cm long. Mechanical pencil is 13.5 cm long. Diameter of coin is 18 mm.

micro-continental fragments or arc-related plutonic–volcanic rocks, which evolved independently between 3.6 and 2.7 Ga. The latter (e.g. the English River, Quetico, and Pontiac subprovinces) are dominated by variably metamorphosed greywackes and volcanogenic turbidites, but also contain pelagic and chemical sediments such as carbonates, chert, and mudstones, and fragments of greenstone lithologies (Percival & Williams, 1989; Breaks & Moore, 1992; Davis, 2002). The depositional settings of these basins have been interpreted as inter-arc basins filled by synorogenic sediments from erosion of adjacent, converging terranes (Langford & Morin, 1976; Percival & Williams, 1989).

Five distinct accretionary events, progressive from north to south, characterize the amalgamation of the Superior Craton between 2.72 and 2.68 Ga, during which time the intervening sedimentary basins were trapped in the collisional zones (Percival & Easton, 2007). The basin sediments underwent high-temperature metamorphism, sometimes reaching granulite-facies conditions, resulting in widespread partial melting and migmatization (e.g. Southwick, 1991; Southwick & Sims, 1979; Pan *et al.*, 1997; Fig. 3a and b). Many of these sedimentary provinces (and some of the plutonic provinces) contain a suite of c. 2.6–2.8 Ga SPGs

that have been interpreted as resulting from the burial and melting of the sediments during orogenic collision (Fig. 3c and d). The sub-provinces of the Superior Craton that preserve these SPGs include the Pontiac sub-province (e.g. Feng & Kerrich, 1992a, 1992b), the English River sub-province (Breaks *et al.*, 2003), the boundary of the Winnipeg River and Wabigoon sub-provinces (Breaks & Moore, 1992), the Quetico sub-province (e.g. Percival & Williams, 1989; Southwick, 1991), and the Wawa subprovince (Boerboom & Zartman, 1993) (see Table 1 for details). For a detailed discussion and review of occurrences of SPGs in Ontario, we refer the reader to the comprehensive report of Breaks *et al.* (2003).

### Wyoming Province, USA

The Archean Wyoming Province can broadly be divided into three sub-provinces: (1) the Montana metasedimentary province; (2) the Beartooth–Bighorn magmatic zone (BBMZ); (3) the southern accreted terranes (SAT) (Chamberlain *et al.*, 2003; Mueller & Frost 2006). The Montana metasedimentary sub-province is located in the NW part of province and comprises Neoproterozoic quartzites, pelites, and carbonates together with Paleoproterozoic quartzofeldspathic gneiss (Mogk *et al.*,



1988, 1992; Mueller *et al.*, 1993; Mueller & Frost, 2006). The BBMZ is primarily characterized by ~2.80–2.55 Ga tonalities and granodiorites (Mueller *et al.*, 1996, 1998; Frost & Fanning, 2006; Bagdonas *et al.*, 2016). The Wyoming Province grew in the Neoproterozoic through accretion of southern terranes (including both recently formed magmatic terranes as well as those composed of older continental crust) between 2.68 and 2.63 Ga to form the SAT (Chamberlain *et al.*, 2003; Mueller & Frost, 2006; Souders & Frost, 2006; Bagdonas *et al.*, 2016). A widespread, but minor subset of the Neoproterozoic granites in the BBMZ and SAT are SPGs. These include the Mt Owen batholith (~2.55 Ga) in the Teton Range (Frost *et al.*, 2006, 2018), the South Pass granites (~2.55 Ga) in the southern Wind River Range (Frost *et al.*, 1998), and the Tin Cup Spring and Long Creek Mountain granites (~2.65 Ga) of the western Granite Mountains (Stuckless & Miesch, 1981; Wall, 2004). The Bear Mountain granite of the Black Hills, South Dakota (~2.6 Ga) is thought to be part of an extension of the Wyoming Province basement, but definitive correlation between the identified sub-provinces in Wyoming is not certain (Gosselin *et al.*, 1988, 1990; McCombs *et al.*, 2004). The strongly peraluminous compositions and Sr and Nd isotope whole-rock data for the Wyoming Province SPGs suggest that they formed through crustal melting of psammitic or pelitic metasedimentary rocks (Gosselin *et al.*, 1990; Frost *et al.*, 2006).

#### *Slave Craton, Canada*

The rocks of the Slave Craton can broadly be divided into three temporally and lithologically distinct groups: (1) basement gneisses (4.1–2.8 Ga); (2) the Yellowknife Supergroup (YKS, 2.8–2.6 Ga); (3) syn- to post-orogenic granitoid rocks (<2.6 Ga). The YYS is a heterogeneous package of metasedimentary rocks and metavolcanic rocks. The upper member of the YYS includes turbidites deposited in the Burwash Basin c. 2.67–2.65 Ga, which has been interpreted as a back-arc basin whose closure marked the onset of final amalgamation and assembly of the Slave Craton (Henderson, 1972; Bleeker, 2003). This accretion was characterized by deformation beginning at c. 2.64 Ga, characterized by NE–SW structural trends, overthickening of the crust resulting in high-temperature–low-pressure metamorphism, and anatexis of metasedimentary rocks to produce SPGs at c. 2.61–2.59 Ga (Henderson, 1985; Davis & Bleeker, 1999; Bleeker, 2003). SPGs occur throughout the province from the vicinity of Yellowknife near the Great Slave Lake (e.g. Prosperous Granite; Kretz, 1989) to the Contwoyto Lake area in the north-central part of the craton (Contwoyto Intrusive Suite; King *et al.*, 1992; Davis *et al.*, 1994). Metasedimentary protoliths of the YYS, probably quartz-feldspathic metagreywackes of the Burwash Basin, have been proposed as the source rock of the SPGs (Drury, 1979; Meintzer, 1987; Davis *et al.*, 1994).

#### *Yilgarn Craton, Australia*

The geological framework of Western Australia consists of two cratonic nuclei, the Pilbara Craton in the north and Yilgarn Craton in the south. The southwestern part of the Yilgarn Craton, known as the Western Gneiss terrane, is thought to represent the deepest exposed section of the craton and is characterized by charnockites, minor granulite-facies metavolcanic and metasedimentary rocks, and voluminous granitoids. The granitoids have been divided into several geochemical subgroups based on Ca and Ti contents (Champion & Sheraton, 1997; Qui, 1997; Qui & Groves, 1999). A 'low-Ti' subgroup comprises small discrete plutons of post-tectonic garnet-, muscovite-, and tourmaline-bearing SPGs that crystallized between 2.64 and 2.63 Ga (Qui, 1997; Qui & Groves, 1999). Where exposed (e.g. at Griffin's Find gold mine and Nevoria goldmine) they are spatially associated with metasedimentary rocks. Their whole-rock major and trace-element chemistry, peraluminous mineralogy, and abundance of inherited zircon support derivation from partial melting of metasedimentary rocks (Qui, 1997). Similar low-Ti granitoids are exposed in the Fraser's, Marvel Loch, Bounty and Edward's Find gold mines in the Southern Cross greenstone belts in the central part of the Yilgarn Craton (Qui, 1997). Their widespread geographical distribution suggests that there was a regional high-temperature thermal event in the lower crust, possibly as a result of lithospheric delamination at c. 2635 Ma (Qui, 1997; Qui & Groves, 1999).

#### *Kaapvaal Craton, South Africa*

The Kaapvaal Craton of southern Africa forms the oldest part of the African continent and ranges in age between ~3.6 and ~2.7 Ga (Poujol *et al.*, 2003). It comprises four geographical domains (Northern, Eastern, Central, and Western) characterized by granite–greenstone belts. SPGs in the Kaapvaal Craton are found in the Eastern and Northern domains. The Eastern domain is the oldest portion of the craton and includes the 3.45–3.25 Ga Barberton greenstone belt and the 3.1–2.9 Ga Pongola Supergroup (Hegner *et al.*, 1984). A suite of granites intruding the Pongola metasediments are referred to as the 'post-Pongola granites' (Matthews, 1985). These plutons include marginally peraluminous granites (ASI = 1–1.1) such as the Mooihock, Mhlosheni, and Spekboom plutons, as well as SPGs such as the Sinceni and Godlwayo plutons (ASI > 1.1; Meyer *et al.*, 1994). These plutons have all been classified as either 'S-type' or 'ilmenite-series' granites (Meyer *et al.*, 1994; Ishihara *et al.*, 2002). The Sinceni pluton may be as old as ~3.07 Ga [Pb–Pb evaporation zircon age, Maphalala & Kröner, 1993; although see Robb *et al.* (2006) questioning the >3 Ga age and Trumbull (1993) reporting a Rb–Sr whole-rock isochron age of 2990 ± 43 Ma], whereas the other leucogranites formed between 2.86 and 2.82 Ga (Maphalala & Kröner, 1993). The younger plutons are leucogranites that

display field relationships with the Pongola Supergroup suggesting high-temperature interaction and assimilation, such as contact migmatites and xenoliths of quartzite and pelitic hornfels along their margins (Matthews, 1985). In contrast, the intrusive relationship with the Pongola Basin metasediments is unknown for the Sinceni pluton, which is a coarse-grained granite with minor amounts of biotite, muscovite, and tourmaline (Blamart *et al.*, 1993; Trumbull, 1993). In addition to peraluminous mineralogy, the initial  $^{87}\text{Sr}/^{86}\text{Sr}$  ratio of the Sinceni pluton is radiogenic at  $0.7113 \pm 0.007$  (Trumbull, 1993) suggesting derivation from an older crustal source.

Other SPGs in the Kaapvaal Craton are found in the southern portion of the Murchison greenstone belt of the Northern domain (e.g. the 2.99–2.80 Ga Lekkersmaak suite, including the Willie and Discovery plutons; Poujol & Robb, 1999; Poujol, 2001; Zeh *et al.*, 2009), which range in size from large plutons (20–30 km in diameter) to pegmatitic dikes. Typically, they are biotite- and muscovite-bearing leucogranites with sporadic occurrences of garnet and tourmaline (Jaguin *et al.*, 2010). It has been suggested that the source rock to the granites is similar to metapelite of the La France domain schists found in the Murchison greenstone belt (Vearncombe, 1988; Jaguin *et al.* 2010; Block *et al.*, 2013).

#### *Grunehogna Craton, Antarctica*

The Grunehogna Craton in East Antarctica is thought to have formed as part of or adjacent to the Kalahari Craton of southern Africa, but remained attached to Antarctica during the breakup of Gondwana in the Jurassic (e.g. Fitzsimons, 2000). The Archean basement of the craton is exposed solely as a small, glacier-bound exposure or nunatak of granite with cross-cutting garnet-bearing pegmatite dikes at Annandagstoppane (or 'Boxing Day Peaks') (Barton *et al.*, 1987; Marschall *et al.*, 2010). The crystallization age of the granite has been dated at  $3067 \pm 8$  Ma (U–Pb zircon; Marschall *et al.*, 2010), but the granite contains inherited grains as old as  $3433 \pm 7$  Ma, which constrain the maximum depositional age of the sediments from which the granites were derived. Although specific sedimentary source material cannot be identified owing to the limited exposure of the granite, whole-rock chemistry and zircon Hf and oxygen isotopes suggest a supracrustal sedimentary source (Barton *et al.*, 1987; Marschall *et al.*, 2010).

#### **Paleo- and Mesoproterozoic localities**

##### *Wopmay orogen, Canada*

The Wopmay orogen is an Early Proterozoic (c. 2.1–1.9 Ga) collisional belt located on the western edge of the Slave Craton (Hoffman & Bowring, 1984; St-Onge & Davis, 2018). The eastern part of the Wopmay comprises the Coronation Supergroup, which preserves a west-dipping sedimentary prism with rift-fill, passive margin, and foredeep flysch–molasses sequences that

accumulated within a back-arc basin (Hoffman, 1980; Hildebrand *et al.*, 1987; Lalonde, 1989). In the western part of the Coronation Supergroup, these sedimentary units were thrust onto underlying Archean basement, translated eastward, and subsequently intruded and metamorphosed by the Hepburn intrusive suite during the Calderian orogeny at c. 1885 Ma (Hoffman & Bowring, 1984; King, 1986). The Hepburn intrusive suite is composed of ~100 plutons with 2750 km<sup>2</sup> of exposure along two north–south-trending belts (Lalonde, 1989). The plutons of the Hepburn intrusive suite are variable, ranging continuously from gabbro to granite, but are dominated by peraluminous monzogranites and syenogranites. The Hepburn intrusive suite has been interpreted as the product of mantle-derived basalt generated in a back-arc setting, which subsequently assimilated and/or partially melted significant amounts of the sedimentary basin host rocks (Hoffman *et al.*, 1980; Lalonde, 1989).

##### *Talston magmatic zone, Canada*

The Talston–Thelon orogen is an ~2500 km long orogenic belt marking the suture between the 2.0–2.4 Ga Buffalo Head terrane to the west and the Archean Churchill province to the east (Bostock *et al.*, 1987; Hoffman, 1988; Ross *et al.*, 1991). In the southern part of the orogen, the Talston magmatic zone in Alberta and the Northwest Territories is composed of granitoids that intrude pre-2.0 Ga basement characterized by ortho- and paragneisses, high-grade pelitic metasedimentary rocks, and amphibolites (Bostock *et al.*, 1991; van Breemen *et al.*, 1992b; McNicoll *et al.*, 1994; Chacko *et al.*, 2000; De *et al.*, 2000). The granitoid series are characterized by an early phase of biotite and hornblende–biotite granodioritic to granitic intrusions at c. 1.99–1.93 Ga, which was followed by the intrusion of a large volume of SPGs from 1.95 to 1.93 Ga (see summary given by Chacko *et al.*, 2000). The latter include the biotite ± garnet ± cordierite ± spinel granitoids of the Slave and Konth suites (Bostock *et al.*, 1987, 1991; Bostock & Loveridge, 1988) and the biotite ± garnet granitoids of the Arch Lake suite (McNicoll *et al.*, 1993). The SPGs often contain enclaves of basement metapelites (Bostock *et al.*, 1987; Thériault, 1992; Chacko & Creaser, 1995; Grover *et al.*, 1997). Based on U–Pb zircon and monazite ages, Bostock & van Breemen (1994) concluded that the protoliths of the metapelites were originally deposited in the Rutledge River basin, a rift-related basin on the western margin of the Churchill Province, between 2.17 and 2.04 Ga. Whole-rock chemistry, peraluminous mineralogy, abundance of metasedimentary enclaves, and similarities in Nd and oxygen isotopes between metapelites and the SPGs suggest an origin of the latter primarily through partial melting of the basement metasedimentary rocks (De *et al.*, 2000; Thériault, 1992; Chacko *et al.*, 1994, 2000).

### *Trans-Hudson orogen, Canada and USA*

The Trans-Hudson Orogeny (THO) was a major collisional event closing the Manikewan Ocean and suturing the Superior Province with the Wyoming and Rae–Hearne cratons at c. 2.0–1.8 Ga, and marks the largest Paleoproterozoic orogenic belt in the world (Corrigan *et al.*, 2009). Two well-documented occurrences of SPGs occur in the THO, including those in the Wollaston domain of Saskatchewan (Annesley *et al.*, 2005; McKechnie *et al.*, 2012a, 2012b) and the Harney Peak Granite and satellite intrusions in the Black Hills of South Dakota (Redden *et al.*, 1982, 1990; Duke *et al.*, 1992; Nabelek *et al.*, 1992a, 1992b, 1999, 2001; Shearer *et al.*, 1992). The Wollaston domain comprises metasedimentary rocks deposited unconformably on the margins of the Hearne craton during rifting and formation of the Manikewan Ocean in the early Proterozoic (Madore & Annesley, 1996). Sedimentary rocks of the Wollaston domain include a succession of arkoses, conglomerates, and graphitic pelites towards the base, which are overlain by calcareous clastic units, marbles, and iron formations, and are interpreted as a rift-fill sequence deposited between 2.3 and 2.1 Ga (Madore & Annesley, 1996; Ansdell, 2005). During the Trans-Hudson Orogeny, these sediments were buried to depths equivalent to 0.6–0.9 GPa and reached peak temperatures of 720–825°C, which, combined with basaltic underplating in the lower crust, initiated large-scale crustal melting (Annesley *et al.*, 2005). Peraluminous leucogranites and granitic pegmatites occur ubiquitously throughout the Wollaston Group and are interpreted as the products of partial melting of the Wollaston domain metasedimentary rocks (Annesley *et al.*, 2005; McKechnie *et al.*, 2012a, 2012b, 2013).

The Harney Peak granite (1715 ± 3 Ma; Redden *et al.*, 1990) marks the culmination of the Trans-Hudson Orogeny during collision of the Wyoming Province and the western boundary of either the Superior Craton or the Dakota block (DeWitt *et al.*, 1986; Nabelek *et al.*, 1999). This collision resulted in the thrusting of Proterozoic metasedimentary rocks to the west over the Wyoming Craton and low-pressure (0.3–0.4 GPa), high-temperature regional metamorphism of late Archean and early Proterozoic (deposited 2100–1880 Ma) metasedimentary rocks exposed around and within the granite (Redden *et al.*, 1982, 1990; DeWitt *et al.*, 1986; Helms & Labotka, 1991; Nabelek & Bartlett, 1998). The metasedimentary rocks are dominantly quartz + muscovite ± biotite ± garnet schists with metapelite and greywacke protoliths (Walker *et al.*, 1986; Redden *et al.*, 1990). The Harney Peak granite consists of a main pluton with numerous satellite intrusions and isolated sills. The main intrusion is zoned with respect to mineralogy and oxygen isotopes, with a core composed of ‘low- $\delta^{18}\text{O}$ ’ muscovite + biotite granites and an outer zone with ‘high- $\delta^{18}\text{O}$ ’ muscovite + garnet + tourmaline (Nabelek *et al.*, 1992a). Based on whole-rock chemistry, mineral chemistry, and isotopic constraints, Nabelek *et al.*

(1992a) suggested that the core of the pluton formed through high degrees of melting of an immature Archean metasedimentary source. The ascent of these hot melts may then have triggered lower degree of melting of Proterozoic schists higher in the crust to produce the high- $\delta^{18}\text{O}$  series and satellite intrusions.

### *Southwestern USA (Colorado and Arizona)*

The time period from 1600 to 1300 Ma in Laurentia was characterized by extensive magmatism resulting in a transcontinental belt of granitoids across the USA and Canada (e.g. Anderson & Bender, 1989; Anderson & Morrison, 2005). This magmatism has been classically considered to be ‘anorogenic’, resulting from low degrees of partial melting of dominantly Paleoproterozoic or older crustal sources (Anderson & Bender, 1989; Anderson & Morrison, 2005; Rämö *et al.*, 2003). However, it has also been suggested that the magmatism was an in-board expression of orogenesis on the margin of Laurentia (Nyman *et al.*, 1994; Kirby *et al.*, 1995; Nyman & Karlstrom, 1997; Karlstrom *et al.*, 2001). Although most of these intrusions are metaluminous, biotite + hornblende granites (Anderson & Bender, 1989; Anderson & Morrison, 2005), a third group, and the ones considered here, are c. 1400–1500 Ma peraluminous, two-mica granites forming a distinct province from Colorado to central Arizona and New Mexico, such as the Silver Plume and St Vrain granites of Colorado (Anderson & Thomas, 1985; Anderson & Cullers, 1999) and the Ak Chin, Ruin, Sierra Estrella, and Oracle granites of Arizona (Anderson & Bender, 1989). The SPGs have been divided into two petrographic groups: (1) Silver Plume-type granites (located in Colorado) are relatively water-poor based on the occurrence of magmatic sillimanite and late crystallization of muscovite, biotite, and fluorite (Anderson & Thomas, 1985); (2) Oracle-type granites (located in Arizona) were emplaced under more hydrous conditions, demonstrated by the early crystallization of biotite and muscovite, and lack sillimanite and fluorite as accessory phases (Anderson & Bender, 1989). Granites from both these groups are similar to SPGs in orogenic belts in terms of their peraluminous nature and high whole-rock  $\delta^{18}\text{O}$  values (10.2–11.6‰; Anderson & Morrison, 1992).

The Silver Plume and St Vrain batholiths of Colorado intrude Paleoproterozoic paragneisses and schists of the Idaho Springs Formation (Gable & Sims, 1969; Tweto & Schoenfeld, 1979; Anderson & Thomas, 1985) and range in composition from two-mica monzogranite to syenogranite, with primary sillimanite occurring in the more evolved lithologies ( $\text{SiO}_2 > \sim 70\text{ wt } \%$ ). Although Sr isotope compositions of the granites have been used to suggest that the Idaho Springs Formation is not itself the source material, the granites were probably derived through crustal melting of a similar peraluminous quartzo-feldspathic source at pressures of 0.7–1.0 GPa (DePaolo, 1981; Anderson & Thomas,



1985). Robust crystallization ages are not available for the Silver Plume and St Vrain batholiths; however, Rb–Sr whole-rock and mineral isochrons suggest crystallization from 1420 to  $1450 \pm 30$  Ma (Peterman *et al.*, 1968).

Nd isotope studies on the peraluminous Oracle-type granites of Arizona concluded that they were derived from Proterozoic crust (Farmer & DePaolo, 1984; Nelson & DePaolo, 1985). Although specific source materials were not identified, whole-rock major and trace element and oxygen isotope compositions are consistent with melting of a peraluminous, quartz-feldspathic sedimentary source (Anderson & Bender, 1989; Anderson & Morrison, 2005). Peraluminous two-mica granites from Arizona have crystallization ages varying from  $1440 \pm 20$  Ma (U/Pb zircon age) for the Oracle and Ruin granites to c. 1380 Ma (Rb/Sr whole-rock age) for the Sierra Estrella granite (see summary by Anderson & Bender, 1989).

### *Svecofennian orogen, Finland*

The Svecofennian orogen formed through accretion of island arc complexes and older crustal fragments to the Archean basement of the Karelian craton between 1.91 and 1.87 Ga (Gaál & Gorbatshev, 1987; Lahtinen, 1994; Nironen, 1997). The main collision at c. 1.88 Ga produced significant quantities of syn-orogenic predominantly metaluminous granitoids (Huhma, 1986; Front & Nurmi, 1987; Gaál & Gorbatshev, 1987). However, in southernmost Finland a later generation of peraluminous granitic melts intruded between 1.84 and 1.81 Ga, forming a 500 km long and 100 km wide belt of intrusions (Huhma, 1986; Vaasjoki & Sakko, 1988; Suominen, 1991; Ehlers *et al.*, 1993; Väisänen *et al.*, 2000). These granites are associated with granulite metamorphism and extensive migmatization (Sederholm, 1926; Hopgood *et al.*, 1976; Edelman & Jaanus-Järkkälä, 1983; Korsman *et al.*, 1984) in what is known as the late Svecofennian granite–migmatite (LSGM) zone. The country rocks include pelitic and psammitic garnet–cordierite  $\pm$  spinel gneisses with intercalations of volcanic rocks and tonalitic sheets (Väisänen & Hölttä, 1999). The cause for high-temperature metamorphism (c. 800°C and 0.5–0.7 GPa) in the area, which resulted in partial melting of the metasedimentary rocks, is controversial, as both transpressional (Ehlers *et al.*, 1993) and extensional (Korja & Heikkinen, 1995; Nironen, 1997) tectonic models have been proposed; however, mafic underplating as a heat source has been suggested to be an important process (Schreurs & Westra 1986; Van Duin & Nieman, 1993; Väisänen *et al.*, 2000). Perhaps the best evidence for mafic underplating is the presence of contemporaneous mafic plutonic rocks in the LSGM zone (Väisänen *et al.*, 2000). The SPGs commonly occur as a stromatic network or garnet-, cordierite-, and biotite-bearing leucosomes in migmatitic metapelitic rocks. However, at higher metamorphic grades the volumes of granitic

melt increase and garnet- and cordierite-bearing pegmatitic dikes and sheets are common (Väisänen *et al.*, 2000). The metasedimentary rocks hosting the migmatites and the SPGs have detrital zircon age populations similar to local basement rocks. Maximum depositional ages of pre-Svecofennian quartzites are shown to shortly precede deformation and range from 1.87 to 1.84 Ga (Bergman *et al.*, 2008).

### *Kondalite belt, North China Craton, China*

The North China craton (NCC) coalesced in the Late Paleoproterozoic through amalgamation and collision of terranes along three large suture zones now preserved as the Khondalite belt, the Trans-North China orogen, and the Jiao-Liao-Ji belt (e.g. Zhao *et al.*, 2001, 2005; Wilde *et al.*, 2002; Zhao & Zhai, 2013). The Khondalite belt consists of khondalites (i.e. high-grade sillimanite–garnet paragneisses), which are intruded by or display transitional contacts with SPGs. The khondalites are thought to have formed during the culmination of a continental collision between the Yinshan terrane and southern Huai'an (or Ordos) terrane at c. 1.95 Ga (e.g. Qiao *et al.*, 2016). The protoliths to the khondalites are metapelites, metasandstones, and minor marbles deposited between 2.0 and 1.96 Ga and metamorphosed under both granulite-facies conditions (c. 1.95 Ga) and ultra-high-temperature (UHT) metamorphism (1.93–1.92 Ma) (Santosh *et al.*, 2006; Peng *et al.*, 2010; Wang *et al.*, 2011). The SPGs are garnet-bearing granites and occur as isolated plutons over an area of about 220 km  $\times$  80 km. At least three episodes of SPG magmatism occurred during partial melting of the khondalites at  $\sim$ 1.95, 1.93–1.90, and  $\sim$ 1.85 Ga (Yin *et al.*, 2009, 2011; Peng *et al.*, 2012; Dan *et al.*, 2014; Zhang *et al.*, 2017a; Wang *et al.*, 2018). As an alternative mechanism to crustal thickening and burial, underplating of mantle-derived basalts, potentially during ridge subduction, has been evoked as an origin for both the UHT metamorphism and SPG generation in the eastern portion of the Khondalite belt near Liangcheng (Peng *et al.*, 2012; Wang *et al.*, 2018). Input from basaltic magmas is supported by the presence of numerous syn-magmatic gabbro-norite intrusions and mafic dikes, and basaltic enclaves within the SPGs (Wang *et al.*, 2018).

Muscovite- and garnet-bearing SPGs are also found in the Helanshan region located in the western part of the Khondalite belt (Dan *et al.*, 2014; Zhang *et al.*, 2017a). Based on zircon Hf and oxygen isotope compositions, geochronology, and field relationships, Dan *et al.* (2014) suggested that the Helanshan SPGs formed during a slab break-off event at which time mafic magmas intruded into and partially melted the khondalite source rocks. (Zhang *et al.* 2017a) presented a further study of the Helanshan SPGs and, based on similar trace element patterns, zircon Hf model ages, and whole-rock Nd model ages between the khondalites and SPGs, also suggested derivation of the SPGs

through partial melting of the khondalites following a collisional orogenic event.

#### *Nangrim Massif, Imjingang Belt, and Yeongnam Massif granites, North and South Korea*

Precambrian basement rocks in the Korean peninsula comprise Archean and Proterozoic metasediments and granitoids of the Nangrim (called elsewhere 'Rangnim') Massif, Imjingang Belt, Gyeonggi Massif, Okcheon Belt and Yeongnam Massif from north to south. In the northern part of North Korea Proterozoic metasedimentary rocks belong to the Paleoproterozoic Jungsan and Machollyong Groups in the Nangrim Massif and Imjingang Belt. The Jungsan group comprises primarily pelitic schists, although amphibolites, hornblende-biotite gneisses, and calc-silicate rocks are also present (Zhang *et al.*, 2017b). The Machollyong Group occurs along a NW–SE-trending belt that has been interpreted as a Paleoproterozoic rift zone and consists of a stratigraphically lower unit of metamorphosed arkoses and volcanic rocks, a carbonate-rich middle unit (now marbles and calc-silicate rocks), and an upper unit dominated by argillaceous metasediments (Zhang *et al.*, 2017b). Intruding into the Jungsan and Machollyong groups are garnet  $\pm$  sillimanite granites, which are interpreted as partial melts of the metasedimentary rocks (Zhao *et al.*, 2006). At their margins the garnet-sillimanite granites are gradational with the metasedimentary rocks, varying from migmatites with leucosomes into SPGs with metasedimentary enclaves (Zhao *et al.*, 2006). However, in the cores of the plutons, the granites become massive and homogeneous. Weighted averages of  $^{207}\text{Pb}/^{206}\text{Pb}$  zircon ages from two samples of the SPGs yielded crystallization ages of  $1908 \pm 12$  and  $1903 \pm 49$  Ma (Zhao *et al.*, 2006). One of these two samples yielded inherited zircon ages between 2.5 and 2.1 Ga, placing a maximum constraint on depositional age.

SPGs and related pegmatites also occur in South Korea at the boundary of the Ogcheon Belt and the Yeongnam Massif. The Yeongnam Massif is primarily composed of pelitic to psammo-pelitic metasedimentary rocks and orthogneiss, as well as Mesozoic granites. Detrital zircon constraints on the metasedimentary rocks from the Yeongnam Massif constrain the depositional age to c. 2.00 Ga (Kim *et al.*, 2012). Both small volumes of garnet-bearing leucogranites dikes, sills, and stocks (Kim & Cho, 2003) and the larger (5–20 km<sup>2</sup> in areal extent) biotite + muscovite  $\pm$  tourmaline  $\pm$  garnet-bearing Nonggeori and Naedeokri leucocratic granites (Lee *et al.*, 2005) intruded into the metamorphic rocks. The Nonggeori and Naedeokri granites are characterized by low magnetic susceptibilities [ $(0.08\text{--}0.3) \times 10^{-3}$  SI], suggesting that they belong to the 'ilmenite-series' (Jin *et al.*, 2001). A Sm–Nd whole-rock-garnet isochron yielded an age of  $1926 \pm 41$  Ma for the garnet-bearing leucogranites (Kim & Cho, 2003), whereas K–Ar muscovite ages range from  $1802 \pm 18$  to

$1732 \pm 16$  Ma for the Nonggeori granite and from  $1787 \pm 19$  to  $1773 \pm 18$  Ma for the Naedeokri granite (see summary by Lee *et al.*, 2005). Although the tectonic history of this region is not well constrained, Lee *et al.* (2005) concluded, on the basis of mineralogy, whole-rock chemistry, and Nd isotopes, that the Nonggeori and Naedeokri granites were derived from partial melting of 'crustal rocks represented by the gneissic basement of the Sino-Korean craton'.

#### *Guyana Shield granites, Brazil*

The Roraima State located in the Guyana Shield may be divided into four major geological domains (Surumu, Parima, Central Guyana, and Uatumã–Anauá), which are characterized by an intense period of Paleoproterozoic magmatism (Reis *et al.*, 2000; Almeida *et al.*, 2007, 2008). Two of these domains contain SPGs: the garnet-bearing Curuxium, Taiano, and Amajari granites of the Central Guyana domain (CGD) and the muscovite  $\pm$  cordierite  $\pm$  sillimanite-bearing Serra Dourada granite of the Uatumã–Anauá domain (UAD). The crystallization ages of the Taiano and Serra Dourada granites have been constrained via zircon U–Pb geochronology at  $1969 \pm 4$  Ma (CPRM, 2003) and  $1962 \pm 2$  Ma respectively (Almeida *et al.*, 2007). Based on whole-rock chemistry and mineralogy, Almeida *et al.* (2007) suggested that the Serra Dourada granite was probably derived from partial melting of metagraywackes during collision of older Paleoproterozoic domains of the Guyana Shield. Both the Serra Dourada and the Taiano granites contain zircon with inherited cores ranging from 2138 Ma to 2047–2072 Ma, respectively, suggesting a maximum depositional age of their source sediment in the earliest Paleoproterozoic. Although future field studies and geochronology are required to understand the detailed origin of these granites, they were probably formed during the collision of the Paleoproterozoic Anauá magmatic arc with Transamazon (2.2–2.0 Ga) and Central Amazonian (>2.3 Ga) terranes (Almeida *et al.*, 2007).

#### *Jacobina–Contendas Mirante belt, São Francisco craton, Brazil*

The Jacobina–Contendas Mirante (JCM) belt is a north-south-trending dominantly volcano-sedimentary belt in the eastern part of the São Francisco craton. The JCM belt is situated between two Archean crustal blocks: the Jequié domain and Atlantic coast 'mobile belt' to the east and the Gavião domain to the west. The Gavião domain comprises migmatitic gneisses and amphibolites that represent the basement of the JCM supracrustal sequences. The convergence between the Jequié and Gavião domains in the Paleoproterozoic was marked by the formation of basins in which the JCM belt volcanic and sedimentary rocks were deposited (Barbosa & Sabaté, 2004). The Serra de Jacobina series of the JCM belt is an ~10 km wide by >200 km long belt of meta-quartzite, meta-conglomerates, mica-schists, banded



iron formations, and minor intercalated meta-ultramafic rocks (Cuney *et al.*, 1990; Marinho *et al.*, 1993). Two lithostratigraphic units have been defined in the Contendas Mirante belt: a lower unit of basalts and andesites with interbedded clastic and chemical sediments and an upper unit of greywackes, pelites and argillites with conglomerate layers (Marinho *et al.*, 1993). A maximum depositional age defined by detrital U–Pb zircon ages from the Contendas–Mirante upper unit is  $2168 \pm 18$  Ma (Nutman & Cordani, 1993; Nutman *et al.*, 1994).

Numerous (>20) SPGs intrude the Gavião basement rocks and the JCM belt. These include, but are not limited to, the Gameleira, Riacho das Pedras, Aliança, Caetano, Lagoa Grande, and Lagoinha plutons in Contendas Mirante belt and the Campo Formos and Carnaíba plutons in the Serra de Jacobina series (Cuney *et al.*, 1990; Sabaté *et al.*, 1990; Marinho *et al.*, 1993; Leal *et al.*, 2000). Rb/Sr whole-rock isochrons for the granites yield ages between  $1974 \pm 36$  and  $1883 \pm 87$  Ma (Sabaté *et al.*, 1990). The granites are muscovite + biotite ± garnet-bearing and sometimes associated with late muscovite-, garnet-, and tourmaline-bearing pegmatites (Cuney *et al.*, 1990; Sabaté *et al.*, 1990). Biotite-rich layered enclaves thought to be representative of restitic source material are present in the plutons (Cuney *et al.*, 1990). Based on whole-rock and mineral chemistry, Sr and Nd isotope ratios, geochronology, and field relationships, the SPGs are thought to be derived through partial melting of supracrustal material during the c. 2 Ga collision of the Jequié and Gavião domains (Cuney *et al.*, 1990). Based on whole-rock Sr isotope ratios, Sabaté *et al.* (1990) suggested that the Archean Gavião terrane was the most likely source rock; however, Nd isotopes are in conflict with this interpretation and instead are consistent with derivation from rocks of the Contendas Mirante metasedimentary rocks.

#### *Cape Coast suite granites, Baoulé Mossi domain, Ghana and Côte d'Ivoire*

The Baoulé Mossi domain of the West African craton is a composite terrane composed of NE–SW-trending belts of early Paleoproterozoic (~2.35–2.20 Ga) tholeiitic to calc-alkaline metavolcanic rocks and metasedimentary rocks of the Birimian and Tarkwaian groups, all of which were intruded by granites at ~2.1–2.0 Ga (Boher *et al.*, 1992; Taylor *et al.*, 1992; Vidal & Alric, 1994; Hirdes *et al.*, 1996; Gasquet *et al.*, 2003; Baratoux *et al.*, 2011). The metasedimentary rocks of the Birimian Supergroup consist of metamorphosed volcanoclastic rocks, turbidite-related greywackes, carbonaceous argillites, cherts, carbonates, and Mn-rich sediments, interpreted as having formed in a basin proximal to a volcanic front (Leube *et al.*, 1990). There are four main suites of granite; the Winneba, Cape Coast, Dixcove, and Bongo. Of interest here are the Cape Coast granites, which are peraluminous muscovite + biotite-bearing granitoids that predominantly occur as batholiths

hosted in the Birmain metasedimentary rocks (Leube *et al.*, 1990). Metasedimentary xenoliths in the granites (up to 10 m in size) have been observed (Petersson *et al.*, 2016). These granites represent the latest stage of magmatism in the domain and formed during the accretion of various oceanic arc terranes at ~2.1–2.0 Ga (Boher *et al.*, 1992; Pouclet *et al.*, 1996; Gasquet *et al.*, 2003).

Leube *et al.* (1990) analyzed 25 samples from the Cape Coast granite suite for whole-rock major and trace element chemistry and found that although all samples were peraluminous, only seven were strongly peraluminous. In addition, initial  $^{87}\text{Sr}/^{86}\text{Sr}$  ratios ( $0.70150 \pm 42$ ) and  $\epsilon_{\text{Nd}}$  (+3.7) values suggested a relatively depleted (i.e. mantle-like) source for these granites. A more recent study of the U–Pb and Hf isotopes in zircon of three different muscovite-bearing granodioritic, granitic, and pegmatitic samples from the Cape Coast suite yielded  $^{207}\text{Pb}/^{206}\text{Pb}$  crystallization ages of  $2125 \pm 18$  Ma,  $2093 \pm 20$  Ma, and  $2092 \pm 40$  Ma respectively and initial  $\epsilon_{\text{Hf}}$  values of +2.1 to +5.5 (Petersson *et al.*, 2016). The existing collective radiogenic isotope data suggest that there is a strong mantle-derived component in the Cape Coast granites. Leube *et al.* (1990) suggested that the peraluminous character of the granites may have resulted from large-scale contamination of the ascending melts by volcanoclastic sediments. However, radiogenic isotope data exist for only three samples with well-described petrology (i.e. muscovite-bearing granites) and whole-rock data for these samples do not exist. We therefore have decided to include these granites in this compilation based on the strongly peraluminous nature of some of the granites, their described primary mineralogy, and their field relationships suggesting intimate association with the Birimian sedimentary rocks. However, Leube *et al.* (1990) reported only an average whole-rock chemistry of the 25 samples they analyzed, so our analysis of geochemical data from this suite in subsequent discussion is hindered.

#### PETROGRAPHY AND MINERAL CHEMISTRY

The corundum-normative nature of SPGs requires that in addition to quartz and two feldspars they have one or more aluminous major phase such as biotite, muscovite, garnet, cordierite, aluminosilicates (sillimanite, andalusite, or kyanite), tourmaline, topaz, spinel, or corundum (Clarke, 1981). These phases can have a magmatic origin (i.e. crystallizing directly from the granitic melt) or can be entrained restitic phases (e.g. biotite and garnet; White & Chappell, 1977; Stevens *et al.*, 2007). If these are primary magmatic phases, the crystallization of these phases is controlled by temperature, pressure, bulk composition, fluid composition, and oxygen fugacity. As such, careful interpretation of the mineral crystallization textures, reaction relationships, and chemistry can be used to constrain these intensive variables during crystallization. As a comprehensive discussion of petrography and mineral chemistry in SPGs

**Table 2:** Summary of mineral assemblages and compositions for SPG localities

No.	Locality	Aluminous mineral assemblage(s) (not including feldspars)	Accessory phases	% Anorthite	Fe <sup>2+</sup> /(Fe <sup>2+</sup> +Mg)			Garnet compositions	References
				Plg	Bt	Ms	Tur	Crd	
<b>Archean Superior Craton</b>									
1	Preissac-Lacorne-Lamotte-Moly Hill granites + Pontiac garnet-muscovite granites (GMG)	bt+ms, ms, ms±grt	ilm, mnz, xnt, ap, zrc, mo, col-tan, sp	7–15	0.7–0.85	0.65–0.85	—	Sps(30–60), Alm(59–37)	Mulja <i>et al.</i> , 1995a
2	Allison Lake batholith	bt+ms±grt, ms±grt	F-ap, tur	—	—	0.60–0.71	—	Sps(22–58), Alm(39–69), Pyr(2–7), And(0–3), Grs(0–2)	Tindle <i>et al.</i> , 2002; Breaks <i>et al.</i> , 2003
3	Wenasaga Lake batholith	bt+ms±grt±crd	F-ap, mnz, xnt	—	0.65–0.66	0.60–0.63	—	Sps(8–21), Alm(71–80), Pyr(6–11), Grs(1–2)	Tindle <i>et al.</i> , 2002; Breaks <i>et al.</i> , 2003
4	Root Bay pluton	ms±tur	F-ap	—	—	0.80–0.84	—	—	Tindle <i>et al.</i> , 2002; Breaks <i>et al.</i> , 2003
5	Sharpe Lake batholith	bt+ms±grt	tur, F-ap	—	—	—	—	—	C. Buchholz, field observations
6	Twiname Lake stock and Caron Lake pluton	bt+ms±grt, ms±grt	tur, F-ap	—	—	0.72–0.75	—	Sps(28–39), Alm(58–68), Pyr(1–3), And(0–1)	Tindle <i>et al.</i> , 2002; Breaks <i>et al.</i> , 2003
7	Ghost Lake batholith (and Zealand stock)	bt+crd, bt+ms, bt±grt+ms, grt+ms±tur	zrc, mnz, F-ap, brl, 3–28 py	—	0.59–0.79	0.50–0.87	—	Sps(15–24), Alm(68–83), Pyr(4–6), Grs(1–2)	Breaks & Jones, 1991; Breaks & Moore, 1992; Buchholz <i>et al.</i> , 2018
8	Medicine Lake pluton	bt+ms, ms±grt	tur, brl	—	—	—	—	Sps(12–25), Alm(72–82), Pyr(1–5), Grs(0–1)	Tindle <i>et al.</i> , 2002; Breaks <i>et al.</i> , 2003
9	Separation Rapids pluton + Treeline Lake complex	grt+crd+bt, grt+bt	F-ap, mnz, zrc, rt, sil, ghn	—	0.61–0.70	0.60 (1 sample)	—	—	Pan & Breaks, 1997; Buchholz <i>et al.</i> , 2018
10	Cat Lake-Winnipeg River pegmatite field (associated leucogranites)	bt+ms±grt, ms±grt	tur, crd, zrc, ap, mnz, ghn, btl, col-tan, mo, apy	3–6	—	—	—	Sps(7–50)	Černý <i>et al.</i> , 1981; Goad & Černý, 1981
11	Georgia Lake granites (e.g. Glacier Lake batholith, Barbara Lake stock)	grt+bt, crd+bt, bt+ms, ms±grt±tur	F-ap, brl	—	—	0.49–0.89	—	Sps(4–49), Alm(50–77), Pyr(0–22), And(0–2), Grs(0–3)	Tindle <i>et al.</i> , 2002; Breaks <i>et al.</i> , 2003
12	Armstrong Highway area	bt+ms±grt, bt+grt, ms±grt, crd, grt+crd	tur, F-ap, brl	—	—	—	—	Sps(5–50), Alm(49–83), Pyr(2–17), And(1–2)	Tindle <i>et al.</i> , 2002; Breaks <i>et al.</i> , 2003
13	Sturgeon Lake and Vermillion granites	bt+ms±grt±sil±crd±tur	arc, mnz, ap, fl	—	0.61–0.72	0.63–0.70	—	Sps(6), Alm(81), Pyr(11), Grs(2) (1 sample)	Percival, 1986; Buchholz <i>et al.</i> , 2018
14	Shannon Lake granite	bt+ms, tur+grt+beryl in pegmatites	ap, ttu, zrc, aln	—	0.71–0.75	—	—	—	Boerboom & Zartman, 1993; Buchholz <i>et al.</i> , 2018
<b>Wyoming Craton</b>									
15	Mt Owen batholith	bt+ms±grt	zrc, aln, mnz, sil needles in qtz	—	0.81	0.81	—	Sps(10), Alm(84), Pyr(4), Grs(2) (1 sample)	Frost <i>et al.</i> , 2006; Buchholz <i>et al.</i> , 2018
16		bt+ms±grt	not described	—	—	—	—	—	(continued)

Table 2: Continued

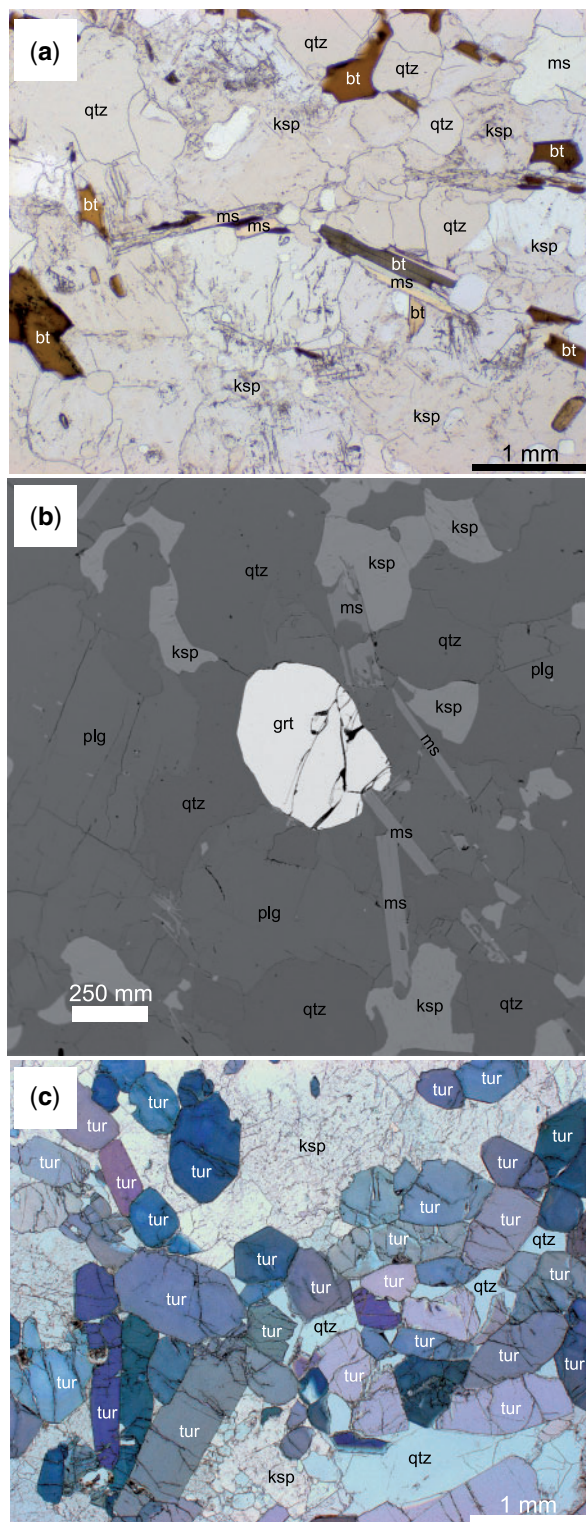
No.	Locality	Aluminous mineral assemblage(s) (not including feldspars)	Accessory phases	% Anorthite	$Fe^{T}/(Fe^{T}+Mg)$				Garnet compositions	References
				Plg	Bt	Ms	Tur	Crd		
South Pass granites (South Pass and Sweetwater plutons)										
17	Tin Cup Spring granite	bt+ms±grt±tur	ep, ttu, zrc, aln	—	—	—	—	—	—	C. Bucholz, field observations
18	Bear Mountain granite	ms±bt±grt	ap, 'opaques'	2–11	—	—	—	—	—	Langstaff, 1995; Meredith, 2005; Gosselin <i>et al.</i> , 1988, 1990
Slave Craton										
19	Yellowknife granite-pegmatite field (e.g. Prosperous Lake, Sparrow Lake, and Prestige plutons)	bt+ms±tur±grt	ap, mnz	5	0.74	0.54	0.62–0.67	—	—	Meintzer <i>et al.</i> , 1984; Kretz <i>et al.</i> , 1989
20	Contwoyto plutonic suite	bt+ms±tur±sil	ap, zrc, mnz	—	—	—	—	—	—	Davis, 1992; Davis <i>et al.</i> , 1994
Yilgarn Craton										
21	'post-tectonic, low-Ti' peraluminous granites	bt+grt+ms±tur	zrc, mgt	—	—	—	—	—	—	Qui, 1997; Qui & Groves, 1999
Kaapvaal Craton										
22	'low-Ca' granites (Sinceni, Mooihoek, Mhlosheni, Godlwayo, Spekboom, and Kwetta plutons)	Sinceni: bt±ms±tur; others: bt±ms	zrc, ap, xnt, thr, mnz, aln, rt, ilm, mgt	5–30	0.70–0.85	0.64–0.78	0.65–0.83	—	—	Trumbull, 1993; Meyer <i>et al.</i> , 1994
23	Lekkersmaak suite granites (including Willie granite and Discovery pluton)	bt+ms±grt	not described	—	—	—	—	—	—	Jaguin <i>et al.</i> , 2010
Grunehogna Craton										
24	Annandagstoppane granite	bt+ms	zrc, ap, ep, mnz	—	—	—	—	—	—	Barton <i>et al.</i> , 1987; Marschall <i>et al.</i> , 2010
Proterozoic Wopmay Orogen										
25	Hepburn intrusive suite	bt+ms±grt (accessory sill & tur in some units)	zrc, aln, fl, 'opaques'	—	0.61–0.78	0.49–0.54	—	—	—	Lalonde, 1986; Lalonde & Bernard, 1993
Tasmanian magmatic zone										
26	Arch Lake, Slave, and Konth intrusive suites	bt±grt±±crd±sp	mnz, ilm, zrc, ap, opx	2–30	—	—	—	0.27–0.30	Sp(1–2), Alm(65–73), Pyr(2–31), Grs(3–5)	Thériault, 1992; Berman & Bostock, 1997; De <i>et al.</i> , 2000
Trans-Hudson Orogen										
27	Cree Lake granites	bt±ms±grt±sill±rare tur	mnz, zrc, ap, ilm, mgt, urn, gr, fl	—	—	—	—	—	—	Annesley <i>et al.</i> , 1997, 2003; McKechnie <i>et al.</i> , 2013
28	Harney Peak granite (+ satellite intrusions; e.g. Calamity Peak pluton)	bt±ms±grt, ms±grt±tur	ap, zrc, mnz	30 Oct	0.63–0.86	0.52–0.84	0.52–0.82	—	Sps(15–53), Alm(38–76), Pyr(1–9), Grs(1–4)	Shearer <i>et al.</i> , 1987; Redden <i>et al.</i> , 1990; Nabelek <i>et al.</i> , (continued)

Table 2: Continued

No.	Locality	Aluminous mineral assemblage(s) (not including feldspars)	Accessory phases	% Anorthite	Fe <sup>2+</sup> /(Fe <sup>2+</sup> +Mg)	Plg	Bt	Ms	Tur	Crd	Garnet compositions	References
<i>Mesoproterozoic southwest USA</i>												
29	Silver Plume and St Vrain batholiths.	bt+ms±sill	mgt, ilm, mnz	15–33	0.55–0.69	0.63–0.74	—	—	—	—	—	1992a; Bucholz <i>et al.</i> , 2018
30	Ak-Chin, Maricopa, Oracle, Sierra Estrella, Dells, and Lawler Peak granites	bt+ms±grt±tur	ilm, mgt, rt, zrc, fl, aln, mnz, ap, xnt, thr	10–39	0.52–0.58	0.58–0.70	—	—	—	—	—	Anderson & Thomas, 1985; Bucholz <i>et al.</i> , 2018 Anderson & Bender, 1989
<i>Svecofennian Orogen</i>												
31	Late Svecofennian granite–migmatite zone	bt+grt (in granites), bt±grt±crd in leucosomes	not described	18–25	0.52–0.55	—	—	—	—	0.36–0.40	—	Johannes <i>et al.</i> , 2003
<i>North China Craton</i>												
32	Liangcheng granitoids	grt±crd±bt	sp, ilm zrc, mnz, ap, py	—	—	—	—	—	—	—	Sp(1), Alm(56–66), Pyr(27–40), Grs(2–6)	Lan, 2007; Wang <i>et al.</i> , 2018
33	Helanshan complex	bt+ms, bt±grt, grt	sp, ilm, mgt, zrc	—	—	—	—	—	—	—	—	Dan <i>et al.</i> , 2014
34	Peraluminous granites associated with Jungsan and Machollyong sediments	grt±sill	not described	—	—	—	—	—	—	—	—	Zhao <i>et al.</i> , 2006
35	Nonggeori and Naadeokri granites and grt-bearing leucogranites	bt+ms±grt±tur±crd±sill	zrc, ap, ttn, ilm	3–15	—	—	—	—	—	—	Sps(14), Alm(77), Pyr(8), Grs(1)	Kim & Cho, 2003; Lee <i>et al.</i> , 2005
<i>Guyana Shield</i>												
36	Serra Dourada granite	bt+ms±crd±sill	zrc, mnz, xnt	—	—	—	—	—	—	—	—	Almeida <i>et al.</i> , 2007
37	Curuxim, Taiano, and Amajari granites	bt+ms±grt	not described	—	—	—	—	—	—	—	—	Almeida <i>et al.</i> , 2007
<i>São Francisco Craton</i>												
38	Gamaleira Massif	bt+ms	zrc, ap, ttn, mgt, ilm	—	—	—	—	—	—	—	—	Sabaté <i>et al.</i> , 1990; Marinho <i>et al.</i> , 1993
<i>West Africa Craton</i>												
39	Cape Coast granites	bt+ms, ms	zrc	—	—	—	—	—	—	—	—	Leube <i>et al.</i> , 1990

ap, arsenopyrite; aln, almandine; ap, apatite; brl, beryl; bt, biotite; col-tan, columbite-tantalite; crd, cordierite; ep, epidote; F-ap, fluorapatite; fl, fluorite; ghn, garnet; gr, graphite; hm, hematite; ilm, ilmenite; mgt, magnetite; mo, molybdenite; mnz, monazite; ms, muscovite; opx, orthopyroxene; py, pyrite; qtz, quartz; rt, rutile; sil, sillimanite; sp, sphalerite; thr, thorite; ttn, titanite; tur, tourmaline; urn, uraninite; xnt, xenotime; zrc, zircon.





**Fig. 4.** Examples of mineralogy observed in Archean and Proterozoic SPGs. (a) Photomicrograph in plane-polarized light of biotite + muscovite granite from the Ghost Lake batholith (sample E19-8). (Note interlocking growth of biotite and muscovite.) (b) Back-scattered electron image of biotite + muscovite + garnet granite from the Ghost Lake batholith (sample F11-4). (c) Photomicrograph in cross-polarized light of tourmaline-rich granite from a satellite intrusion associated with Harney Peak granite (sample HP-39a from Nabelek *et al.*, 1992a, 1992b). bt, biotite; ksp, K-feldspar; ms, muscovite; plg, plagioclase; qtz, quartz; tur, tourmaline.

merits a paper unto itself (e.g. Clarke, 1981; Clemens & Wall, 1988; Zen, 1988; Holtz *et al.*, 1992), we focus our discussion on an overview of Archean and Proterozoic SPG phase assemblages and mineral chemistry between these temporally distinct groups, which can inform our understanding of their intensive parameters during crystallization, whether they changed across the Archean–Proterozoic transition, and the implications these differences have for their sedimentary source material across this transition. We summarize reported mineral assemblages (including accessory phases) and compositions (when available) in Table 2.

All of the SPGs considered here contain biotite and/or muscovite and sometimes other peraluminous minerals, dominantly garnet (Figs 3c, d and 4a, b). In addition, many include major to accessory minerals such as cordierite, aluminosilicates, tourmaline, or beryl, typical of SPGs (Tables 1 and 2; Fig. 4c). Within certain SPG plutons, zoning in mineralogy and composition is observed. For example, the Ghost Lake batholith, which has been the subject of a detailed study by Breaks & Moore (1992), demonstrates mineralogical zoning from west to east from a more primitive biotite + cordierite granite to a highly evolved garnet + muscovite ( $\pm$  tourmaline  $\pm$  beryl) granite. This was interpreted as the petrological and geochemical consequences of *in situ* differentiation (Breaks & Moore, 1992). Another example of a zoned intrusion is the Harney Peak granite, where biotite is the dominant ferromagnesian mineral in the core of the pluton, whereas tourmaline dominates along the perimeter, as well as in satellite intrusions (Nabelek *et al.*, 1992a). (Nabelek *et al.* 1992a) ascribed this difference in mineralogy to different source regions for the biotite- versus tourmaline-bearing granites, as well as extents of melting. The biotite granites were proposed to have formed through high extents of biotite dehydration melting of immature greywackes, whereas the tourmaline granites (see example in Fig. 4c) were concluded to have formed through a lower extent of melting of metapelites, producing melts with high boron concentrations.

### Biotite

Other than feldspar, biotite is generally the dominant aluminous mineral in the SPGs considered here and becomes rare to absent only in the more evolved leucogranites or tourmaline-dominated granites. Biotites from SPGs of all ages are more aluminous than members of the phlogopite–annite solid solution with significant eastonite–siderophyllite components (Abdel-Rahman, 1994; Bucholz *et al.*, 2018). With the limited dataset available, no distinctions in major and minor elements in biotite (e.g.  $\text{TiO}_2$ , halogens, etc.) from Archean and Proterozoic SPGs are observed, except for  $\text{Fe}^{\text{T}}/\text{Mg}$  ratios. Biotite  $\text{Fe}^{\text{T}}/\text{Mg}$  (where  $\text{Fe}^{\text{T}} = \text{Fe}^{2+} + \text{Fe}^{3+}$ ) ratios are highly sensitive to oxygen fugacity ( $f_{\text{O}_2}$ ) during crystallization, with higher values being stable at lower  $f_{\text{O}_2}$  (Wones & Eugster, 1965; Czamanske &



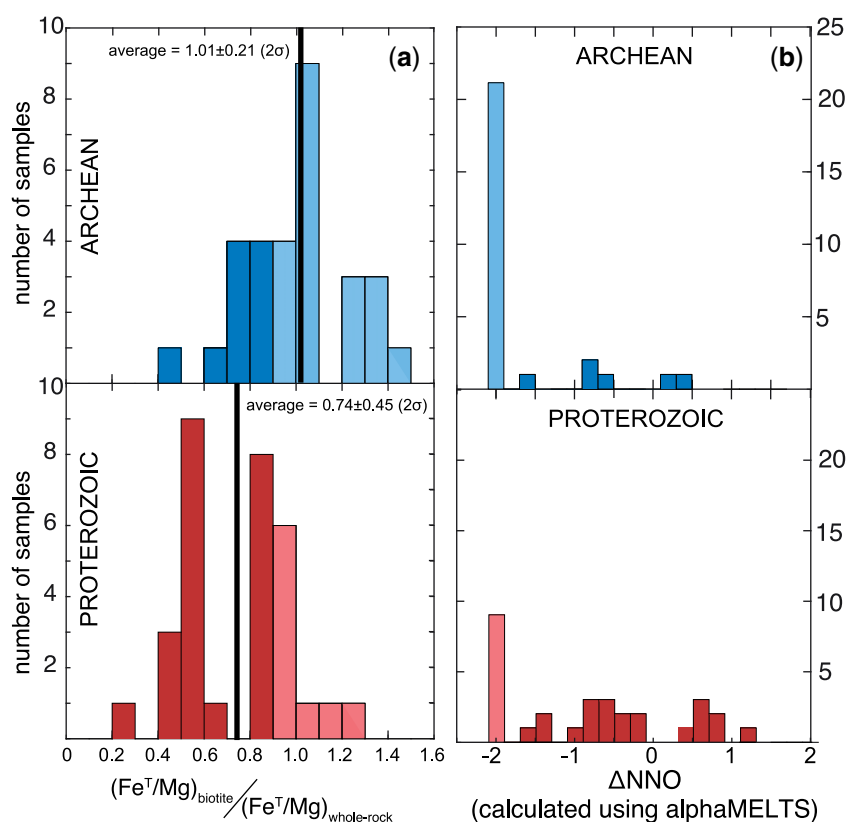
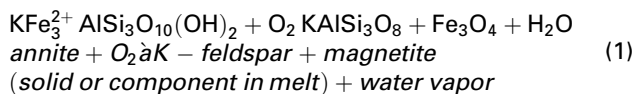


**Fig. 5.** Histograms of (a)  $\text{Fe}^{\text{T}}/\text{Mg}$  biotite–WR (whole-rock) partition coefficient [ $K(\text{bt-WR})$ ] and (b) calculated oxygen fugacity (relative to the Ni–NiO buffer) for Archean and Proterozoic SPGs using the method of Bucholz *et al.* (2018), which utilizes biotite and bulk-rock compositions and alphaMELTS modeling. In (a) and (b) samples in lighter blue and red indicate those not amenable to modeling via alphaMELTS [owing to  $K(\text{bt-WR}) > 0.9$ ; see Bucholz *et al.*, 2018, for details]. For these samples, although a specific  $f_{\text{O}_2}$  could not be calculated, their elevated  $K(\text{bt-WR})$  values impose a maximum limit of 2 log units below the Ni–NiO buffer ( $\text{NNO} - 2$ ).

Wones, 1973; Ague & Brimhall, 1988). This arises as a result of the breakdown of the annite component in biotite with increasing  $f_{\text{O}_2}$  to produce K-feldspar, magnetite (or hematite component in hemo-ilmenite or  $\text{Fe}_2\text{O}_3$  component in the melt), and  $\text{H}_2\text{O}$  via a reaction such as



Therefore, as  $f_{\text{O}_2}$  increases in a melt the total percentage of the Fe in the bulk system (i.e. melt + crystals) hosted within biotite will decrease as  $\text{Fe}^{3+}$  is preferentially partitioned into an oxide phase or the melt. As such, the  $\text{Fe}^{\text{T}}/\text{Mg}$  partition coefficient between biotite and whole-rock [ $K_{\text{bt-wr}}^{\text{Fe}^{\text{T}}/\text{Mg}} = (\text{Fe}^{\text{T}}/\text{Mg})_{\text{biotite}}/(\text{Fe}^{\text{T}}/\text{Mg})_{\text{whole-rock}}$ ] decreases as  $f_{\text{O}_2}$  increases (Bucholz *et al.*, 2018). If independent estimates of temperature, pressure, and water activity are available, quantitative estimates of  $f_{\text{O}_2}$  can be obtained through thermodynamic modeling using alphaMELTS software (Smith & Asimow, 2005).

Developing and using this method, Bucholz *et al.* (2018) modeled variations in  $\text{Fe}^{\text{T}}/\text{Mg}$  ratios in biotite from Archean and Proterozoic SPGs to understand

whether they were characterized by differences in  $f_{\text{O}_2}$  during crystallization. They found that the average  $K_{\text{bt-bulk}}^{\text{Fe}^{\text{T}}/\text{Mg}}$  for Archean SPGs was  $1.01 \pm 0.21$  versus  $0.74 \pm 0.45$  for Proterozoic granites (Fig. 5a). The majority (>80%) of Archean SPGs considered in the study crystallized at  $f_{\text{O}_2}$  values near the maximum stability of graphite in equilibrium with a water-saturated C–O–H fluid, whereas only ~40% of the Proterozoic samples did. The other Proterozoic samples crystallized at higher  $f_{\text{O}_2}$  values [up to one log unit above the Ni–NiO (NNO) buffer; Fig. 5b]. The simplest explanation for this observation is that the sediments from which Archean SPGs were derived had lower bulk redox states than the more oxidized Proterozoic SPGs, possibly reflecting the deposition of Archean SPG source rock sediments under lower partial pressures of atmospheric  $\text{O}_2$  prior to the GOE.

For example, Fe and S, two of the dominant redox-sensitive elements in sediments, are characterized by different bulk redox states in Archean versus Proterozoic sediments. Fe in Archean sediments is dominantly ferrous and S is hosted in sulfides, mainly pyrite, as  $\text{S}^{-1}$ . In contrast, Proterozoic sediments are characterized by the proliferation of red beds stained by ferric Fe (Holland, 1984) and the onset of sulfate

(S<sup>6+</sup>-bearing) deposits (Chandler, 1988). Thus, the variation in  $f_{O_2}$  of SPGs derived from sedimentary rocks deposited on either side of the GOE may reflect this change in Fe and S speciation. Although organic carbon is present in both Archean and Proterozoic sedimentary rocks and certainly exerted a reducing influence on Archean and Proterozoic SPG  $f_{O_2}$ , it was probably the bulk redox state of the sediments that ultimately fixed the  $f_{O_2}$  of SPG magmas. In particular, although the cumulative preserved thicknesses of black shales in the Paleoproterozoic to Mesoproterozoic reached a peak in Earth history, the total organic carbon in these shales (<5 wt %) was on average lower than at other times in Earth history (up to ~30% in the Phanerozoic; Condie *et al.*, 2001; Och & Shields-Zhou, 2012). The simultaneous decrease in the organic carbon content of sediments (by weight per cent) and increase in amount of other oxidized sedimentary material may explain the relatively elevated  $f_{O_2}$  of Proterozoic SPGs as compared with Phanerozoic and Archean SPGs. Notably, however, many SPGs from both the Archean and Proterozoic crystallized at  $f_{O_2}$  values controlled by reduced carbon in their source region (samples at NNO – 2 in Fig. 5b), suggesting that burial of organic carbon in the sedimentary source regions for the SPGs has exerted an important control on the  $f_{O_2}$  of the SPGs across the transition (and indeed also for Phanerozoic SPGs; Flood & Shaw, 1977; Blevin & Chappell, 1992; Nabelek, 2019).

### White mica

White mica is a common mineral in SPGs and can be either primary or secondary in origin. Primary white mica occurs as large euhedral books or phenocrysts (Fig. 4a), whereas secondary white mica shows textural relationships suggesting that it formed through the breakdown of feldspars, biotite, or other aluminosilicates during cooling and potential ingress of fluids (Miller, 1981). In addition to textural arguments, primary versus secondary white mica can be identified based on its chemistry. Miller (1981) suggested that magmatic white mica is consistently richer in Ti, Na, and Al, but poorer in Mg and Si, than secondary white mica. Bucholz *et al.* (2018) compiled and screened existing white mica compositional data for Archean and Proterozoic SPGs. In both the Archean and Proterozoic granites, white mica does not occur as pure end-member muscovite [K<sub>2</sub>Al<sub>4</sub>(Si<sub>6</sub>Al<sub>2</sub>O<sub>20</sub>)] but rather exhibits solid solution towards paragonite [Na<sub>2</sub>Al<sub>4</sub>(Si<sub>6</sub>Al<sub>2</sub>O<sub>20</sub>)(OH)<sub>4</sub>] and celadonite [K<sub>2</sub>Al<sub>2</sub>(Fe,Mg)<sub>2</sub>(Si<sub>8</sub>O<sub>20</sub>)(OH)<sub>4</sub>] (Bucholz *et al.*, 2018). Primary white mica was identified in all SPG samples from that study and no systematic compositional differences in white mica (e.g. Na contents, halogens, etc.) from Archean and Proterozoic SPGs were observed.

### Garnet

Garnets in SPGs display variable compositions from one intrusion to another, mostly in relationship to Fe:Mg:Mn ratios. In both Archean and Proterozoic

SPGs, garnets are almandine–spessartine solid solutions, having only a minor pyrope and grossular component (generally <10 mol. %; Table 2). Some garnets in the highly evolved SPGs from both the Archean and Proterozoic can attain spessartine-rich compositions (e.g. 50–60 mol %), probably owing to high Mn/(Mn + Fe<sup>2+</sup> + Mg) in evolved peraluminous melts. However, no systematic differences in composition between Archean and Proterozoic samples are observed in the existing data. Garnet in SPGs can have a number of origins, including direct crystallization from the granitic melt (Hall & Tyler, 1965; Joyce, 1973; Green, 1977), derivation from restitic material (White & Chappell, 1977; Stevens *et al.*, 2007; Villaros *et al.*, 2009) or surrounding host rock (Allan & Clarke, 1981), or reaction between early formed phases and silicate melt (e.g. liquid + biotite → garnet + muscovite; Miller & Stoddard, 1981). Combined careful textural, petrographic, and geochemical studies are required to determine the origin for garnet in SPGs, which are currently lacking for SPGs from the Archean and Paleo- to Mesoproterozoic. Therefore, at this time using garnet compositions to understand either the crystallization conditions or the characteristics of the source rocks of these granites is difficult, but would provide a fruitful avenue for future study.

### Other peraluminous indicator minerals and accessory phases

Other peraluminous indicator minerals present in both Archean and Proterozoic SPGs include cordierite, tourmaline, sillimanite, and beryl. Cordierite is found in less evolved granites (e.g. parts of the Ghost Lake batholith, the Treelined Lake complex, the Talston Magmatic Zone, and the Liangcheng granites) (Breaks & Moore, 1992; Pan & Breaks, 1997; De *et al.*, 2000; Wang *et al.*, 2018). In contrast, tourmaline is a phase dominantly found coexisting with muscovite and garnet in more evolved SPGs and only rarely with biotite (Fig. 4c; Breaks & Moore, 1992; Nabelek *et al.*, 1992a). The water content of the melt is probably the determining factor controlling whether tourmaline or biotite crystallizes from a B-bearing strongly peraluminous melt. For example, Scaillet *et al.* (1991) found that in a strongly peraluminous granitic melt biotite is the stable liquidus phase at high water activities (when the mole fraction of water in the coexisting vapor phase is <0.7), whereas tourmaline is stable only at lower water activities. Elevated Ti contents in strongly peraluminous melts may also stabilize biotite over tourmaline (Nabelek, 2019). No systematic differences in either abundances or compositions of these phases are observed between Archean and Proterozoic SPGs based on existing, albeit limited data.

Dominant accessory phases in the SPGs include (fluor-)apatite, monazite, thorite, zircon, titanite, allanite, spinel, uraninite, graphite, ilmenite, magnetite, and rutile. Notably, Archean SPGs predominantly contain ilmenite as the sole stable Fe–Ti oxide [although

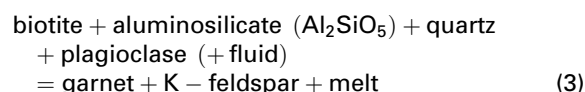
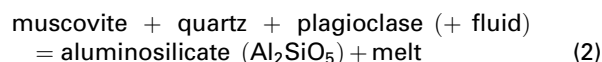
magnetite has been described in granites from the Yilgarn and Kaapvaal craton (Trumbull, 1993; Qui, 1997)], whereas magnetite is found in a number of the Proterozoic SPGs (e.g. Cree Lake granites, Mesoproterozoic granites of the southwestern USA, the Helanshan complex, and SPGs of the Transamazonian Orogeny). The presence of magnetite in these granites indicates that they crystallized at sufficiently elevated  $f_{O_2}$  for magnetite to be a stable crystallizing phase (e.g. Ishihara, 1977). As discussed in the section on biotite chemistry, this transition in  $f_{O_2}$  values of crystallization may reflect a shift in the bulk redox state of the sedimentary source rocks across the GOE.

## WHOLE-ROCK MAJOR AND TRACE ELEMENT CHEMISTRY

Whole-rock major and trace element chemistry for SPGs can be difficult to interpret in the framework of melt compositions because of the potential for restitic material to be entrained in the granitic melt during extraction from the source (White & Chappell, 1977; Chappell *et al.*, 1987; Stevens *et al.*, 2007). [However, see Wall *et al.* (1987) and Clemens (1989) for points raised against the restite model.] In addition, melt compositions, and in particular some trace element concentrations, are highly sensitive to the degree of melting, the source rock composition, and the presence and abundance of accessory minerals in the restite. With these caveats in mind, we present an analysis of the whole-rock chemistry of both Archean and Proterozoic SPGs, both compiled from the existing literature and newly acquired data. A complete dataset with references is available in [Supplementary Data Table S1](#); [supplementary data](#) are available for downloading at <http://www.petrology.oxfordjournals.org>. Newly acquired major and trace element whole-rock chemistry for 50 samples from the St Vrain and Silver plume granites (Colorado, USA), Mt Owen batholith (Wyoming, USA), and the Superior Craton was obtained via X-ray fluorescence (XRF) at Caltech ( $n=47$ ) and Washington State University ( $n=3$ ). Sample information (i.e. locality, lithology, sampling GPS coordinates) for the newly acquired data is provided in [Supplementary Data Table S2](#). Whole-rock sample preparation and analytical methods are described in the [Supplementary Data](#). From an initially larger dataset including all available whole-rock data from the localities listed in [Table 1](#), we culled the samples to include only whole-rock compositions normalized to 100% on an anhydrous basis that contained 68–80 wt %  $SiO_2$  and <5 wt %  $FeO + MgO + TiO_2$ , and had  $ASI > 1.1$ ; 586 Archean and 255 Proterozoic whole-rock analyses of SPGs are considered.

To frame our discussion, a brief overview of partial melting of metasedimentary rocks is merited. We direct the reader to more detailed discussions in the literature, as a wealth of work has been done on this subject, through both experimental studies (Le Breton &

Thompson, 1988; Vielzeuf & Holloway, 1988; Patiño Douce & Johnston, 1991; Icenhower & London, 1995; Vielzeuf & Montel, 1994; Montel & Vielzeuf, 1997; Stevens *et al.*, 1997; Patiño Douce & Harris, 1998; Pickering & Johnston, 1998) and detailed geochemical modeling (e.g. Clemens & Vielzeuf, 1987; Harris *et al.*, 1993, 1995; Sylvester, 1998; Spear *et al.*, 1999; Nabelek, 2019). A critical factor controlling the amount of melt produced during the partial melting of metasedimentary rocks is the presence or absence of excess fluid (see Clemens & Vielzeuf, 1987, for a detailed discussion). In both the presence and absence of excess fluid, the primary melting reactions that occur involve the breakdown of either muscovite or biotite:



In [equations \(2\) and \(3\)](#), if excess fluid is present (indicated by ‘+ fluid’ in parentheses), the reactions proceed until one of the phases on the left-hand side of the reaction is exhausted. When fluid is absent, sometimes referred to as dehydration melting, the amount of either muscovite [[equation \(2\)](#)] or biotite [[equation \(3\)](#)] in the source controls the amount of melt produced. Quantitative modeling of these reactions to determine trace element concentrations in the derivative melts will strongly rest upon assumptions concerning equilibrium between the melt and solid phases and the choice of partition coefficients used (e.g. Harris *et al.*, 1993). For trace elements that reside predominantly in major phases (e.g. Rb, Sr, and Ba in micas and feldspars), it is reasonable to infer that trace element modeling of biotite- and muscovite-breakdown reactions [[equations \(2\) and \(3\)](#)] will generally capture the range of compositions produced in nature. Other trace elements that predominantly reside in accessory phases (e.g. REE, Zr, Th, and Nb) are dominantly controlled by dissolution of these minor phases, which in turn are dependent on the solubility of the phases in various melt compositions and, potentially, incomplete separation between the melt and restitic minerals (e.g. Barbero *et al.*, 1995; Ayres & Harris, 1997; Zeng *et al.*, 2005a, 2005b). Trace element modeling based on the reactions in [equations \(2\) and \(3\)](#), therefore, is restricted to Rb, Sr, and Ba. (Zr, however, can potentially yield information on maximum temperatures of melting through zircon saturation temperature modeling as discussed in more detail below.)

Archean and Proterozoic SPGs are relatively similar in terms of most major element concentrations, because as a whole they represent near minimum melts in the peraluminous haplogranite system. Most (>90%) of the analyses fall within the following compositional brackets: 13.5–17.0 wt %  $Al_2O_3$ , <0.4 wt %  $TiO_2$ , 0.3–2.5 wt % CaO, and 3–7 wt %  $Na_2O$ .  $K_2O$  contents are

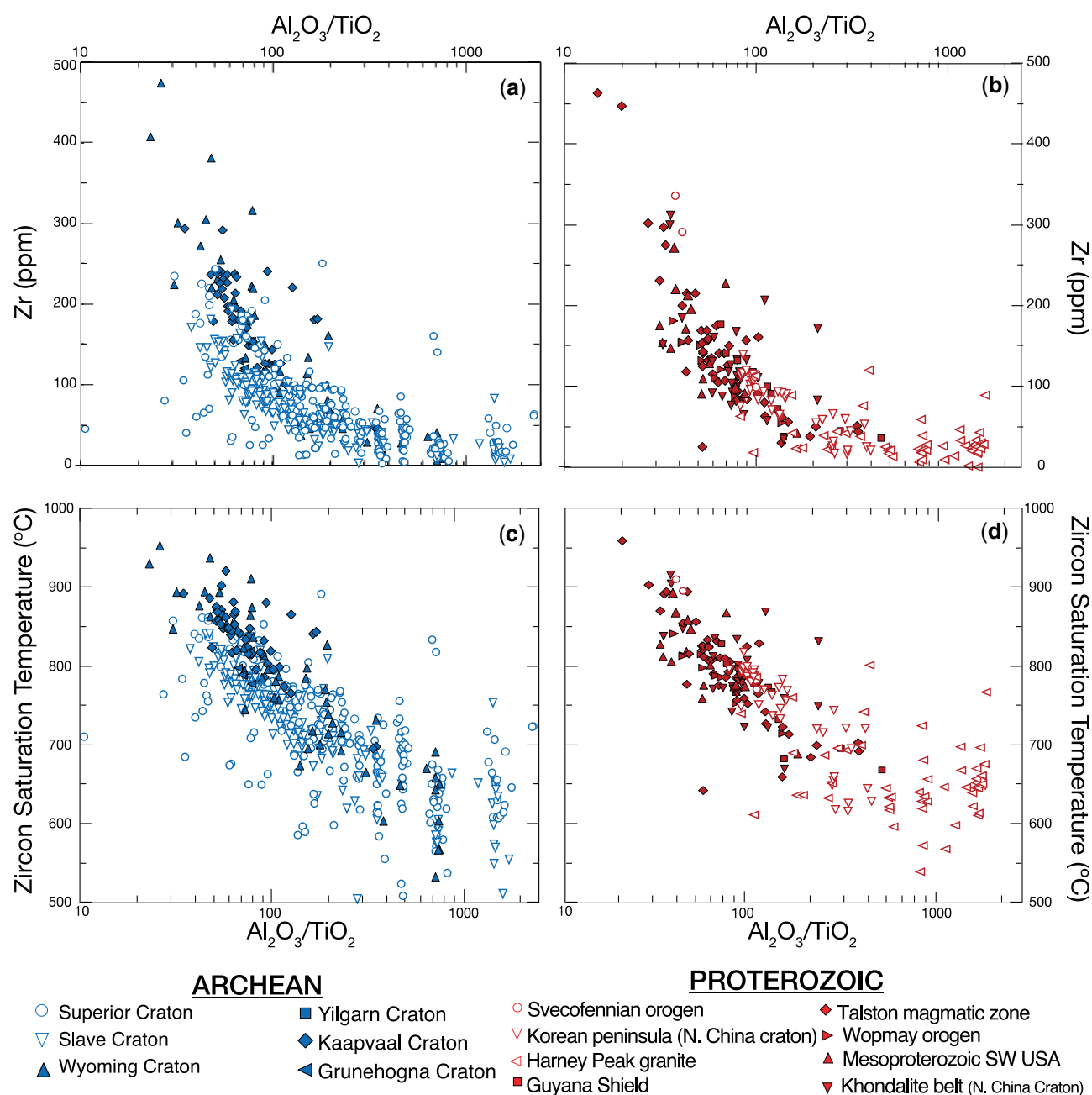


**Fig. 6.** Summary of whole-rock geochemistry indicative of temperature of melting. Zr (a, b) and zircon saturation temperature (c, d) for Archean (a, c) and Proterozoic (b, d) SPGs versus whole-rock  $\text{Al}_2\text{O}_3/\text{TiO}_2$ . Zircon saturation temperature is calculated using distribution coefficient of Zr between zircon and melt as parameterized by [Boehnke et al. \(2013\)](#). Filled symbols are used for localities that generally plot at higher Zr contents and zircon saturation temperatures, and lower  $\text{Al}_2\text{O}_3/\text{TiO}_2$  ratios.

more variable, between 1 and 8 wt %. According to the granite classification of [Frost et al. \(2001\)](#), the SPGs considered here span a range of compositions from magnesian to ferroan and calcic to alkalic. The only consistent compositional features (as defined by the compositional constraints imposed on the compilation) are that they are strongly peraluminous and have high  $\text{SiO}_2$  contents (70–80 wt %). Although there is variability between localities in both Archean and Proterozoic SPGs, their major and trace element concentrations are similar to those observed in Phanerozoic SPGs (see

[Sylvester, 1998; Nabelek, 2019](#)). However, several major and trace element characteristics of Archean and Proterozoic samples indicative of temperature of melting and source lithology merit discussion.

#### $\text{Al}_2\text{O}_3/\text{TiO}_2$ and Zr—melting temperatures

In an analysis of experimental studies on partial melting of sediments, [Sylvester \(1998\)](#) found that  $\text{Al}_2\text{O}_3/\text{TiO}_2$  values in the partial melts are primarily controlled by the temperature of melting. Whereas  $\text{Al}_2\text{O}_3$  contents remain relatively constant in partial melts owing to the



stability of refractory aluminous phases (e.g. plagioclase, garnet, aluminosilicates) in the restite,  $\text{TiO}_2$  contents will increase with increasing temperatures owing to the breakdown of Ti-bearing phases such as biotite and ilmenite. If whole-rock SPG compositions are considered pure partial melts (i.e. they have not experienced mixing with another melt, assimilation, or fractional crystallization) their whole-rock  $\text{Al}_2\text{O}_3/\text{TiO}_2$  should reflect the temperature of melt generation. If this assumption is valid, SPGs produced as a result of partial melting at higher temperatures will have lower  $\text{Al}_2\text{O}_3/\text{TiO}_2$  on average than those produced at lower temperatures. Similarly, Zr concentrations and calculated zircon saturation temperatures have also been used as an indicator of magmatic temperature for silicic magmas (e.g. Watson & Harrison, 1983; Miller *et al.*, 2003; Boehnke *et al.*, 2013). Zr solubility in magmas is primarily a function of magmatic composition and temperature, with higher concentrations of Zr capable of being dissolved in melts at higher  $(\text{Na} + \text{K} + 2\text{Ca})/(\text{Al} \times \text{Si})$  ratios and higher temperatures (Watson & Harrison, 1983; Boehnke *et al.*, 2013). If a rock is saturated in zircon, calculated zircon saturation temperatures using whole-rock Zr contents provide a maximum magmatic temperature estimate (Miller *et al.*, 2003).

These two geochemical variables (whole-rock  $\text{Al}_2\text{O}_3/\text{TiO}_2$  ratios and calculated zircon saturation temperatures) portray a consistent story concerning magmatic temperatures in SPGs. Both whole-rock Zr concentrations and zircon saturation temperatures covary with whole-rock  $\text{Al}_2\text{O}_3/\text{TiO}_2$  ratios (Fig. 6). That is, Archean and Proterozoic SPGs with low  $\text{Al}_2\text{O}_3/\text{TiO}_2$  ratios ( $<100$ ) have higher Zr contents (generally  $>100$  ppm) and Zr saturation temperatures (average  $807 \pm 105^\circ\text{C}$ ,  $2\sigma$ ), whereas SPGs with  $\text{Al}_2\text{O}_3/\text{TiO}_2$  ratios  $>100$  have lower Zr contents (generally  $<100$  ppm) and Zr saturation temperatures ( $688 \pm 145^\circ\text{C}$ ,  $2\sigma$ ) (Fig. 6). Whether these temperatures reflect the primary temperatures of partial melting versus secondary temperatures during cooling (and fractional crystallization of biotite and zircon) is unclear (see Finger & Schiller, 2012). However, SPGs with high Zr saturation temperatures and low  $\text{Al}_2\text{O}_3/\text{TiO}_2$  ratios certainly obtained elevated temperatures and were probably derived through relatively high-temperature melting above the biotite-dehydration curve ( $>800^\circ\text{C}$ ). In contrast, SPGs with low Zr concentrations and zircon saturation temperatures and high  $\text{Al}_2\text{O}_3/\text{TiO}_2$  whole-rock ratios may have formed under conditions of relatively cool, muscovite-dehydration melting (which occurs between  $650$  and  $725^\circ\text{C}$  at  $0.4$ – $1.0$  GPa). These 'cooler' peraluminous granitic melts would have been saturated in zircon in the source (along with potentially other refractory restitic trace phases such as monazite or apatite).

Sylvester (1998) compared whole-rock  $\text{Al}_2\text{O}_3/\text{TiO}_2$  ratios in SPGs from different Phanerozoic orogens with known metamorphic histories to test the idea that 'low-temperature' versus 'high-temperature' orogens would preserve SPGs with different whole-rock compositions

indicative of temperature of melting. His observations suggested that a distinction may be made between SPGs from (1) 'low-temperature, high-pressure' collisions [e.g. the Alps and Himalayas, where small- to moderate-volume 'cool', post-collisional SPGs formed by decompression melting of over-thickened crust ( $>50$  km thick) heated by *in situ* decay of radiogenic elements] and (2) high-temperature collisions (e.g. the Hercynides or the Lachlan fold belt) in which large-volume, 'hot' post-collisional SPGs formed by mantle-derived heating of crust  $\leq 50$  km thick after lithospheric delamination. Indeed, Sylvester (1998) found that Phanerozoic SPGs from 'low-' and 'high-temperature' collisions tended to have high and low  $\text{Al}_2\text{O}_3/\text{TiO}_2$  ratios, respectively. Archean and Proterozoic SPGs span the range in  $\text{Al}_2\text{O}_3/\text{TiO}_2$  values observed by Sylvester (1998) for Phanerozoic SPGs (20–500), although some samples in both temporal groups extend to higher  $\text{Al}_2\text{O}_3/\text{TiO}_2$  values (up to 2000; Fig. 6). [It should be noted that the samples with the highest  $\text{Al}_2\text{O}_3/\text{TiO}_2$  values are primarily due to low  $\text{TiO}_2$  concentrations with limited reported significant digits (e.g. 0.01 and 0.02 wt %), giving rise to near-vertical trends in Zr or zircon saturation temperature versus  $\text{Al}_2\text{O}_3/\text{TiO}_2$ .]

For Archean SPGs, those from the Yilgarn, Kaapvaal, and Grunehogna Cratons (filled blue symbols) define a more tightly clustered range of values at lower  $\text{Al}_2\text{O}_3/\text{TiO}_2$  and higher Zr concentrations and zircon saturation temperatures than those from the Superior, Slave, and Wyoming cratons (open symbols), which display more variable values extending to lower Zr contents and higher  $\text{Al}_2\text{O}_3/\text{TiO}_2$  values (Fig. 6a and c). This geographical distinction is notable, as it suggests that the SPGs from the Yilgarn, Kaapvaal, and Grunehogna Cratons were derived predominantly through higher temperatures of melting ( $>800^\circ\text{C}$ ). In contrast, SPGs from the Superior, Slave, and Wyoming cratons appear to have formed through cooler melting conditions ( $<750^\circ\text{C}$ ). In the Proterozoic SPGs, the Harney Peak granite of the Trans-Hudson Orogeny (open left-pointing triangles) defines the high  $\text{Al}_2\text{O}_3/\text{TiO}_2$  and low zircon saturation temperature end of the distribution of samples in our dataset (Fig. 6b and d), suggesting derivation at relatively low temperatures of melting. In contrast, the Proterozoic SPGs from the SW USA, the Talston magmatic zone, Guyana Shield, and Khondalite belt of north China (filled red symbols) define the low  $\text{Al}_2\text{O}_3/\text{TiO}_2$  end of the data array, suggestive of partial melting at higher temperatures. Although specific localities cluster towards high or low  $\text{Al}_2\text{O}_3/\text{TiO}_2$  values, these variations occur in both Archean and Proterozoic SPGs. As such, this suggests that variations in temperatures of sediment melting and likely tectonic mechanisms of producing melting (e.g. burial during a collisional orogeny, mafic underplating, ridge subduction, etc.) were locality specific and tectonically viable from the Mesoproterozoic ( $\sim 3.0$  Ga) into the Paleoproterozoic.



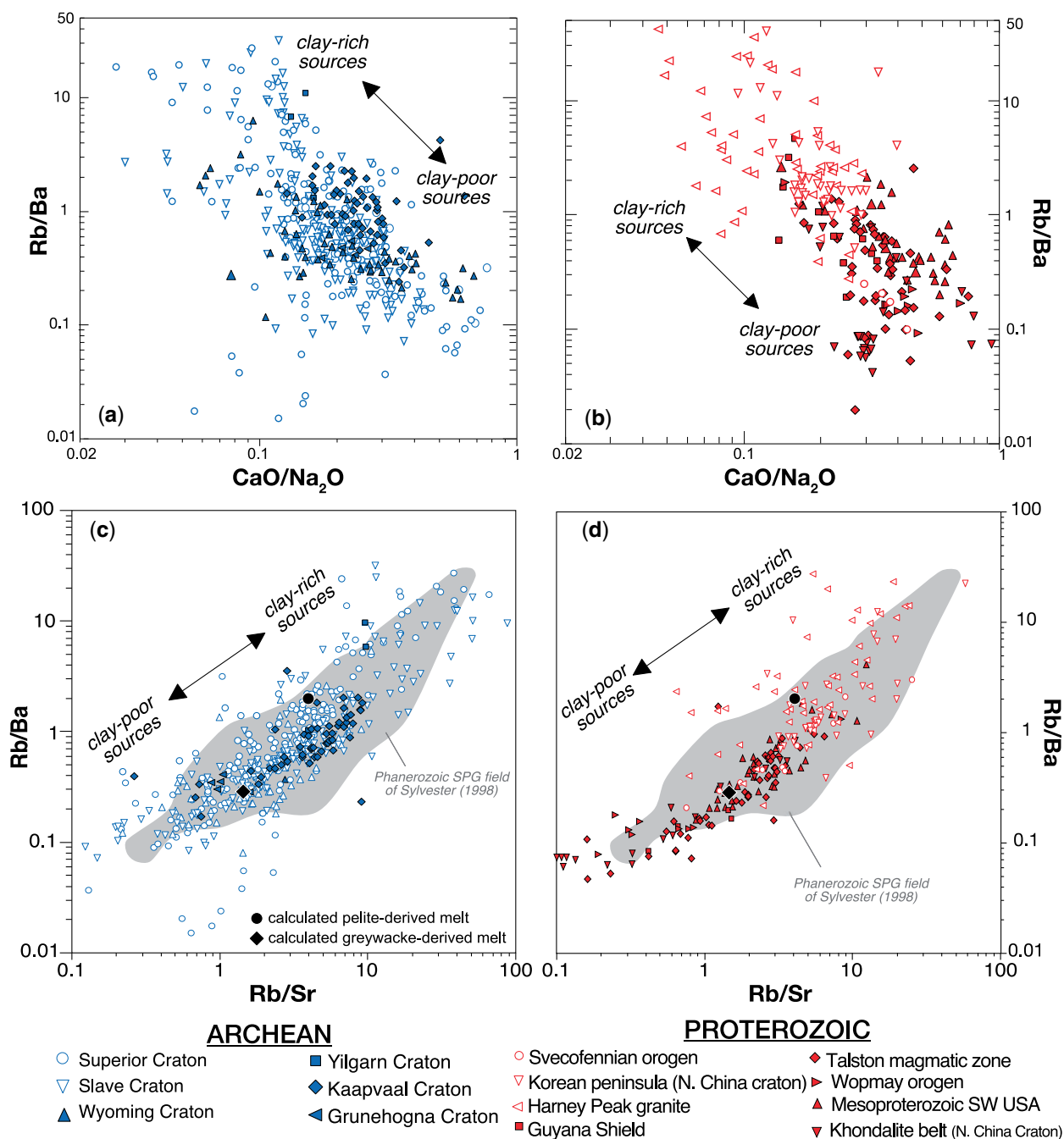


**Fig. 7.** Summary of bulk-rock geochemistry indicative of source rock lithology. Rb/Ba versus CaO/Na<sub>2</sub>O (a, b) and Rb/Sr (c, d) for Archean (a, c) and Proterozoic (b, d) SPGs. Symbols as in Fig. 5. In (c) and (d), calculated pelite- and greywacke-derived melts are from Sylvester (1998).

### CaO/Na<sub>2</sub>O, Rb/Sr, and Rb/Ba—source lithologies

In his analysis of partial melting experiments on metasedimentary rocks and SPG whole-rock compositions, Sylvester (1998) also demonstrated that CaO/Na<sub>2</sub>O, Rb/Sr, and Rb/Ba whole-rock values of SPGs could be used to understand variation in source lithologies. SPGs produced through partial melting of plagioclase-rich, clay-poor sources (greywackes) will have higher CaO/Na<sub>2</sub>O ratios than those produced through partial melting of clay-rich pelites owing to the contribution of CaO to the

melt from plagioclase (Patiño Douce & Johnston, 1991; Patiño Douce & Beard, 1995). Extent of melting, pressure, and H<sub>2</sub>O activity will also affect these ratios; however, the abundance of plagioclase in the source lithology is the strongest control (Sylvester, 1998). The systematics of Rb/Sr and Rb/Ba ratios of SPG whole-rock compositions are slightly more complicated. Comprehensive partial melting modeling of various source materials suggest that two primary factors control Rb/Sr and Rb/Ba ratios (Harris & Inger, 1992; Harris

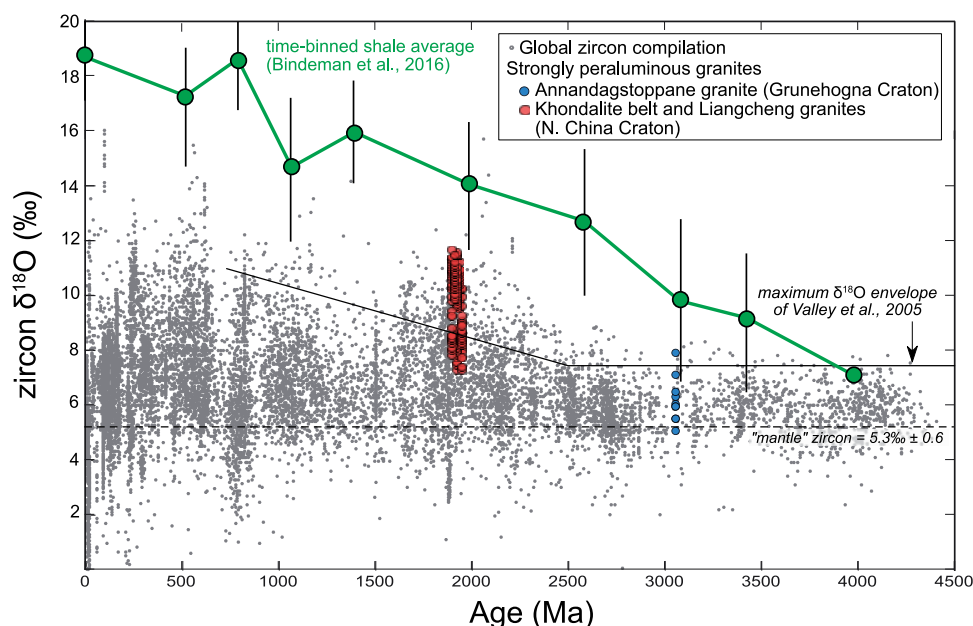


**Fig. 8.** Zircon and shale  $\delta^{18}\text{O}$  (‰) values with age (Ma). Global zircon compilation (grey dots) is from [Spencer et al. \(2017\)](#) and includes both detrital zircons and zircons separated from igneous rocks. Time binned averages of shale compositions are from [Bindeman et al. \(2016\)](#) with  $1\sigma_{\text{SD}}$  errors on average. Data for the Archean Annandagstoppane granite (blue dots) are from [Marshall et al. \(2010\)](#), and for the Proterozoic granites from the Khondalite belt and Liangcheng granites of the North China Craton are from [Dan et al. \(2014\)](#) and [Wang et al. \(2017, 2018\)](#).

[et al., 1993](#)). First, vapor-absent melting produces higher Rb/Sr and Ba/Sr ratios in the partial melt owing to lower melt fractions and the presence of significant feldspar (both plagioclase and K-feldspar) in the restite, which will retain Sr. Second, muscovite- or biotite-rich, plagioclase-poor rocks (i.e. metapelites) will yield higher Rb/Sr and Rb/Ba ratios than plagioclase-rich, mica-poor sediments (i.e. greywackes) owing to higher Rb concentrations in the source rocks ([Harris et al., 1993](#); [Sylvester 1998](#)). [Sylvester \(1998\)](#) pointed out that the Rb/Sr and Rb/Ba ratios of Phanerozoic SPGs generally fall on a log-linear array of increasing Rb/Sr with Rb/Ba. In addition, he noted that SPGs with low  $\text{CaO}/\text{Na}_2\text{O}$  ratios generally have higher Rb/Sr and Rb/Ba ratios than do those with high  $\text{CaO}/\text{Na}_2\text{O}$  ratios, although there is some overlap. As such, [Sylvester \(1998\)](#) suggested that Rb/Sr and Rb/Ba ratios in SPGs are dominantly controlled by the characteristics of the source rock, with higher Rb/Sr and Rb/Ba ratios reflecting clay-rich sources.

In Archean and Proterozoic SPGs, whole-rock  $\text{CaO}/\text{Na}_2\text{O}$  is negatively correlated with both Rb/Sr and Rb/Ba ([Fig. 7a](#) and [b](#)). In addition, whole-rock compositions of Archean and Proterozoic SPGs define a similar, positively correlated trend of Rb/Sr and Rb/Ba to the Phanerozoic SPG compilation presented by [Sylvester \(1998\)](#) ([Fig. 7c](#) and [d](#)). Localities with lower  $\text{CaO}/\text{Na}_2\text{O}$  values tend to have higher Rb/Sr and Rb/Ba ratios and vice versa, suggesting derivation from clay-rich and clay-poor source regions, respectively. For example, for the Proterozoic SPGs, the Harney Peak granite of the Trans-Hudson Orogeny (open left-pointing triangles) defines the low  $\text{CaO}/\text{Na}_2\text{O}$  and high Rb/Sr and Rb/Ba end of the

distribution of samples in our dataset ([Fig. 7b](#) and [d](#)), suggesting derivation from clay-rich sources. In contrast, the Proterozoic SPGs from the SW USA, the Talston magmatic zone, Guyana Shield, and Khondalite belt of north China (filled red symbols) define the high- $\text{CaO}/\text{Na}_2\text{O}$  and low Rb/Sr and Rb/Ba of the data array ([Fig. 7b](#) and [d](#)), suggestive of partial melting of greywacke-rich (i.e. clay-poor) source rocks. SPGs from other localities appear to have formed through melting of both plagioclase- and clay-rich source rocks, such as those from the Superior, Slave, and Wyoming cratons.

No systematic difference in the ranges or distributions of  $\text{CaO}/\text{Na}_2\text{O}$ , Rb/Sr, or Rb/Ba values is observed between Archean and Proterozoic SPG populations as a whole, suggesting that clay-rich and clay-poor sediments were present in the source rocks of both Archean and Proterozoic SPGs. Therefore, on a broad scale the sedimentary source regions for SPGs may have been similar in terms of maturity (i.e. clay component) across the Archean–Proterozoic transition. However, we recognize that this suggestion is based upon a relatively limited dataset of both Archean and Proterozoic SPGs ([Fig. 7](#)). A larger compilation of Archean and Proterozoic SPG whole-rock chemistry from more localities, in addition to quantitative trace element modeling of partial melting of specific representative source rocks, would be useful to explore this idea in greater detail.

## STABLE ISOTOPES

Given the existing petrological and geochemical data indicating an origin through partial melting of

metasedimentary rocks, Archean and Proterozoic SPGs should preserve stable (e.g. oxygen) and radiogenic isotope signatures suggesting derivation from weathered, continental material (e.g. elevated  $^{18}\text{O}/^{16}\text{O}$  ratios and initial  $^{87}\text{Sr}/^{86}\text{Sr}$  ratios). The available oxygen isotope data for the SPGs, however limited, clearly demonstrate this, as explained in detail below. We do not discuss the radiogenic isotope compositions of the SPGs because of the difficulties involved in their interpretation. Melts derived through the partial melting of metasedimentary rocks have complicated trace element and radiogenic isotope signatures owing (in part) to the disequilibrium nature of crustal anatexis at relatively low temperatures (e.g. Watson & Harrison, 1983; Hammouda *et al.*, 1996; Patiño Douce & Harris, 1998; Knesel & Davidson, 2002; Zeng *et al.*, 2005a, 2005b). As a result of incomplete dissolution of accessory phases (e.g. apatite, monazite, or zircon), some trace elements (e.g. Pb and REE) and radiogenic isotope characteristics (e.g. those of Nd, Pb, and Hf) of anatectic melts are not representative of their source rock, but rather the degree to which the accessory phases have participated in the partial melting process (Hogan & Sinha, 1991; Nabelek & Glascock, 1995; Zeng *et al.*, 2005a, 2005b; Farina *et al.*, 2014; Tang *et al.*, 2014). Therefore, the radiogenic isotope signatures of SPGs are controlled by two factors, which are difficult to untangle: (1) the age of the crust from which the sedimentary material was derived and subsequently melted (which is highly dependent on location and geological history); (2) disequilibrium melting during partial melting of refractory mineral phases. Therefore, we focus here on a review of existing oxygen isotope data, as other stable isotopes have not been measured in the SPGs to so great an extent as to merit a comparison between Archean and Proterozoic samples [although see Nabelek *et al.* (1992b) for H isotopes of the Harney Peak granite].

## Oxygen isotopes

### Background

Studies of oxygen isotopes in igneous and detrital zircon demonstrate that zircon  $\delta^{18}\text{O}$  values in the Archean are mostly between 5 and 7‰, suggesting crystallization from dominantly mantle-derived melts, whereas zircon  $\delta^{18}\text{O}$  shifts abruptly in the Proterozoic to higher and more variable values (up to 10‰) (Valley, 2003; Valley *et al.*, 2005; Spencer *et al.*, 2014, 2017; Payne *et al.*, 2015; Fig. 8). Possible causes for the shift in  $\delta^{18}\text{O}_{\text{zircon}}$  values may be related to several, non-mutually exclusive factors (see discussion by Valley *et al.*, 2005) including the following: (1) the onset or acceleration of subduction at the end of the Archean, which would enhance the recycling of sediments into the source regions of magmas; (2) the quantity and composition of sediments available for recycling owing to the emergence of a subaerial, evolved crust in the Proterozoic (Spencer *et al.*, 2014); (3) differences in weathering across the GOE, giving rise to higher- $\delta^{18}\text{O}$

Proterozoic sediments that were ultimately assimilated into magmas (Bindeman *et al.*, 2016; Spencer *et al.*, 2019). Support for the latter two causes comes from what is known about the ancient sedimentary record. Archean sediments are characterized by immature, subaqueous volcanoclastic material and shales with low  $\delta^{18}\text{O}$  values (Ronov, 1964; Longstaffe & Schwarcz, 1977; Shieh & Schwarcz, 1978; Lowe, 1994; Veizer & Mackenzie, 2003; Bindeman *et al.*, 2016; Fig. 8). In contrast, Proterozoic sedimentary sequences mark the onset of subaerial weathering, characterized by high- $\delta^{18}\text{O}$ , mature sediments such as clays, and chemical sediments (e.g. carbonates and evaporates) (Ronov, 1964; Grotzinger & James, 2000; Veizer & Mackenzie, 2003; Campbell & Davies, 2017). In addition, the rise of atmospheric oxygen diversified the number of clay minerals (e.g.  $\text{Fe}^{3+}$ -bearing smectites) through oxidative weathering of subaerial continental crust (Hazen *et al.*, 2013).

Testing whether the secular change in  $\delta^{18}\text{O}_{\text{zircon}}$  values was primarily due to a change in sediment composition or volume or in tectonic regime is difficult using zircon from a broadly sampled igneous record. First, igneous rocks often have a complicated origin and may have both mantle and crustal source components. Second, detrital zircons (which are the primary dataset for more recent studies demonstrating a secular trend in  $\delta^{18}\text{O}_{\text{zircon}}$  values) have no petrological context to understand their origin (see Spencer *et al.*, 2019). As SPGs are derived entirely from the partial melting of metasedimentary rocks, they therefore should preserve a pure sedimentary signal in their oxygen isotope values. If a stepwise change is observed, this suggests that the increase in  $\delta^{18}\text{O}$  values of igneous zircon at c. 2.3–2.4 Ga was due, at least in part, to the increasing  $\delta^{18}\text{O}$  of sediments. On the other hand, if there is no shift across the Archean–Proterozoic transition in the  $\delta^{18}\text{O}$  values of the SPGs, then sedimentary rocks must have been incorporated into magmas in more abundant amounts via enhanced crustal recycling (through the formation of larger volumes of sediments or enhanced subduction). In addition, mineral  $\delta^{18}\text{O}$  values of SPGs are a complementary, and in some cases, more robust record than the sedimentary archive as the  $\delta^{18}\text{O}$  values of some minerals (such as zircon) are more resistant to subsequent alteration than whole-rock values (Valley, 2003). Although diagenesis and metamorphism (prerequisites prior to partial melting) certainly will affect the  $\delta^{18}\text{O}$  values of the source rocks for the SPGs, SPGs should still faithfully record relative variations in sedimentary  $\delta^{18}\text{O}$  values as these processes should affect the  $\delta^{18}\text{O}$  values of Archean and Proterozoic sedimentary rocks equally.

### Oxygen isotopes in Archean and Proterozoic SPGs

Archean SPGs with previously measured  $\delta^{18}\text{O}$  values (of both whole-rocks and minerals) include the

**Table 3:** Archean and Proterozoic SPG oxygen isotope literature data summary

Locality	WR/min*	Range (‰)†	Av. (‰)†	1σ (‰)	n	References	Notes
<b>Archean</b>							
<i>Superior Craton</i>							
[1] Preissac–Lacorne batholith	WR	7.8–8.6	8.2	0.6	7	Feng <i>et al.</i> , 1993	
	qtz	8.3–10.1	9.4	0.7	7	Feng <i>et al.</i> , 1993	
	ksp	6.4–9.1	7.4	1.1	7	Feng <i>et al.</i> , 1993	
	grt	4.3–6.5	5.4	0.7	7	Feng <i>et al.</i> , 1993	
	ms	5.5–6.4	6.0	0.3	6	Feng <i>et al.</i> , 1993	
	bt	1.7–3.4	2.7	0.6	5	Feng <i>et al.</i> , 1993	
	WR	8.1–9.8	8.6	0.3	9	Mulja <i>et al.</i> , 1995b	
[9] Treelined Lake complex	WR	9.0–11.6	10.0	0.9	8	Pan & Breaks, 1997	
[9] Separation Rapid pluton	WR	9.2–11.8	10.3	0.9	6	Pan & Breaks, 1997	
[10] Winnipeg River pegmatite field–per-aluminous leucogranites	WR	8.1–12.4	10.1	1.4	30	Longstaffe <i>et al.</i> , 1981	Data from Eaglenest Lake, Greer Lake, Osis Lake, and Tin Lake intrusions. Whole-rock δ <sup>18</sup> O are homogeneous within individual intrusions, but vary between bodies (e.g. Greer Lake: +8.1 to +8.7‰ v. Osis Lake: +11.1 to +12.4‰)
	qtz	9.8–13.4	11.6	1.4	9	Longstaffe <i>et al.</i> , 1981	
	ksp	7.7–11.4	9.3	1.5	9	Longstaffe <i>et al.</i> , 1981	
	bt	3.3–5.9	4.8	1.2	6	Longstaffe <i>et al.</i> , 1981	
	ms	6.3–9.6	7.6	1.5	7	Longstaffe <i>et al.</i> , 1981	
<i>Slave Craton</i>							
[19] Yellowknife granite–pegmatite field	WR	8.8–11.0	10.3	0.7	12	Meintzer, 1987	
<i>Kaapvaal Craton</i>							
[22] Sinceni pluton	WR	10.0–11.1	10.5	0.37	8	Blamart, 1993	
<i>Grunehogna Craton</i>							
[24] Annandagstoppane granite	zrc†	5.4–7.8	6.2	0.8	9	Marschall <i>et al.</i> , 2010	zircon from 3 granodiorite to granite samples (values only from zircon with crystallization ages; i.e. not inherited)
<b>Proterozoic</b>							
<i>Wopmay Orogen</i>							
[25] Hepburn intrusive suite	WR	8.7–12.1	10.1	0.7	28	Lalonde, 1989	only data from peraluminous granodiorites to granites compiled (whole-rock >65 wt % SiO <sub>2</sub> )
<i>Trans-Hudson Orogen</i>							
[28] Harney Peak granite ('low-δ <sup>18</sup> O' series)	WR	10.4–13.3	11.5	0.6	—	Nabelek <i>et al.</i> , 1992a, 1992b	averages are those reported by Nabelek <i>et al.</i> , 1992b
[28] Harney Peak granite ('high-δ <sup>18</sup> O' series)	WR	10.4–13.3	13.2	0.8	—	Nabelek <i>et al.</i> , 1992a, 1992b	averages are those reported by Nabelek <i>et al.</i> , 1992b
[28] Calamity Peak pluton	WR	12.9–14.3	13.7	0.5	6	Rockhold <i>et al.</i> , 1987	
[26] Arch Lake granite, Talston Magmatic Zone	WR	9.7–10.9	10.4	0.5	6	De <i>et al.</i> , 2000	
[26] Slave granite, Talston Magmatic Zone	WR	9.6–11.8	10.9	0.9	6	De <i>et al.</i> , 2000	
<i>SW USA—Colorado</i>							
[29] Silver Plume & St Vrain granites	WR	10.4–11.6	10.8	0.5	5	Anderson & Morrison, 2005	
<i>SW USA—Arizona</i>							
[30] Ruin, Sierra Estrella, Oracle, Ak-Chin granites	WR	10.2–11.2	10.6	0.4	6	Anderson & Morrison, 2005	
<i>North China Craton</i>							

(continued)



**Table 3:** Continued

Locality	WR/min*	Range (‰)†	Av. (‰)†	1σ (‰)	n	References	Notes
[33] Helanshan complex	zrc‡	7.3–10.6	9.4	1	37	Dan <i>et al.</i> , 2014	zircon data from two different granite samples
[32] Liangcheng granites	zrc‡	9.2–11.6	10.5	0.5	143	Wang <i>et al.</i> , 2018	5 different samples of grt–bt to grt–opx granitoids; only values from zircon with ‘magmatic’ textures included
	zrc‡	7.2–9.1	8.2	0.5	45	Wang <i>et al.</i> , 2017	3 different samples of ‘meta-leucogranites’ (grt-, bt-, and sil-bearing); only values from zircon with ‘magmatic’ textures included

Locality number in brackets is locality number in Table 1.

\*Indicates whether reported values are for whole-rock (WR) or mineral separates. qtz, quartz; ksp, K-feldspar; grt, garnet; ms, muscovite; bt, biotite; zrc, zircon.

†O isotope values are reported in per mil notation relative to the Vienna Standard Mean Ocean Water (VSMOW).

‡Measured *in situ* via secondary ion mass spectrometry.

Annandagstoppane granite of Antarctica (~3.1 Ga; Marschall *et al.*, 2010), the Preissac–Lamotte–Lacorne–Moly Hill granites of Quebec (~2.6 Ga; Feng *et al.*, 1993; Mulja *et al.*, 1995b), the Treelined Lake complex (Pan & Breaks, 1997); the Yellowknife granite–pegmatite field (Prosperous granite, Meintzer, 1987), the Winnipeg River pegmatite field (Longstaffe *et al.*, 1981), and the Sinceni pluton of the Kaapvaal Craton (Blamart, 1993). Paleoproterozoic SPGs with previously measured  $\delta^{18}\text{O}$  values are the Harney Peak granite and satellite intrusions (Walker *et al.*, 1986; Rockhold *et al.*, 1987; Shearer *et al.*, 1987; Nabelek *et al.*, 1992b), the Helanshan Complex (Dan *et al.*, 2014) and Liangcheng granites (Wang *et al.*, 2017, 2018) of the North China Craton, and the Taltson Magmatic Zone of Saskatchewan (De *et al.*, 2000). A summary of oxygen isotope data from the literature is provided in Table 3.

Average whole-rock, zircon, and quartz  $\delta^{18}\text{O}$  values from SPGs all increase from the Archean to the Paleoproterozoic (Fig. 9a–f). Among mineral phases in high-silica rocks, zircon is generally taken as the most reliable recorder of magmatic  $\delta^{18}\text{O}$  values owing to its slow O self-diffusivity and robustness to alteration (Valley, 2003; Bindeman *et al.*, 2018). [Garnet, although considered a phase often resistant to weathering, is not always present in high-silica rocks, with SPGs being a notable exception (King & Valley, 2001).] Zircon  $\delta^{18}\text{O}$  values in Archean SPGs are limited in number and derive solely from the Annandagstoppane granite (Marschall *et al.*, 2010) with a mean value of  $6.1 \pm 1.6\text{‰}$  ( $2\sigma_{\text{SD}}$ ,  $n = 10$ ; Fig. 9c). Available zircon  $\delta^{18}\text{O}$  data for Paleoproterozoic SPGs exist only for the Helanshan Complex (Dan *et al.*, 2014) and the Liangcheng granites (Wang *et al.*, 2017, 2018) of the North China Craton and yield significantly higher average values of  $9.9 \pm 2.2\text{‰}$  ( $2\sigma_{\text{SD}}$ ,  $n = 225$ ) (Fig. 9d). However, as the present zircon  $\delta^{18}\text{O}$  data are limited [from one Archean locality (with 10 analyses) and two Paleoproterozoic localities], we discuss whole-rock and quartz  $\delta^{18}\text{O}$  values as well, even

though these materials are known to be more susceptible to alteration of primary magmatic  $\delta^{18}\text{O}$  values by weathering (for whole-rock samples) or sub-solidus re-equilibration (e.g. for quartz; Giletti & Yund, 1984; Eiler *et al.*, 1992). The averages of all available quartz  $\delta^{18}\text{O}$  values from Archean and Proterozoic SPG localities are  $10.6 \pm 3.2\text{‰}$  ( $2\sigma_{\text{SD}}$ ,  $n = 16$ ) and  $13.4 \pm 2.5\text{‰}$  ( $2\sigma_{\text{SD}}$ ,  $n = 61$ ), respectively, whereas whole-rock  $\delta^{18}\text{O}$  values are  $9.8 \pm 2.5\text{‰}$  and  $11.0 \pm 3.3\text{‰}$  (Fig. 9a, b, e and f; Table 3). The average zircon, quartz, and whole-rock  $\delta^{18}\text{O}$  values from the Archean and Proterozoic are statistically distinguishable with *t*-test *p* values of  $<0.001$ .

Magmatic  $\delta^{18}\text{O}$  values can increase through differentiation and concomitant  $\text{SiO}_2$  enrichment in the melt (Eiler, 2001; Bindeman *et al.*, 2004; Bucholz *et al.*, 2017). However, the difference in whole-rock  $\delta^{18}\text{O}$  values is not simply a function of an increase in whole-rock  $\text{SiO}_2$  contents. Indeed, in the oxygen isotope compilation, the Archean samples skew to higher  $\text{SiO}_2$  contents than the Proterozoic samples while maintaining distinctly lower  $\delta^{18}\text{O}$  values (Fig. 9g). Unfortunately, for most studies included in the compilation, mineral pairs were not measured, rendering implementation of oxygen isotope thermometry impossible. An exception to this is the study of Nabelek *et al.* (1992b) in which the authors comprehensively measured quartz, feldspar, garnet, muscovite, biotite, and tourmaline  $\delta^{18}\text{O}$  values from over 50 samples from the Harney Peak granite and associated pegmatites. Calculated oxygen isotope equilibration temperatures are widely variable (408–848°C, excluding feldspar–quartz pairs, which yielded a lower range of 300–550°C), suggesting that in many samples significant subsolidus re-equilibration of oxygen isotopes in quartz and other minerals occurred. Further such detailed studies involving mineral pair oxygen isotope measurements (e.g. zircon and garnet) will need to be undertaken to verify which values are representative of magmatic  $\delta^{18}\text{O}$  values. Although the SPG data summarized in Figs 8 and 9 come from a

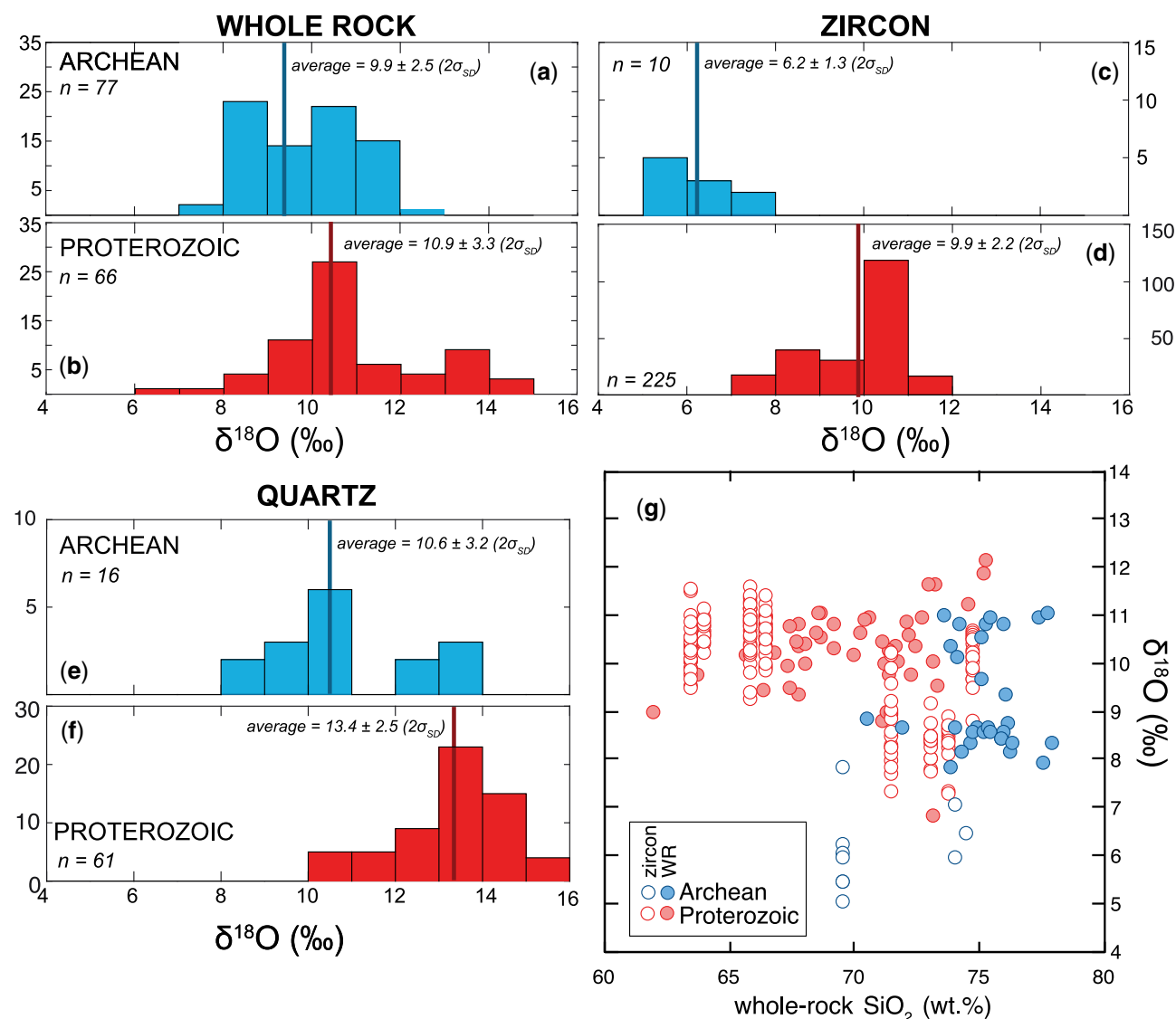


**Fig. 9.** Oxygen isotope ratios [expressed as  $\delta^{18}\text{O}$  (‰)] of Archean and Proterozoic SPGs. Histograms of whole-rock (a, b), zircon (c, d), and quartz (e, f)  $\delta^{18}\text{O}$  values. (g) Whole-rock and zircon  $\delta^{18}\text{O}$  values versus whole-rock  $\text{SiO}_2$  for samples where whole-rock major element analyses were available. Summary of data and data sources are given in Table 3.

relatively small set of data, it is nevertheless important to note that the  $\delta^{18}\text{O}$  data from the Archean to Proterozoic SPGs come from four continents (Antarctica, North America, Europe, Asia) and are consistent between zircon, quartz, and whole-rock values. The shift in  $\delta^{18}\text{O}$  mineral and whole-rock values is consistent with the hypothesis that sedimentary  $\delta^{18}\text{O}$  values underwent a dramatic increase across the Archean–Proterozoic transition, potentially owing to the rise of new styles of weathering of subaerial landmasses in an oxygenated atmosphere.

## PERSPECTIVES

The motivation and premise for this review paper is that SPGs may be able to shed light on how variations

at the surface of the Earth and in sedimentary rock compositions across the Archean–Proterozoic transition may have been imprinted on the igneous rock record. In particular, the Archean–Proterozoic transition coincided with both the rise of subaerial weathering and the Great Oxidation Event, both of which profoundly influenced the chemistry and lithologies of sedimentary rocks. Further, SPGs may provide complementary insight into the evolution of sediments across Earth's history as they can mitigate some of the issues associated with poor preservation of the sedimentary rock record. We briefly summarize our key findings.

1. No systematic variations between Archean and Proterozoic SPGs in terms of mineral assemblages are observed. Because of their strongly peraluminous nature, all are characterized by biotite and/or

muscovite, sometimes with another peraluminous indicator mineral such as garnet, cordierite, or tourmaline. Biotite compositions and the presence of magnetite in some Proterozoic SPGs, however, indicate that Archean SPGs on average crystallized from melts characterized by lower oxygen fugacity values, which may reflect derivation from sedimentary source rocks with more reduced bulk redox states prior to the Great Oxidation Event.

2. Whole-rock chemistry indicators of temperatures of melting and source lithology (e.g. greywackes versus pelites) imply that although specific SPGs localities are characterized by coherent patterns (e.g. high-temperature melting of greywackes), there is no systematic difference between Archean and Proterozoic SPGs as a whole. This in turn suggests that the generation of SPGs on either side of the Great Oxidation Event was not characterized by distinct temperatures of melting or maturity of sedimentary source rocks. These conclusions are based on a relatively limited dataset predominantly defined by SPGs that appear to have been derived from both clay-rich and clay-poor source regions.
3. Although interpretation of radiogenic isotopes in SPGs (e.g. Sr or Nd) is complicated owing to disequilibrium melting of accessory phases such as monazite, the oxygen isotope composition of SPGs should reflect variations in source rock oxygen isotope ratios. Whole-rock, quartz, and zircon  $\delta^{18}\text{O}$  values, although currently limited in number and geographical locality, are on average higher in Proterozoic SPGs as compared with Archean SPGs. This shift in  $\delta^{18}\text{O}$  values is consistent with the hypothesis that sedimentary  $\delta^{18}\text{O}$  values increased across the Archean–Proterozoic transition as a result of the onset of oxidative weathering of subaerial landmasses.

Above, we discussed what is known about Archean and Paleoproterozoic SPG localities in terms of petrology and chemistry. However, there exist large gaps in our knowledge of these rocks and there is abundant future work to be done on them. Below we outline several fruitful areas for research and potential avenues forward.

### Detailed field studies, petrology, and geochronology

In this review, we have attempted to catalog and describe all the localities of Archean and Paleoproterozoic SPGs in the literature. The SPGs from the localities listed in Table 1 have been studied to greater or lesser degrees. For some, a combination of careful field mapping and sampling [e.g. the Ghost Lake batholith (Breaks & Moore, 1992) or the Harney Peak granite (Nabelek, 1999, and references therein)] have allowed for a detailed understanding of their petrogenesis and relationship to broader tectonic events. Many others require more detailed studies to understand their

source rock characteristics and ages, crystallization ages through modern geochronological techniques, and crystallization conditions as inferred from quantitative thermobarometry. Many of the granite localities in Table 1 do not have robust age constraints. For example, many localities from the Superior Craton are only known to be Neoproterozoic in age (e.g. Allison Lake batholith) and others, such as the Silver Plume and St Vrain granites, have ages based on Rb–Sr whole-rock and mineral isochrons (Peterman *et al.*, 1968). Precise and accurate age constraints are required to explore the temporal evolution of isotope systems in these granites. To obtain crystallization ages zircon rims should be analyzed, as SPGs are often characterized by zircon with inherited cores owing to partial dissolution of zircon during partial melting (Miller *et al.*, 2003).

A critical objective of any future studies should be to constrain the depositional age of the sedimentary source material. As constraining crustal residence ages through radiogenic isotope systems is complicated in SPGs, analyzing inherited cores of zircon in the granites will provide provenance and maximum depositional age information, analogous to the detrital zircon technique in sediments (Gehrels, 2014). This will allow correlation of geochemical signals in the SPGs not only with the age of crystallization, but also with the age of source rock deposition and will be particularly important for Proterozoic sediments to screen for SPGs that may have been derived from Archean sediments.

### Mineral chemistry

Detailed studies of individual localities and their mineral chemistry can yield information concerning intensive variables during granite formation. For example, in a study of Archean and Proterozoic SPGs from North America, Buchholz *et al.* (2018) used biotite and whole-rock  $\text{Fe}^{\text{T}}/\text{Mg}$  ratios to demonstrate that on average the Archean SPGs crystallized at higher oxygen fugacity values than the Proterozoic SPGs. They related this shift in  $f_{\text{O}_2}$  values to the more oxidized sedimentary sources of the Proterozoic SPGs owing to deposition under oxidative weathering conditions after the GOE. The protocol developed for constraining the  $f_{\text{O}_2}$  during crystallization for SPGs in that paper could be applied to a wider sample suite from different continents and a wider temporal range. In addition, although based on a limited dataset,  $\text{Fe}^{3+}/\text{Fe}^{\text{T}}$  ratios of biotites in SPGs are generally lower (0.04–0.09) as compared with those of I-type granites (generally  $>0.1$ ) (De Albuquerque, 1973; Ishihara, 1977; Lalonde & Bernard, 1993). Measurement of  $\text{Fe}^{3+}/\text{Fe}^{\text{T}}$  ratios in biotite in Archean and Proterozoic SPGs could be another fruitful way forward, to constrain relative  $f_{\text{O}_2}$  values.

In garnet-bearing SPGs, detailed studies of garnet textures and compositions (e.g. Taylor & Stevens, 2010), as well as garnet–biotite thermometry (e.g. Holdaway, 2000), can yield information on garnet formation mechanisms (e.g. through peritectic reactions)

and crystallization conditions. This information, in turn, will inform how bulk-rock compositions should be interpreted (as melt or a mixture of melt + restite) and SPG formation mechanisms (Stevens *et al.*, 2007).

### Oxygen isotopes

As reviewed above, there is a general paucity of oxygen isotope data on SPGs from the Archean and Proterozoic and, in particular, single mineral oxygen isotope data. Obtaining oxygen isotope ratios for minerals considered relatively robust to subsolidus diffusive oxygen isotope re-equilibration (e.g. zircon and garnet) would inform the long-standing problem concerning secular variation of oxygen isotope ratios in both sedimentary and igneous rocks (see previous section on oxygen isotopes). Obtaining data for mineral pairs from individual samples will be crucial to assess the temperatures at which oxygen isotope equilibrium was achieved and whether the minerals faithfully recording magmatic values (in contrast to sub-solidus conditions).

### Sulfur isotopes

Although our discussion of stable isotopes has concerned only oxygen isotopes, sulfur isotope studies of Archean and Proterozoic SPGs would yield interesting information on several fronts. First, sulfur in the sedimentary record primarily occurs either in its oxidized form as sulfate or its reduced form as sulfide (Canfield, 2001). Sulfate has higher  $^{34}\text{S}/^{32}\text{S}$  ratios as compared with coexisting sulfide at equilibrium (i.e. higher  $\delta^{34}\text{S}$  values). Further, during reduction of sulfate ions by anaerobic bacteria, the remaining sulfate is further enriched in  $^{34}\text{S}$ . The sedimentary sources from which Archean SPGs were derived were probably dominated by sulfide-bearing metasedimentary rocks because of the relatively low  $f_{\text{O}_2}$  values inferred in their genesis (Bucholz *et al.*, 2018). In contrast, Proterozoic SPGs may have been derived from a significantly more oxidized source region, potentially owing to the incorporation of sulfate deposits, which became abundant only in the Proterozoic. If sulfate is the cause of the increase in  $f_{\text{O}_2}$  values of SPGs in the Proterozoic, rocks that preserve evidence for elevated  $f_{\text{O}_2}$  values during crystallization may also have elevated  $\delta^{34}\text{S}$  values. For example, there is some evidence that sulfur isotopes in igneous rocks may mirror the bulk sulfur oxidation state of their source region, with more reduced 'ilmenite-series' granitoids and more oxidized 'magnetite-series' granitoids from Japan and the Sierra Nevada batholith having lower (0 to  $-10\text{‰}$ ) and higher ( $+1$  to  $9\text{‰}$ )  $\delta^{34}\text{S}$  values, respectively (Sasaki & Ishihara, 1979; Ishihara & Sasaki, 1989).

Second, Archean sulfide and (less-abundant) sulfate minerals display mass-independent fractionations (MIF) among the four stable sulfur isotopes, providing evidence for an anoxic atmosphere at that time (e.g. Farquhar *et al.*, 2000; Johnston, 2011; Paris *et al.*, 2014). Examining MIF signatures in sulfur-bearing minerals

has been classically used in the study of Archean sedimentary rocks, but has been extended to igneous rocks through analysis of sulfide inclusions in ocean island basalts (Cabral *et al.*, 2013; Delavault *et al.*, 2016) and diamonds (Farquhar *et al.*, 2002; Thomassot *et al.*, 2009; Smit *et al.*, 2019). For example, small S-MIF ( $<1\text{‰}$ ) have been observed in sulfides from ocean island basalts from Mangaia and Pitcairn and have been interpreted as indicating a deep, long-lived subducted Archean component in their mantle source regions (Cabral *et al.*, 2013; Delavault *et al.*, 2016). However, it is not well understood how sulfur isotopes are transferred to the igneous record, as sulfur isotopes in igneous rocks (and particularly  $^{33}\text{S}$  or  $^{36}\text{S}$ ) are generally not analyzed and have not received much attention. A careful study of Archean SPGs and rocks representative of their metasedimentary source rocks could help shed light on the fundamentals of sulfur isotope transfer from the sedimentary to the igneous rock record.

### Other stable isotopes

Numerous other stable isotope systems in sedimentary rocks have been observed to undergo radical changes across the GOE (e.g. Fe, Rouxel *et al.*, 2005; Mo, Planavsky *et al.*, 2014; Cu, Fru *et al.*, 2016; U, Kendall *et al.*, 2013). These shifts in isotope ratios are hypothesized to have occurred as a result of changing redox conditions during sediment transport and/or deposition. An outstanding question is whether these shifts are also preserved in Archean versus Proterozoic SPGs. Each of these systems will need to be studied in detail to determine how metamorphism and partial melting affected the isotopes of the metasedimentary source rock and ultimately strongly peraluminous magmas derived from such source rocks.

For all these time-variant isotope systems, Archean and Proterozoic SPGs are uniquely situated to offer a complementary archive to the existing sedimentary record. First, SPGs have the unique capability to homogenize large packages of sedimentary rocks, giving an 'average' composition throughout this critical time in Earth history. This helps to eliminate some of the sampling and preservation bias inherent in the sedimentary record. Second, the source rock sediments for SPG formation are often those deposited on continental slopes or in the deep ocean, which represent different lithofacies from the cratonic sequences that are traditionally analyzed in sedimentary studies.

### ACKNOWLEDGEMENTS

During the preparation of this paper conversations about the details of local Archean and Proterozoic geology were conducted with numerous people, including F. Breaks, Y. Pan, P. Weiblen, T. Boerboom, C. Frost, R. Frost, D. Bagdonas, H. Marschall, P. Nabelek, I. Annesley, and L. Anderson. We thank these people for sharing their knowledge of these unique rocks. S. Newall is thanked for assistance with sample



preparation for whole-rock XRF analyses. C. Frost and I. Bindeman provided thoughtful and constructive reviews that improved this paper. We also thank M. Holness for the suggestion to write such a review and her infinite patience while we put this paper together.

## SUPPLEMENTARY DATA

Supplementary data for this paper are available at *Journal of Petrology* online.

## REFERENCES

- Abdel-Rahman, A. F. M. (1994). Nature of biotites from alkaline, calc-alkaline, and peraluminous magmas. *Journal of Petrology* **35**, 525–541.
- Ague, J. J. & Brimhall, G. H. (1988). Regional variations in bulk chemistry, mineralogy, and the compositions of mafic and accessory minerals in the batholiths of California. *Geological Society of America Bulletin* **100**, 891–911.
- Allan, B. D. & Clarke, D. B. (1981). Occurrence and origin of garnets in the South Mountain Batholith, Nova Scotia. *Canadian Mineralogist* **19**, 19–24.
- Almeida, M. E., Macambira, M. J. & Oliveira, E. C. (2007). Geochemistry and zircon geochronology of the I-type high-K calc-alkaline and S-type granitoid rocks from southeastern Roraima, Brazil: Orosirian collisional magmatism evidence (1.97–1.96 Ga) in central portion of Guyana Shield. *Precambrian Research* **155**, 69–97.
- Almeida, M. E., Macambira, M. J. & Valente, S. D. C. (2008). New geological and single-zircon Pb evaporation data from the central Guyana domain, southeastern Roraima, Brazil: tectonic implications for the central region of the Guyana shield. *Journal of South American Earth Sciences* **26**, 318–328.
- Althoff, F., Barbey, P. & Boullier, A. M. (2000). 2.8–3.0 Ga plutonism and deformation in the SE Amazonian craton: the Archaean granitoids of Marajoara (Carajás Mineral Province, Brazil). *Precambrian Research* **104**, 187–206.
- Anderson, J. L. & Bender, E. E. (1989). Nature and origin of Proterozoic A-type granitic magmatism in the southwestern United States of America. *Lithos* **23**, 19–52.
- Anderson, J. L. & Cullers, R. L. (1999). Paleo- and Mesoproterozoic granite plutonism of Colorado and Wyoming. *Rocky Mountain Geology* **34**, 149–164.
- Anderson, J. L. & Morrison, J. (1992). The role of anorogenic granites in the Proterozoic crustal development of North America. In: Condie, K. C. V. (ed.) *Developments in Precambrian Geology, Proterozoic Crustal Evolution*. Amsterdam: Elsevier, **10**, pp. 263–299.
- Anderson, J. L. & Morrison, J. (2005). Ilmenite, magnetite, and peraluminous Mesoproterozoic anorogenic granites of Laurentia and Baltica. *Lithos* **80**, 45–60.
- Anderson, J. L. & Thomas, W. M. (1985). Proterozoic anorogenic two-mica granites: silver plume and St. Vrain batholiths of Colorado. *Geology* **13**, 177–180.
- Annesley, I. R., Madore, C. & Krogh, T. E. (1997). U–Pb geochronology of peraluminous pegmatites from the Wollaston Lake area, northern Saskatchewan. *Geological Association of Canada–Mineralogical Association of Canada, Program with Abstracts* **22**, A-4.
- Annesley, I. R., Madore, C. & Portella, P. (2005). Geology and thermotectonic evolution of the western margin of the Trans-Hudson Orogen: evidence from the eastern sub-Athabasca basement, Saskatchewan. *Canadian Journal of Earth Sciences* **42**, 573–597.
- Ansdell, K. M. (2005). Tectonic evolution of the Manitoba–Saskatchewan segment of the Paleoproterozoic Trans-Hudson orogen, Canada. *Canadian Journal of Earth Sciences* **42**, 741–759.
- Arndt, N. (1999). Why was flood volcanism on submerged continental platforms so common in the Precambrian? *Precambrian Research* **97**, 155–164.
- Arndt, N. T., Coltice, N., Helmstaedt, H. & Gregoire, M. (2009). Origin of Archean subcontinental lithospheric mantle: some petrological constraints. *Lithos* **109**, 61–71.
- Ayres, M. & Harris, N. (1997). REE fractionation and Nd-isotope disequilibrium during crustal anatexis: constraints from Himalayan leucogranites. *Chemical Geology* **139**, 249–269.
- Bagdonas, D. A. (2014). Petrogenesis of the Neoproterozoic Wyoming batholith, Central Wyoming. MSc thesis, University of Wyoming, Laramie, WY.
- Bagdonas, D. A., Frost, C. D. & Fanning, C. M. (2016). The origin of extensive Neoproterozoic high-silica batholiths and the nature of intrusive complements to silicic ignimbrites: insights from the Wyoming batholith, USA. *American Mineralogist* **101**, 1332–1347.
- Baratoux, L., Metelka, V., Naba, S., Jessell, M. W., Grégoire, M. & Ganne, J. (2011). Juvenile Paleoproterozoic crust evolution during the Eburnean orogeny (2.2–2.0 Ga), western Burkina Faso. *Precambrian Research* **191**, 18–45.
- Barbero, L., Villasaca, C., Rogers, G. & Brown, P. E. (1995). Geochemical and isotopic disequilibrium in crustal melting: an insight from the anatectic granitoids from Toledo, Spain. *Journal of Geophysical Research: Solid Earth* **100**, 15745–15765.
- Barbosa, J. S. F. & Sabaté, P. (2004). Archean and Paleoproterozoic crust of the São Francisco craton, Bahia, Brazil: geodynamic features. *Precambrian Research* **133**, 1–27.
- Barker, F. (1979). Trondhjemite: definition, environment and hypotheses of origin. In: Barker, F. (ed.) *Trondhjemites, Dacites and Related Rocks*. Amsterdam: Elsevier, pp. 1–11.
- Barton, J. M., Klemd, R., Allsopp, H. L., Auret, S. H. & Copperthwaite, Y. E. (1987). The geology and geochronology of the Annandagstoppane granite, Western Dronning Maud Land, Antarctica. *Contributions to Mineralogy and Petrology* **97**, 488–496.
- Bayley, R. W., Proctor, P. D. & Condie, K. C. (1973). Geology of the South Pass area, Fremont County, Wyoming. *US Geological Survey, Professional Papers* **793**.
- Bea, F., Fershtater, G. & Corretgé, L. G. (1992). The geochemistry of phosphorus in granite rocks and the effect of aluminum. *Lithos* **29**, 43–56.
- Bekker, A., Karhu, J. A., Eriksson, K. A. & Kaufman, A. J. (2003). Chemostratigraphy of Paleoproterozoic carbonate successions of the Wyoming Craton: tectonic forcing of biogeochemical change? *Precambrian Research* **120**, 279–325.
- Bekker, A., Holland, H. D., Wang, P. L., Rumble, D., III, Stein, H. J., Hannah, J. L., Coetsee, L. L. & Beukes, N. J. (2004). Dating the rise of atmospheric oxygen. *Nature* **427**, 117.
- Bergman, S., Högdahl, K., Nironen, M., Ogenhall, E., Sjöström, H., Lundqvist, L. & Lahtinen, R. (2008). Timing of Palaeoproterozoic intra-orogenic sedimentation in the central Fennoscandian Shield; evidence from detrital zircon in metasandstone. *Precambrian Research* **161**, 231–249.
- Berman, R. G. & Bostock, H. H. (1997). Metamorphism in the northern Taltson magmatic zone. Northwest Territories. *Canadian Mineralogist* **35**, 1069–1091.
- Bindeman, I. N., Ponomareva, V. V., Bailey, J. C. & Valley, J. W. (2004). Volcanic arc of Kamchatka: a province with high- $\delta^{18}\text{O}$  magma sources and large-scale  $^{18}\text{O}/^{16}\text{O}$  depletion of the upper crust. *Geochimica et Cosmochimica Acta* **68**, 841–865.

- Bindeman, I. N., Bekker, A. & Zakharov, D. O. (2016). Oxygen isotope perspective on crustal evolution on early Earth: A record of Precambrian shales with emphasis on Paleoproterozoic glaciations and Great Oxygenation Event. *Earth and Planetary Science Letters* **437**, 101–113.
- Bindeman, I., Schmitt, A., Lundstrom, C. & Hervig, R. (2018). Stability of zircon and its isotopic ratios in high-temperature fluids: long-term (4 months) isotope exchange experiment at 850°C and 50 MPa. *Frontiers in Earth Science* **6**.
- Blamart, D., Trumbull, R. B. & Chaussidou, M. (1993). Oxygen and boron isotopic composition of the Archaean Sinceni pluton: implications for the occurrence of S-type granites in Swaziland. *Abstracts, 16th Colloquium of African Geology, Ezulwini, Swaziland*, pp. 29–31.
- Bleeker, W. (2003). The late Archean record: a puzzle in ca. 35 pieces. *Lithos* **71**, 99–134.
- Blevin, P. L. & Chappell, B. W. (1992). The role of magma sources, oxidation states and fractionation in determining the granite metallogeny of eastern Australia. *Earth and Environmental Science Transactions of the Royal Society of Edinburgh* **83**, 305–316.
- Block, S., Moya, J. F., Zeh, A., Poujol, M., Jaguin, J. & Paquette, J. L. (2013). The Murchison greenstone belt, South Africa: accreted slivers with contrasting metamorphic conditions. *Precambrian Research* **227**, 77–98.
- Blockley, J. G. (1980). *The Tin Deposits of Western Australia, with Special Reference to the Associated Granites. Geological Survey of Western Australia, Mineral Resources Bulletin* 12, 184 pp.
- Boehnke, P., Watson, E. B., Trail, D., Harrison, T. M. & Schmitt, A. K. (2013). Zircon saturation re-visited. *Chemical Geology* **351**, 324–334.
- Boerboom, T. J. & Zartman, R. E. (1993). Geology, geochemistry, and geochronology of the central Giants Range batholith, northeastern Minnesota. *Canadian Journal of Earth Sciences* **30**, 2510–2522.
- Boher, M., Abouchami, W., Michard, A., Albarède, F. & Arndt, N. T. (1992). Crustal growth in West Africa at 2.1 Ga. *Journal of Geophysical Research* **97**, 345–369.
- Bostock, H. H. & Loveridge, W. D. (1988). *Geochronology of the Taltson magmatic zone, and its eastern cratonic margin, District of Mackenzie. Radiogenic age and isotopic studies: report 2. Geological Survey of Canada, Paper* **88-2**, 59–65.
- Bostock, H. H. & van Breemen, O. (1994). Ages of detrital and metamorphic zircons and monazites from a pre-Taltson magmatic zone basin at the western margin of the Rae province. *Canadian Journal of Earth Sciences* **31**, 1353–1364.
- Bostock, H. H., van Breemen, O. & Loveridge, W. D. (1987). *Proterozoic geochronology in the Taltson magmatic zone, N.W.T. Radiogenic age and isotopic studies: report 1. Geological Survey of Canada, Paper* **87-2**, 73–80.
- Bostock, H. H., van Breemen, O. & Loveridge, W. D. (1991). *Further geochronology of plutonic rocks in northern Taltson magmatic Zone, District of Mackenzie, NWT. Radiogenic age and isotopic studies. Report 4. Geological Survey of Canada, Paper* **67-78**, 90–2.
- Bourne, J. & Danis, D. (1987). A proposed model for the formation of reversely zoned plutons based on a study of the Lacorne Complex, Superior Province, Quebec. *Canadian Journal of Earth Sciences* **24**, 2506–2520.
- Breaks, F. W. & Janes, D. A. (1991). *Granite-related mineralization of the Dryden Area, Superior Province of northwestern Ontario. Field Trip B7 Guidebook*. Sudbury, ON: Geological Association of Canada, Toronto'91 Organizing Committee, 71 pp.
- Breaks, F. W. & Moore, J. M. (1992). The Ghost Lake batholith, Superior Province of northwestern Ontario; a fertile, S-type, peraluminous granite–rare-element pegmatite system. *Canadian Mineralogist* **30**, 835–875.
- Breaks, F. W., Selway, J. B. & Tindle, A. G. (2003). *Fertile peraluminous granites and related rare-element mineralization in pegmatites, Superior Province, northwest and northeast Ontario: Operation Treasure Hunt. Ontario Geological Survey, Open File Report* **6099**.
- Breaks, F. W., Selway, J. B. & Tindle, A. G. (2005). Fertile peraluminous granites and related rare element pegmatites, Superior Province of Ontario. In: Linnen, R. L. & Samson, I. M. (eds) *Rare Element Geochemistry and Mineral Deposits. Geological Association of Canada, Short Course Notes* **17**, 87–125.
- Broska, I., Williams, C. T., Uher, P., Konečný, P. & Leichmann, J. (2004). The geochemistry of phosphorus in different granite suites of the Western Carpathians, Slovakia: the role of apatite and P-bearing feldspar. *Chemical Geology* **205**, 1–15.
- Bucholz, C. E., Jagoutz, O., VanTongeren, J. A., Setera, J. & Wang, Z. (2017). Oxygen isotope trajectories of crystallizing melts: insights from modeling and the plutonic record. *Geochimica et Cosmochimica Acta* **207**, 154–184.
- Bucholz, C. E., Stolper, E. M., Eiler, J. M. & Breaks, F. W. (2018). A comparison of oxygen fugacities of strongly peraluminous granites across the Archean–Proterozoic boundary. *Journal of Petrology* **59**, 2123–2156.
- Cabral, R. A., Jackson, M. G., Rose-Koga, E. F., Koga, K. T., Whitehouse, M. J., Antonelli, M. A., Farquhar, J., Day, J. M. & Hauri, E. H. (2013). Anomalous sulphur isotopes in plume lavas reveal deep mantle storage of Archaean crust. *Nature* **496**, 490–493.
- Campbell, I. H. & Davies, D. R. (2017). Raising the continental crust. *Earth and Planetary Science Letters* **460**, 112–122.
- Canfield, D. E. (2001). Biogeochemistry of sulfur isotopes. In: Valley, J. W. & Cole, D. R. (eds) *Stable Isotope Geochemistry. Mineralogical Society of America and Geochemical Society, Reviews in Mineralogy and Geochemistry* **43**, 607–636.
- Canfield, D. E., Habicht, K. S. & Thamdrup, B. (2000). The Archean sulfur cycle and the early history of atmospheric oxygen. *Science* **288**, 658–661.
- Card, K. D. (1990). A review of the Superior Province of the Canadian Shield, a product of Archean accretion. *Precambrian Research* **48**, 99–156.
- Catling, D. C. & Claire, M. W. (2005). How Earth's atmosphere evolved to an oxic state: a status report. *Earth and Planetary Science Letters* **237**, 1–20.
- Černý, P. (1989). Contrasting geochemistry of two pegmatite fields in Manitoba: products of juvenile Apebian crust and polycyclic Archean evolution. *Precambrian Research* **45**, 215–234.
- Černý, P. (1990). Distribution, affiliation and derivation of rare-element granitic pegmatites in the Canadian Shield. *Geologische Rundschau* **79**, 183–226.
- Černý, P. (1991a). Fertile granites of Precambrian rare-element pegmatite fields: is geochemistry controlled by tectonic setting or source lithologies? *Precambrian Research* **51**, 429–468.
- Černý, P. (1991b). Rare-element granitic pegmatites. Part II: regional to global environments and petrogenesis. *Geoscience Canada* **18**, 68–81.
- Černý, P., Trueman, D. L., Ziehlke, D. V., Goad, B. E. & Paul, B. J. (1981). *The Cat Lake–Winnipeg River and the Wekusko Lake Pegmatite Fields, Manitoba*. Manitoba Department of Energy and Mines, Mineral Resources Division, Economic Geology Report **ER80**.
- Černý, P., Masau, M., Goad, B. E. & Ferreira, K. (2005). The Greer Lake leucogranite, Manitoba, and the origin of lepidolite-subtype granitic pegmatites. *Lithos* **80**, 305–321.

- Chacko, T. & Creaser, R. A. (1995). Hercynite bearing granites and associated metasedimentary enclaves from the Taltson Magmatic Zone, Alberta, Canada: a natural example of high temperature pelite melting. In: Brown, M. & Piccoli, P. M. (eds) *Origin of Granites and Related Rocks, Third Hutton Symposium Abstracts, US Geological Survey, Circular* **1129**, 32–33.
- Chacko, T., Creaser, R. A. & Poon, D. (1994). Spinel + quartz granites and associated metasedimentary enclaves from the Taltson magmatic zone, Alberta, Canada: a view into the root zone of a high temperature S-type granite batholith. *Mineralogical Magazine* **8A**, 161–162.
- Chacko, T., De, S. K., Creaser, R. A. & Muehlenbachs, K. (2000). Tectonic setting of the Taltson magmatic zone at 1.9–2.0 Ga: a granitoid-based perspective. *Canadian Journal of Earth Sciences* **37**, 1597–1609.
- Chamberlain, K. R., Frost, C. D. & Frost, B. R. (2003). Early Archean to Mesoproterozoic evolution of the Wyoming Province: Archean origins to modern lithospheric architecture. *Canadian Journal of Earth Sciences* **40**, 1357–1374.
- Champion, D. C. & Sheraton, J. W. (1997). Geochemistry and Nd isotope systematics of Archean granites of the Eastern Goldfields, Yilgarn Craton, Australia: implications for crustal growth processes. *Precambrian Research* **83**, 109–132.
- Champion, D. C. & Smithies, R. H. (2001). Archean granites of the Yilgarn and Pilbara Cratons, Western Australia. In: Cassidy, K. F., Dunphy, J. M. & Van Kranendonk, M. J. (eds) *Geoscience Australia 2001*, **4**, 134–136.
- Chandler, F. W. (1988). Diagenesis of sabkha-related, sulphate nodules in the early Proterozoic Gordon Lake formation, Ontario, Canada. *Carbonates and Evaporites* **3**, 75–94.
- Chappell, B. W. & White, A. J. R. (1974). Two contrasting granite types. *Pacific Geology* **8**, 173–174.
- Chappell, B. W., White, A. J. R. & Wyborn, D. (1987). The importance of residual source material (restite) in granite petrogenesis. *Journal of Petrology* **28**, 1111–1138.
- Chorlton, L. B. (2007). *Generalized geology of the world: bed-rock domains and major faults in GIS format: a small-scale world geology map with an extended geological attribute database. Geological Survey of Canada, Open File* **5529**.
- Chough, S. K. (2013). *Geology and Sedimentology of the Korean Peninsula*. Amsterdam: Elsevier, 348 pp.
- Clarke, D. B. (1981). The mineralogy of peraluminous granites; a review. *Canadian Mineralogist* **19**, 3–17.
- Clemens, J. D. (1989). The importance of residual source material (restite) in granite petrogenesis: a comment. *Journal of Petrology* **30**, 1313–1316.
- Clemens, J. D. & Vielzeuf, D. (1987). Constraints on melting and magma production in the crust. *Earth and Planetary Science Letters* **86**, 287–306.
- Clemens, J. D. & Wall, V. J. (1988). Controls on the mineralogy of S-type volcanic and plutonic rocks. *Lithos* **21**, 53–66.
- Collins, W. J. (1996). Lachlan Fold Belt granitoids: products of three-component mixing. *Earth and Environmental Science Transactions of the Royal Society of Edinburgh* **87**, 171–181.
- Condie, K. C. (1989). Geochemical changes in basalts and andesites across the Archean–Proterozoic boundary: identification and significance. *Lithos* **23**, 1–18.
- Condie, K. C. (1994). Greenstones through time. In: Condie, K. C. (ed.) *Archean Crustal Evolution, Developments in Precambrian Geology*, **11**. Amsterdam: Elsevier, pp. 85–120.
- Condie, K. C. (1998). Episodic continental growth and supercontinents: a mantle avalanche connection? *Earth and Planetary Science Letters* **163**, 97–108.
- Condie, K. C. & O'Neill, C. (2010). The Archean–Proterozoic boundary: 500 My of tectonic transition in Earth history. *American Journal of Science* **310**, 775–790.
- Condie, K. C., Des, M. D. J. & Abbott, D. (2001). Precambrian superplumes and supercontinents: a record in black shales, carbon isotopes, and paleoclimates. *Precambrian Research* **106**, 22.
- Condie, K. C., O'Neill, C. & Aster, R. C. (2009). Evidence and implications for a widespread magmatic shutdown for 250 My on Earth. *Earth and Planetary Science Letters* **282**, 294–298.
- Cook, P. J. & McElhinny, M. W. (1979). A reevaluation of the spatial and temporal distribution of sedimentary phosphate deposits in the light of plate tectonics. *Economic Geology* **74**, 315–330.
- Corrigan, D., Pehrsson, S., Wodicka, N. & De Kemp, E. (2009). The Palaeoproterozoic Trans-Hudson Orogen: a prototype of modern accretionary processes. In: Murphy, J. B., Keppie, J. D. & Hynes, A. J. (eds) *Ancient Orogens and Modern Analogues. Geological Society, London, Special Publications* **327**, 457–479.
- CPRM (2003). *Programa Levantamentos Geológicos Básicos do Brasil. Geologia, Tectônica e Recursos Minerais do Brasil: sistema de informações geográficas—SIG*. Rio de Janeiro: CPRM, Mapas Escala 1:2.500.000, 4 CDs ROM [abstract in English].
- Cuney, M., Sabaté, P., Vidal, P., Marinho, M. M. & Conceição, H. (1990). The 2 Ga peraluminous magmatism of the Jacobina–Contendas Mirante Belt (Bahia) Brazil: major and trace-element geochemistry and metallogenic potential. *Journal of Volcanology and Geothermal Research* **44**, 23–141.
- Czamanske, G. K. & Wones, D. R. (1973). Oxidation during magmatic differentiation, Finnmarka complex, Oslo Area, Norway: part 2, the mafic silicates. *Journal of Petrology* **14**, 349–380.
- Dan, W., Li, X. H., Wang, Q., Wang, X. C., Liu, Y. & Wyman, D. A. (2014). Paleoproterozoic S-type granites in the Helanshan complex, Khondalite belt, North China Craton: implications for rapid sediment recycling during slab break-off. *Precambrian Research* **254**, 59–72.
- Davis, D. W. (2002). U–Pb geochronology of Archean metasedimentary rocks in the Pontiac and Abitibi subprovinces, Quebec, constraints on timing, provenance and regional tectonics. *Precambrian Research* **115**, 97–117.
- Davis, W. J. (1992). Granitoid geochemistry and crustal evolution in the central Slave Province. PhD thesis, Memorial University of Newfoundland, St John's, NL.
- Davis, W. J. & Bleeker, W. (1999). Timing of plutonism, deformation, and metamorphism in the Yellowknife Domain, Slave Province, Canada. *Canadian Journal of Earth Sciences* **36**, 1169–1187.
- Davis, W. J. & Hegner, E. (1992). Neodymium isotopic evidence for the tectonic assembly of Late Archean crust in the Slave Province, northwest Canada. *Contributions to Mineralogy and Petrology* **111**, 493–504.
- Davis, W. J., Fryer, B. J. & King, J. E. (1994). Geochemistry and evolution of late Archean plutonism and its significance to the tectonic development of the Slave craton. *Precambrian Research* **67**, 207–241.
- Dawson, K. R. (1966). *A comprehensive study of Preissac–Lacorne batholith, Abitibi county, Quebec. Geological Survey of Canada Bulletin* **142**, 1–76.
- Day, W. C. & Weiblen, P. W. (1986). Origin of late Archean granite: geochemical evidence from the Vermilion granitic complex of northern Minnesota. *Contributions to Mineralogy and Petrology* **93**, 283–296.
- De, S. K., Chacko, T., Creaser, R. A. & Muehlenbachs, K. (2000). Geochemical and Nd–Pb–O isotope systematics of granites from the Taltson magmatic zone, NE Alberta: implications

- for Early Proterozoic tectonics in western Laurentia. *Precambrian Research* **102**, 221–249.
- De Albuquerque, C. A. (1973). Geochemistry of biotites from granitic rocks, northern Portugal. *Geochimica et Cosmochimica Acta* **37**, 1779–1802.
- Delavault, H., Chauvel, C., Thomassot, E., Devey, C. W. & Dazas, B. (2016). Sulfur and lead isotopic evidence of relic Archean sediments in the Pitcairn mantle plume. *Proceedings of the National Academy of Sciences of the USA* **113**, 12952–12956.
- DePaolo, D. J. (1981). Neodymium isotopes in the Colorado Front Range and crust–mantle evolution in the Proterozoic. *Nature* **291**, 193–197.
- DeWitt, E., Redden, J. A., Burack-Wilson, A. & Buscher, D. (1986). Mineral Resource Potential and Geology of the Black Hills National Forest, South Dakota and Wyoming. *US Geological Survey Bulletin* **1580**, 135 pp.
- Dhuime, B., Hawkesworth, C. J., Cawood, P. A. & Storey, C. D. (2012). A change in the geodynamics of continental growth 3 billion years ago. *Science* **335**, 1334–1336.
- Drury, S. A. (1979). Rare-earth and other trace element data bearing on the origin of Archean granitic rocks from Yellowknife, Northwest Territories. *Canadian Journal of Earth Sciences* **16**, 809–815.
- Duarte, K. D., Pereira, E. D., Dall'Agnol, R. & Lafon, J. M. (1991). Geologia e geocronologia do Granito Mata Surrão-sudoeste de Rio Maria (Pa). *Simpósio De Geologia da Amazônia* **3**, 7–20.
- Ducharme, Y., Stevenson, R. K. & Machado, N. (1997). Sm–Nd geochemistry and U–Pb geochronology of the Preissac and Lamotte leucogranites, Abitibi Subprovince. *Canadian Journal of Earth Sciences* **34**, 1059–1071.
- Duke, E. F., Papike, J. J. & Laul, J. C. (1992). Geochemistry of a boron-rich peraluminous granite pluton; the Calamity Peak layered granite–pegmatite complex, Black Hills, South Dakota. *Canadian Mineralogist* **30**, 811–833.
- Edelman, N. & Jaanus-Jiirkilii, M. (1983). A plate tectonic interpretation of the Precambrian of the archipelago of southwestern Finland. *Geological Survey of Finland Bulletin* **325**, 4–33.
- Ehlers, C., Lindroos, A. & Selonen, O. (1993). The late Svecofennian granite–migmatite zone of southern Finland: a belt of transpressive deformation and granite emplacement. *Precambrian Research* **64**, 295–309.
- Eiler, J. M. (2001). Oxygen isotope variations of basaltic lavas and upper mantle rocks. In: Valley, J. W. & Cole, D. R. (eds) *Stable Isotope Geochemistry. Mineralogical Society of America and Geochemical Society, Reviews in Mineralogy and Geochemistry* **43**, 319–364.
- Eiler, J. M., Baumgartner, L. P. & Valley, J. W. (1992). Intercrystalline stable isotope diffusion: a fast grain boundary model. *Contributions to Mineralogy and Petrology* **112**, 543–557.
- Farina, F., Dini, A., Rocchi, S. & Stevens, G. (2014). Extreme mineral-scale Sr isotope heterogeneity in granites by disequilibrium melting of the crust. *Earth and Planetary Science Letters* **399**, 103–115.
- Farmer, G. L. & DePaolo, D. J. (1984). Origin of Mesozoic and Tertiary granite in the western United States and implications for pre-Mesozoic crustal structure: 2. Nd and Sr isotopic studies of unmineralized and Cu- and Mo-mineralized granite in the Precambrian Craton. *Journal of Geophysical Research: Solid Earth* **89**, 10141–10160.
- Farquhar, J., Bao, H. & Thiemens, M. (2000). Atmospheric influence of Earth's earliest sulfur cycle. *Science* **289**, 756–758.
- Farquhar, J., Wing, B. A., McKeegan, K. D., Harris, J. W., Cartigny, P. & Thiemens, M. H. (2002). Mass-independent sulfur of inclusions in diamond and sulfur recycling on early Earth. *Science* **298**, 2369–2372.
- Feng, R. & Kerrich, R. (1991). Single zircon age constraints on the tectonic juxtaposition of the Archean Abitibi greenstone belt and Pontiac subprovince, Quebec, Canada. *Geochimica et Cosmochimica Acta* **55**, 3437–3441.
- Feng, R. & Kerrich, R. (1992a). Geochemical evolution of granitoids from the Archean Abitibi Southern Volcanic Zone and the Pontiac subprovince, Superior Province, Canada: implications for tectonic history and source regions. *Chemical Geology* **98**, 23–70.
- Feng, R. & Kerrich, R. (1992b). Geodynamic evolution of the southern Abitibi and Pontiac terranes: evidence from geochemistry of granitoid magma series (2700–2630 Ma). *Canadian Journal of Earth Sciences* **29**, 2266–2286.
- Feng, R., Fan, J. & Kerrich, R. (1993). Noble metal abundances and characteristics of six granitic magma series, Archean Abitibi belt, Pontiac subprovince: relationships to metallogeny and overprinting of mesothermal gold deposits. *Economic Geology* **88**, 1376–1401.
- Finger, F. & Schiller, D. (2012). Lead contents of S-type granites and their petrogenetic significance. *Contributions to Mineralogy and Petrology* **164**, 747–755.
- Fitzsimons, I. C. W. (2000). A review of tectonic events in the East Antarctic shield and their implications for Gondwana and earlier supercontinents. *Journal of African Earth Sciences* **31**, 3–23.
- Flament, N., Coltice, N. & Rey, P. F. (2008). A case for late-Archaean continental emergence from thermal evolution models and hypsometry. *Earth and Planetary Science Letters* **275**, 326–336.
- Flood, R. H. & Shaw, S. E. (1977). Two “S-type” granite suites with low initial  $^{87}\text{Sr}/^{86}\text{Sr}$  ratios from the New England Batholith, Australia. *Contributions to Mineralogy and Petrology* **61**, 163–173.
- Frost, C. D., Frost, B. R., Chamberlain, K. R. & Hulsebosch, T. P. (1998). The late Archean history of the Wyoming province as recorded by granitic magmatism in the Wind River Range, Wyoming. *Precambrian Research* **89**, 145–173.
- Front, K. & Nurmi, P. A. (1987). Characteristics and geological setting of synkinematic Svecofennian granitoids in southern Finland. *Precambrian Research* **35**, 207–224.
- Frost, B. R., Barnes, C. G., Collins, W. J., Arculus, R. J., Ellis, D. J. & Frost, C. D. (2001). A geochemical classification for granitic rocks. *Journal of Petrology* **42**, 2033–2048.
- Frost, B. R., Frost, C. D., Cornia, M., Chamberlain, K. R. & Kirkwood, R. (2006). The Teton–Wind River domain: a 2.68–2.67 Ga active margin in the western Wyoming Province. *Canadian Journal of Earth Sciences* **43**, 1489–1510.
- Frost, B. R., Swapp, S. M., Frost, C. D., Bagdonas, D. A. & Chamberlain, K. R. (2018). Neoproterozoic tectonic history of the Teton Range: record of accretion against the present-day western margin of the Wyoming Province. *Geosphere* **14**, 1008–1030.
- Frost, C. D. & Fanning, C. M. (2006). Archean geochronological framework of the Bighorn Mountains, Wyoming. *Canadian Journal of Earth Sciences* **43**, 1399–1418.
- Fru, E. C., Rodríguez, N. P., Partin, C. A., Lalonde, S. V., Andersson, P., Weiss, D. J., El Albani, A., Rodushkin, I. & Konhauser, K. O. (2016). Cu isotopes in marine black shales record the Great Oxidation Event. *Proceedings of the National Academy of Sciences of the USA* **113**, 4941–4946.
- Gable, D. J. & Sims, P. K. (1969). *Geology and regional metamorphism of some high-grade cordierite gneisses, Front Range, Colorado*. Geological Society of America, Special Papers **128**, 69 pp.



- Gaál, G. & Gorbatshev, R. (1987). An outline of the Precambrian evolution of the Baltic Shield. *Precambrian Research*, **35**, 15–52.
- Gasquet, D., Barbey, P., Adou, M. & Paquette, J. L. (2003). Structure, Sr–Nd isotope geochemistry and zircon U–Pb geochronology of the granitoids of the Dabakala area (Côte d'Ivoire): evidence for a 2.3 Ga crustal growth event in the Paleoproterozoic of West Africa? *Precambrian Research*, **127**, 329–354.
- Gehrels, G. (2014). Detrital zircon U–Pb geochronology applied to tectonics. *Annual Review of Earth and Planetary Sciences*, **42**, 127–149.
- Giletti, B. J. & Yund, R. A. (1984). Oxygen diffusion in quartz. *Journal of Geophysical Research: Solid Earth*, **89**, 4039–4046.
- Goad, B. E. & Černý, P. (1981). Peraluminous pegmatitic granites and their pegmatite aureoles in the Winnipeg River district, southeastern Manitoba. *Canadian Mineralogist*, **19**, 177–194.
- Gosselin, D. C., Papike, J. J., Zartman, R. E., Peterman, Z. E. & Laul, J. C. (1988). Archean rocks of the Black Hills, South Dakota: reworked basement from the southern extension of the Trans-Hudson orogen. *Geological Society of America Bulletin*, **100**, 1244–1259.
- Gosselin, D. C., Papike, J. J., Shearer, C. K., Peterman, Z. E. & Laul, J. C. (1990). Geochemistry and origin of Archean granites from the Black Hills, South Dakota. *Canadian Journal of Earth Sciences*, **27**, 57–71.
- Gray, C. M. (1984). An isotopic mixing model for the origin of granitic rocks in southeastern Australia. *Earth and Planetary Science Letters*, **70**, 47–60.
- Green, D. C. & Baadsgaard, H. (1971). Temporal evolution and petrogenesis of an Archean crustal segment at Yellowknife, NWT, Canada. *Journal of Petrology*, **12**, 177–217.
- Green, D. C., Baadsgaard, H. & Cumming, G. L. (1968). Geochronology of the Yellowknife area, Northwest Territories, Canada. *Canadian Journal of Earth Sciences*, **5**, 725–735.
- Green, T. H. (1977). Garnet in silicic liquids and its possible use as a PT indicator. *Contributions to Mineralogy and Petrology*, **65**, 59–67.
- Grotzinger, J. P. & James, N. P. (2000). Precambrian carbonates: evolution of understanding. In: Grotzinger, J. P. & James, N. P. (eds) *Carbonate Sedimentation and Diagenesis in the Evolving Precambrian World. Society for Sedimentary Geology, Special Publications* **67**, 3–20.
- Grove, T. L. & Parman, S. W. (2004). Thermal evolution of the Earth as recorded by komatiites. *Earth and Planetary Science Letters*, **219**, 173–187.
- Grover, T. W., Pattison, D. R. M., McDonough, M. R. & McNicoll, V. J. (1997). Tectonometamorphic evolution of the southern Taltson Magmatic Zone and associated shear zones, Northeastern Alberta. *Canadian Mineralogist*, **35**, 1051–1067.
- Gumsley, A. P., Chamberlain, K. R., Bleeker, W., Söderlund, U., de Kock, M. O., Larsson, E. R. & Bekker, A. (2017). Timing and tempo of the Great Oxidation Event. *Proceedings of the National Academy of Sciences of the USA*, **114**, 1811–1816.
- Guo, J.-H., Zhai, M.-G. & Xu, R.-H. (2001). Timing of the granulite-facies metamorphism in the Sanggan area, North China craton: zircon U–Pb geochronology. *Science in China Series D: Earth Sciences*, **44**, 1010–1018.
- Guo, Q., Strauss, H., Kaufman, A. J., Schröder, S., Gutzmer, J., Wing, B., Baker, M. A., Bekker, A., Jin, Q., Kim, S. T. & Farquhar, J. (2009). Reconstructing Earth's surface oxidation across the Archean–Proterozoic transition. *Geology*, **37**, 399–402.
- Hall, A. & Tyler, R. C. (1965). The origin of accessory garnet in the Donegal granite. *Mineralogical Magazine and Journal of the Mineralogical Society*, **35**, 628–633.
- Halla, J., Whitehouse, M. J., Ahmad, T. & Bagai, Z. (2017). Archean granitoids: an overview and significance from a tectonic perspective. In: Betterton, J., Craig, J., Mendum, J. R., Neller, R. & Tanner, J. (eds) *Aspects of the Life and Works of Archibald Geikie. Geological Society, London, Special Publications* **449**, 1–18.
- Hammouda, T., Pichavant, M. & Chaussidon, M. (1996). Isotopic equilibration during partial melting: an experimental test of the behaviour of Sr. *Earth and Planetary Science Letters*, **144**, 109–121.
- Harris, N. B. W. & Inger, S. (1992). Trace element modelling of pelite-derived granites. *Contributions to Mineralogy and Petrology*, **110**, 46–56.
- Harris, N., Massey, J. & Inger, S. (1993). The role of fluids in the formation of High Himalayan leucogranites. In: Treloar, P. J. & Searle, M. P. (eds) *Himalayan Tectonics. Geological Society, London, Special Publications* **74**, 391–400.
- Harris, N., Ayres, M. & Massey, J. (1995). Geochemistry of granitic melts produced during the incongruent melting of muscovite: implications for the extraction of Himalayan leucogranite magmas. *Journal of Geophysical Research: Solid Earth*, **100**, 15767–15777.
- Harrison, T. M. & Watson, E. B. (1984). The behavior of apatite during crustal anatexis: equilibrium and kinetic considerations. *Geochimica et Cosmochimica Acta*, **48**, 1467–1477.
- Hausel, W. D. (1991). *Economic geology of the South Pass granite greenstone belt, southern Wind River Range, western Wyoming. Geological Survey of Wyoming Report of Investigations* **44**, 129 pp.
- Hazen, R. M., Papineau, D., Bleeker, W., Downs, R. T., Ferry, J. M., McCoy, T. J., Sverjensky, D. A. & Yang, H. (2008). Mineral evolution. *American Mineralogist*, **93**, 1693–1720.
- Hazen, R. M., Sverjensky, D. A., Azzolini, D., Bish, D. L., Elmore, S. C., Hinnov, L. & Milliken, R. E. (2013). Clay mineral evolution. *American Mineralogist*, **98**, 2007–2029.
- Healy, B., Collins, W. J. & Richards, S. W. (2004). A hybrid origin for Lachlan S-type granites: the Murrumbidgee Batholith example. *Lithos*, **78**, 197–216.
- Hegner, E., Kröner, A. & Hofmann, A. W. (1984). Age and isotope geochemistry of the Archean Pongola and Usushwana Suites in Swaziland, southern Africa. *Earth and Planetary Science Letters*, **70**, 267–279.
- Helms, T. S. & Labotka, T. C. (1991). Petrogenesis of Early Proterozoic pelitic schists of the southern Black Hills, South Dakota: constraints on regional low-pressure metamorphism. *Geological Society of America Bulletin*, **103**, 1324–1334.
- Henderson, J. B. (1972). Sedimentology of Archean turbidites at Yellowknife, Northwest Territories. *Canadian Journal of Earth Sciences*, **9**, 882–902.
- Henderson, J. B. (1985). *Geology of the Yellowknife–Hearne Lake Area, District of Mackenzie: A Segment across an Archean Basin. Geological Survey of Canada Memoir* **414**, 135 pp.
- Herzberg, C., Condie, K. & Korenaga, J. (2010). Thermal history of the Earth and its petrological expression. *Earth and Planetary Science Letters*, **292**, 79–88.
- Hildebrand, R. S., Hoffman, P. F. & Bowring, S. A. (1987). Tectono-magmatic evolution of the 1.9-Ga Great Bear magmatic zone, Wopmay Orogen, northwestern Canada. *Journal of Volcanology and Geothermal Research*, **32**, 99–118.
- Hill, R. I., Chappell, B. W. & Campbell, I. H. (1992). Late Archean granites of the southeastern Yilgarn Block, Western Australia: age, geochemistry, and origin. *Earth and*

- Environmental Science Transactions of the Royal Society of Edinburgh* **83**, 211–226.
- Hirdes, W., Davis, D. W., Lüdtke, G. & Konan, G. (1996). Two generations of Birimian (Paleoproterozoic) volcanic belts in northeastern Côte d'Ivoire (West Africa): consequences for the Birimian controversy. *Precambrian Research* **80**, 173–191.
- Hoffman, P. F. (1980). Wopmay Orogen: a Wilson cycle of Early Proterozoic age in the northwest of the Canadian Shield. *Geoscience Canada* **6**, 523–549.
- Hoffman, P. F. (1988). United Plates of America. *Annual Review of Earth and Planetary Sciences* **16**, 543–603.
- Hoffman, P. F. & Bowring, S. A. (1984). Short-lived 1.9 Ga continental margin and its destruction, Wopmay orogen, north-west Canada. *Geology* **12**, 68–72.
- Hoffman, P. F., St Onge, M. R., Easton, R. M., Grotzinger, J. & Schulze, D. E. (1980). *Syntectonic Plutonism in North-Central Wopmay Orogen (Early Proterozoic), Hepburn Lake Map Area*. Geological Survey of Canada, Current Research Part A, District of Mackenzie, **80**, 171–177.
- Hogan, J. P. & Sinha, A. K. (1991). The effect of accessory minerals on the redistribution of lead isotopes during crustal anatexis: a model. *Geochimica et Cosmochimica Acta* **55**, 335–348.
- Holdaway, M. J. (2000). Application of new experimental and garnet Margules data to the garnet-biotite geothermometer. *American Mineralogist*, **85**, 881–892.
- Holland, H. D. (1984). *The Chemical Evolution of the Atmosphere and Oceans*. Princeton, NJ: Princeton University Press, 598 pp.
- Holland, H. D. (2002). Volcanic gases, black smokers, and the great oxidation event. *Geochimica et Cosmochimica Acta* **66**, 3811–3826.
- Holland, H. D. (2005). 100th anniversary special paper: sedimentary mineral deposits and the evolution of Earth's near-surface environments. *Economic Geology* **100**, 1489–1509.
- Holland, H. D. (2006). The oxygenation of the atmosphere and oceans. *Philosophical Transactions of the Royal Society of London, Series B* **361**, 903–915.
- Holtz, F., Johannes, W. & Pichavant, M. (1992). Peraluminous granites: the effect of alumina on melt composition and coexisting minerals. *Earth and Environmental Science Transactions of the Royal Society of Edinburgh* **83**, 409–416.
- Hopgood, A. M., Bowes, D. R. & Addison, J. (1976). Structural development of migmatites near Skäldö, southwest Finland. *Bulletin of the Geological Society of Finland* **48**, 43–62.
- Hopkinson, T. N., Harris, N. B. W., Warren, C. J., Spencer, C. J., Roberts, N. M. W., Horstwood, M. S. A. & Parrish, R. R. (2017). The identification and significance of pure sediment-derived granites. *Earth and Planetary Science Letters* **467**, 57–63.
- Huhma, H. (1986). Sm–Nd, U–Pb and Pb–Pb isotopic evidence for the origin of the Early Proterozoic Svecofennian crust in Finland. *Geological Survey of Finland Bulletin* **337**, 48 pp.
- Icenhower, J. & London, D. (1995). An experimental study of element partitioning among biotite, muscovite, and coexisting peraluminous silicic melt at 200 MPa (H<sub>2</sub>O). *American Mineralogist* **80**, 1229–1251.
- Ishihara, S. (1977). The magnetite-series and ilmenite-series granitic rocks. *Mining Geology* **27**, 293–305.
- Ishihara, S. & Sasaki, A. (1989). Sulfur isotopic ratios of the magnetite-series and ilmenite-series granitoids of the Sierra Nevada batholith—a reconnaissance study. *Geology* **17**, 788–791.
- Ishihara, S., Robb, L. J., Anhaeusser, C. R. & Imai, A. (2002). Granitoid series in terms of magnetic susceptibility: a case study from the Barberton region, South Africa. *Gondwana Research* **5**, 581–589.
- Jaguin, J., Moyaen, J. F., Boulvais, P., Poujol, M., Tyler, I. M. & Knox, R. (2010). Mid-Archean granites south of the Murchison Greenstone Belt, South Africa: the oldest large biotite–muscovite leucogranite bodies. In: Tyler, I. M. & Robinson, K. (eds) *Abstracts, Fifth International Archean Symposium*. Perth, WA: Geological Survey of Western Australia, p. 78.
- Jaguin, J., Gapais, D., Poujol, M., Boulvais, P. & Moyaen, J. F. (2012). The Murchison greenstone belt (South Africa): a general tectonic framework. *South African Journal of Geology* **115**, 65–76.
- Jin, M.-S., Lee, Y. S. & Ishihara, S. (2001). Granitoids and magnetic susceptibility in South Korea. *Resource Geology* **51**, 189–203.
- Johannes, W., Ehlers, C., Kriegsman, L. M. & Mengel, K. (2003). The link between migmatites and S-type granites in the Turku area, southern Finland. *Lithos* **68**, 69–90.
- Johnston, D. T. (2011). Multiple sulfur isotopes and the evolution of Earth's surface sulfur cycle. *Earth-Science Reviews* **106**, 161–183.
- Joshi, K. B., Bhattacharjee, J., Rai, G., Halla, J., Ahmad, T., Kurhila, M., Heilimo, E. & Choudhary, A. K. (2017). The diversification of granitoids and plate tectonic implications at the Archean–Proterozoic boundary in the Bundelkhand Craton, Central India. In: Halla, J., Whitehouse, M. J., Ahmad, T. & Bagai, Z. (eds) *Crust–Mantle Interactions and Granitoid Diversification: Insights from Archean Cratons*. Geological Society, London, Special Publications **449**, 123–157.
- Joyce, A. S. (1973). Chemistry of the minerals of the granitic Murrumbidgee batholith, Australian Capital Territory. *Chemical Geology* **11**, 271–296.
- Karlstrom, K. E., Åhäll, K. I., Harlan, S. S., Williams, M. L., McLelland, J. & Geissman, J. W. (2001). Long-lived (1.8–1.0 Ga) convergent orogen in southern Laurentia, its extensions to Australia and Baltica, and implications for refining Rodinia. *Precambrian Research* **111**, 5–30.
- Kasting, J. F. (2001). The rise of atmospheric oxygen. *Science* **293**, 819–820.
- Kay, S. V. & Stott, G. M. (1985). Economic geology of the Lake St. Joseph area. *Summary of Field Work and Other Activities 1985, Ontario Geological Survey, Miscellaneous Paper* **126**, 26–35.
- Kendall, B., Brennecke, G. A., Weyer, S. & Anbar, A. D. (2013). Uranium isotope fractionation suggests oxidative uranium mobilization at 2.50 Ga. *Chemical Geology* **362**, 105–114.
- King, E. M. & Valley, J. W. (2001). The source, magmatic contamination, and alteration of the Idaho batholith. *Contributions to Mineralogy and Petrology* **142**, 72–88.
- Keller, B. & Schoene, B. (2018). Plate tectonics and continental basaltic geochemistry throughout Earth history. *Earth and Planetary Science Letters* **481**, 290–304.
- Keller, C. B. & Schoene, B. (2012). Statistical geochemistry reveals disruption in secular lithospheric evolution about 2.5 Gyr ago. *Nature* **485**, 490–493.
- Kemp, A. I. S., Hawkesworth, C. J., Paterson, B. A., Foster, G. L., Kinny, P. D., Whitehouse, M. J. & Maas, R. (2006). Exploring the plutonic–volcanic link: a zircon U–Pb, Lu–Hf and O isotope study of paired volcanic and granitic units from south-eastern Australia. *Transactions of the Royal Society of Edinburgh: Earth Sciences* **97**, 337–355.
- Kemp, A. I. S., Hawkesworth, C. J., Foster, G. L., Paterson, B. A., Woodhead, J. D., Hergt, J. M., Gray, C. M. & Whitehouse, M. J. (2007). Magmatic and crustal differentiation history of granitic rocks from Hf–O isotopes in zircon. *Science* **315**, 980–983.

- Kim, J. & Cho, M. (2003). Low-pressure metamorphism and leucogranite magmatism, northeastern Yeongnam Massif, Korea: implication for Paleoproterozoic crustal evolution. *Precambrian Research* **122**, 235–251.
- Kim, N., Cheong, C. S., Park, K. H., Kim, J. & Song, Y. S. (2012). Crustal evolution of northeastern Yeongnam Massif, Korea, revealed by SHRIMP U–Pb zircon geochronology and geochemistry. *Gondwana Research* **21**, 865–875.
- King, J. E. (1986). The metamorphic internal zone of Wopmay orogen (Early Proterozoic), Canada: 30 km of structural relief in a composite section based on plunge projection. *Tectonics* **5**, 973–994.
- King, J. E., Davis, W. J. & Relf, C. (1992). Late Archean tectono-magmatic evolution of the central Slave Province, Northwest Territories. *Canadian Journal of Earth Sciences* **29**, 2156–2170.
- Kirby, E., Karlstrom, K. E., Andronikos, C. L. & Dallmeyer, R. D. (1995). Tectonic setting of the Sandia pluton: An orogenic 1.4 Ga granite in New Mexico. *Tectonics* **14**, 185–201.
- Knesel, K. M. & Davidson, J. P. (2002). Insights into collisional magmatism from isotopic fingerprints of melting reactions. *Science* **296**, 2206–2208.
- Korenaga, J. (2008). Urey ratio and the structure and evolution of Earth's mantle. *Reviews of Geophysics* **46**, RG2007.
- Korja, A. & Heikkinen, P. (1995). Proterozoic extensional tectonics of the central Fennoscandian Shield: results from the Baltic and Bothnian echoes from the lithosphere experiment. *Tectonics* **14**, 504–517.
- Korsman, K., H., Hautala, T. & Wasenius, P. (1984). *Metamorphism as an indicator of evolution and structure of the crust in eastern Finland*. Geological Survey of Finland *Bulletin* **328**, 40 pp.
- Kretz, R. (1968). *Study of pegmatite bodies and enclosing rocks, Yellowknife–Beaulieu region, District of Mackenzie*. Geological Survey of Canada *Bulletin* **159**, 109 pp.
- Kretz, R. (1985). Chemical composition of the Sparrow pluton and associated pegmatite dikes. *Contributions to the Geology of the Northwest Territories* **2**, 1–13.
- Kretz, R., Garrett, D. & Garrett, R. G. (1982). Na–K–Li geochemistry of the Prestige pluton in the Slave Province of the Canadian Shield. *Canadian Journal of Earth Sciences* **19**, 540–554.
- Kretz, R., Loop, J. & Hartree, R. (1989). Petrology and Li–Be–B geochemistry of muscovite–biotite granite and associated pegmatite near Yellowknife, Canada. *Contributions to Mineralogy and Petrology* **102**, 174–190.
- Kump, L. R. & Barley, M. E. (2007). Increased subaerial volcanism and the rise of atmospheric oxygen 2.5 billion years ago. *Nature* **448**, 1033–1036.
- Kump, L. R., Kasting, J. F. & Barley, M. E. (2001). Rise of atmospheric oxygen and the ‘upside-down’ Archean mantle. *Geochemistry Geophysics. Geosystems* **2**, 1025.
- Lahtinen, R. (1994). Crustal evolution of the Svecofennian and Karelian domains during 2.1–1.79 Ga, with special emphasis on the geochemistry and origin of 1.93–1.91 Ga gneissic tonalites and associated supracrustal rocks in the Rauta–lampi area, central Finland. *Geological Survey of Finland, Bulletin* **378**, 128.
- Lahtinen, R., Korja, A. & Nironen, M. (2005). Paleoproterozoic tectonic evolution. In: Lehtinen, M., Nurmi, P. A. & Rämö, O. T. (eds) *Developments in Precambrian Geology* **14**, 481–531.
- Lalonde, A. E. (1986). The intrusive rocks of the Hepburn metamorphic-plutonic zone of the central Wopmay orogen, N.W.T. PhD thesis, McGill University, Montreal, ON, 258 pp.
- Lalonde, A. E. (1989). Hepburn intrusive suite: Peraluminous plutonism within a closing back-arc basin, Wopmay orogen, Canada. *Geology* **17**, 261–264.
- Lalonde, A. E. & Bernard, P. (1993). Composition and color of biotite from granites; two useful properties in characterization of plutonic suites from the Hepburn internal zone of Wopmay Orogen, Northwest Territories. *Canadian Mineralogist* **31**, 203–217.
- Lan, Z.-W. (2007). Petrogenesis of garnet-bearing granites in the khondalites of North China Craton: mixing mechanism of melt and restite. Master's Degree thesis, Institute of Geology and Geophysics, Chinese Academy of Sciences, Beijing, 43 pp.
- Langford, F. F. & Morin, J. A. (1976). The development of the Superior Province of northwestern Ontario by merging island arcs. *American Journal of Science* **276**, 1023–1034.
- Langstaff, G. D. (1995). Archean Geology of the Granite Mountains, Wyoming. Ph.D. dissertation, Golden, Colorado, Colorado School of Mines, 671 p.
- Larbi, Y., Stevenson, R., Breaks, F., Machado, N. & Gariépy, C. (1999). Age and isotopic composition of late Archean leucogranites: implications for continental collision in the western Superior Province. *Canadian Journal of Earth Sciences* **36**, 495–510.
- Laurent, O., Martin, H., Moyen, J. F. & Doucelance, R. (2014). The diversity and evolution of late-Archean granitoids: evidence for the onset of ‘modern-style’ plate tectonics between 3.0 and 2.5 Ga. *Lithos* **205**, 208–235.
- Leal, L. R. B., Teixeira, W., Cunha, J. C., Leal, A. B. D. M., Macambira, M. J. B. & Rosa, M. D. L. D. S. (2000). Isotopic signatures of Paleoproterozoic granitoids of the Gavião block and implications for the evolution of the São Francisco craton, Bahia, Brazil. *Revista Brasileira de Geociências* **30**, 066–069.
- Le Breton, N. & Thompson, A. B. (1988). Fluid-absent (dehydration) melting of biotite in metapelites in the early stages of crustal anatexis. *Contributions to Mineralogy and Petrology* **99**, 226–237.
- Lee, C. T. A. & Bachmann, O. (2014). How important is the role of crystal fractionation in making intermediate magmas? Insights from Zr and P systematics. *Earth and Planetary Science Letters* **393**, 266–274.
- Lee, S. G., Shin, S. C., Jin, M. S., Ogasawara, M. & Yang, M. K. (2005). Two Paleoproterozoic strongly peraluminous granitic plutons (Nonggeori and Naedeokri granites) at the north-eastern part of Yeongnam Massif, Korea: Geochemical and isotopic constraints in East Asian crustal formation history. *Precambrian Research* **139**, 101–120.
- Leube, A., Hirdes, W., Mauer, R. & Kesse, G. O. (1990). The early Proterozoic Birimian Supergroup of Ghana and some aspects of its associated gold mineralization. *Precambrian Research* **46**, 139–165.
- London, D. (1992). Phosphorus in S-type magmas: the P<sub>2</sub>O<sub>5</sub> content of feldspars from peraluminous granites, pegmatites, and rhyolites. *American Mineralogist* **77**, 126–145.
- London, D., Cerny, P., Loomis, J. & Pan, J. J. (1990). Phosphorus in alkali feldspars of rare-element granitic pegmatites. *Canadian Mineralogist* **28**, 771–786.
- Longstaffe, F. J., Cerny, P. & Muehlenbachs, K. (1981). Oxygen-isotope geochemistry of the granitoid rocks in the Winnipeg River pegmatite district, southeastern Manitoba. *Canadian Mineralogist* **19**, 195–204.
- Longstaffe, F. J. & Schwarcz, H. P. (1977). sol18O16O of Archean clastic metasedimentary rocks: a petrogenetic indicator for Archean gneisses? *Geochimica et Cosmochimica Acta* **41**, 1303–1312.
- Lowe, D. R. (1994). Archean greenstone-related sedimentary rocks. In: Condie, K. C. (ed.) *Archaean Crustal Evolution, Developments in Precambrian Geology*, **11**. Amsterdam: Elsevier, pp. 121–169.

- Ludwig, K. R. & Stuckless, J. S. (1978). Uranium–lead isotope systematics and apparent ages of zircons and other minerals in Precambrian granitic rocks, Granite Mountains, Wyoming. *Contributions to Mineralogy and Petrology* **65**, 243–354.
- Lyons, T. W., Reinhard, C. T. & Planavsky, N. J. (2014). The rise of oxygen in Earth's early ocean and atmosphere. *Nature* **506**, 307–315.
- Madore, C. & Annesley, I. R. (1996). Wollaston EAGLE Project, Basal Wollaston Group: Facies (Segment 2). In: Annesley, R., Madore, C., Shi, R., Quirt, D. H., Dyck, J., Hajnal, Z. & Reilkoff, B. (eds) *Wollaston EAGLE Project: Segment 2 Report. Saskatchewan Research Council Publication R-1420-5-C-96*, 1–122.
- Maphalala, R. M. & Kröner, A. (1993). Pb–Pb single zircon ages for the younger Archaean granitoids of Swaziland, southern Africa. In: *Abstracts of 16th Cochrane Colloquium*, African Geology, Mbabane, Swaziland, **2**, pp. 201–206.
- Marinho, M. M., Sabaté, P. & Barbosa, J. S. F. (1993). The Contendas–Mirante volcano-sedimentary belt. In: Figueirêdo, M. C. H. & Pedreira, A. J. (eds) *Petrological and Geochronologic Evolution of the Oldest Segments of the São Francisco Craton. Boletim de Instituto de Geociências da Universidade de São Paulo*. Bull IG-USP, **17**, 37–72.
- Marschall, H. R., Hawkesworth, C. J., Storey, C. D., Dhuime, B., Leat, P. T., Meyer, H. P. & Tamm-Buckle, S. (2010). The Annandagstoppane Granite, East Antarctica: evidence for Archaean intracrustal recycling in the Kaapvaal–Grünhegna Craton from zircon O and Hf isotopes. *Journal of Petrology* **51**, 2277–2301.
- Martin, H., Moyen, J. F. & Rapp, R. (2009). The sanukitoid series: magmatism at the Archaean–Proterozoic transition. *Earth and Environmental Science Transactions of the Royal Society of Edinburgh* **100**, 15–33.
- Matthews, P. E. (1985). Archaean post-Pongola granites in the southeastern Kaapvaal Craton. *South African Journal of Science* **81**, 479–484.
- McCombs, J. A., Dahl, P. S. & Hamilton, M. A. (2004). U–Pb ages of Neoarchean granitoids from the Black Hills, South Dakota, USA: implications for crustal evolution in the Archaean Wyoming province. *Precambrian Research* **130**, 161–184.
- McCulloch, M. T. & Bennett, V. C. (1994). Progressive growth of the Earth's continental crust and depleted mantle: Geochemical constraints. *Geochimica et Cosmochimica Acta* **58**, 4717–4738.
- McKechnie, C. L., Annesley, I. R. & Ansdell, K. M. (2012a). Radioactive abyssal granitic pegmatites and leucogranites in the Wollaston Domain, northern Saskatchewan, Canada: Mineral compositions and conditions of emplacement in the Fraser Lakes area. *Canadian Mineralogist* **50**, 1637–1667.
- McKechnie, C. L., Annesley, I. R. & Ansdell, K. M. (2012b). Medium- to low-pressure pelitic gneisses of Fraser Lakes Zone B, Wollaston Domain, northern Saskatchewan, Canada: mineral compositions, metamorphic *P–T–t* path, and implications for the genesis of radioactive abyssal granitic pegmatites. *Canadian Mineralogist* **50**, 1669–1694.
- McKechnie, C. L., Annesley, I. R. & Ansdell, K. M. (2013). Geological setting, petrology, and geochemistry of granitic pegmatites and leucogranites hosting U–Th–REE mineralization at Fraser Lakes zone B, Wollaston Domain, northern Saskatchewan, Canada. *Exploration and Mining Geology* **21**, 1–26.
- McNicoll, V. J., McDonough, M. & Grover, T. (1993). Preliminary U–Pb geochronology of the Southern Taltson Magmatic Zone, Northeastern Alberta. In: Ross, G. M. (ed.) *Report of Lithoprobe Alberta Basement Transects Workshop. Lithoprobe Report* **31**, 129–130.
- McNicoll, V. J., McDonough, M. & Grover, T. (1994). U–Pb geochronology of the Southern Taltson Magmatic Zone, Northeastern Alberta. In: Ross, G. M. (ed.) *Report of Lithoprobe Alberta Basement Transects Workshop. Lithoprobe Report* **37**, 270–273.
- Meintzer, R. E. (1987). The mineralogy and geochemistry of the granitoid rocks and related pegmatites of the Yellowknife Pegmatite Field, Northwest Territories. PhD thesis, University of Manitoba, Winnipeg, MB.
- Meintzer, R. E., Wise, M. A. & Černý, P. (1984). Distribution and structural setting of fertile granites and related pegmatites in the Yellowknife pegmatite field, District of Mackenzie. *Current Research, Part A. Geological Survey of Canada, Paper* **84-1A**, 373–381.
- Meredith, M. T. (2005). A Late Archean tectonic boundary exposed at Tin Cup Mountain, Granite Mountains, Wyoming. MS thesis, University of Wyoming, Laramie, WY.
- Meyer, F. M., Robb, L. J., Reimold, W. U. & De Bruijn, H. (1994). Contrasting low- and high-Ca granites in the Archean Barberton Mountain Land, southern Africa. *Lithos* **32**, 63–76.
- Mikkola, P., Lauri, L. S. & Käpyaho, A. (2012). Neoarchean leucogranitoids of the Kianta Complex, Karelian Province, Finland: source characteristics and processes responsible for the observed heterogeneity. *Precambrian Research* **206**, 72–86.
- Miller, C. F. & Stoddard, E. F. (1981). The role of manganese in the paragenesis of magmatic garnet: an example from the Old Woman–Piute Range, California. *Journal of Geology* **89**, 233–246.
- Miller, C. F., Stoddard, E. F., Bradfish, L. J. & Dollase, W. A. (1981). Composition of plutonic muscovite; genetic implications. *Canadian Mineralogist* **19**, 25–34.
- Miller, C. F., McDowell, S. M. & Mapes, R. W. (2003). Hot and cold granites? Implications of zircon saturation temperatures and preservation of inheritance. *Geology* **31**, 529–532.
- Mogk, D. W., Mueller, P. A. & Wooden, J. L. (1988). Archean tectonics of the North Snowy Block, Beartooth Mountains, Montana. *Journal of Geology* **96**, 125–141.
- Mogk, D. W., Mueller, P. A. & Wooden, J. L. (1992). The nature of Archean terrane boundaries: an example from the northern Wyoming Province. *Precambrian Research* **55**, 155–168.
- Montel, J. M. & Vielzeuf, D. (1997). Partial melting of metagreywackes, Part II. Compositions of minerals and melts. *Contributions to Mineralogy and Petrology* **128**, 176–196.
- Morfin, S., Sawyer, E. W. & Bandyayera, D. (2013). Large volumes of anatectic melt retained in granulite facies migmatites: An injection complex in northern Quebec. *Lithos* **168–169**, 200–218.
- Moyen, J. F., Martin, H., Jayananda, M. & Auvray, B. (2003). Late Archaean granites; a typology based on the Dharwar Craton, India. *Precambrian Research* **127**, 103–123.
- Mueller, P., Wooden, J., Nutman, A. & Mogk, D. (1998). Early Archean crust in the northern Wyoming province: evidence from U–Pb systematics in detrital zircons. *Precambrian Research* **91**, 295–307.
- Mueller, P. A. & Frost, C. D. (2006). The Wyoming Province: a distinctive Archean craton in Laurentian North America. *Canadian Journal of Earth Sciences* **43**, 1391–1397.
- Mueller, P. A., Shuster, R. D., Wooden, J. L., Erslev, E. A. & Bowes, D. R. (1993). Age and composition of Archean crystalline rocks from the southern Madison Range, Montana: Implications for crustal evolution in the Wyoming craton. *Geological Society of America Bulletin* **105**, 437–446.



- Mueller, P. A., Wooden, J. L., Mogk, D. W., Nutman, A. P. & Williams, I. S. (1996). Extended history of a 3.5 Ga trondhjemitic gneiss, Wyoming province, USA: evidence from U–Pb systematics in zircon. *Precambrian Research* **78**, 41–52.
- Mulja, T., Williams-Jones, A. E., Wood, S. A. & Boily, M. (1995a). The rare-element-enriched monzogranite–pegmatite–quartz vein systems in the Preissac–Lacorne Batholith, Quebec; I, Geology and mineralogy. *Canadian Mineralogist* **33**, 793–815.
- Mulja, T., Williams-Jones, A. E., Wood, S. A. & Boily, M. (1995b). The rare-element-enriched monzogranite–pegmatite–quartz vein systems in the Preissac–Lacorne Batholith, Quebec; II, Geochemistry and petrogenesis. *Canadian Mineralogist* **33**, 817–833.
- Mysen, B. O., Ryerson, F. J. & Virgo, D. (1981). The structural role of phosphorus in silicate melts. *American Mineralogist* **66**, 106–117.
- Mysen, B. O. (1998). Phosphorus solubility mechanisms in haplogranitic aluminosilicate glass and melt: Effect of temperature and aluminum content. *Contributions to Mineralogy and Petrology* **133**, 38–50.
- Nabelek, P. I. 2019. Petrogenesis of leucogranites in collisional orogens. *Geological Society, London, Special Publications* **491**, SP491–2018.
- Nabelek, P. I. & Bartlett, C. D. (1998). Petrologic and geochemical links between the post-collisional Proterozoic Harney Peak leucogranite, South Dakota, USA, and its source rocks. *Lithos* **45**, 71–85.
- Nabelek, P. I. & Glascock, M. D. (1995). REE-depleted leucogranites, Black Hills, South Dakota: a consequence of disequilibrium melting of monazite-bearing schists. *Journal of Petrology* **36**, 1055–1071.
- Nabelek, P. I., Russ-Nabelek, C. & Denison, J. R. (1992a). The generation and crystallization conditions of the Proterozoic Harney Peak leucogranite, Black Hills, South Dakota, USA: petrologic and geochemical constraints. *Contributions to Mineralogy and Petrology* **110**, 173–191.
- Nabelek, P. I., Russ-Nabelek, C. & Haeussler, G. T. (1992b). Stable isotope evidence for the petrogenesis and fluid evolution in the Proterozoic Harney Peak leucogranite, Black Hills, South Dakota. *Geochimica et Cosmochimica Acta* **56**, 403–417.
- Nabelek, P. I., Sirbescu, M. & Liu, M. (1999). Petrogenesis and tectonic context of the Harney Peak Granite, Black Hills, South Dakota. *Rocky Mountain Geology* **34**, 165–181.
- Nabelek, P. I., Liu, M. & Sirbescu, M. L. (2001). Thermo-rheological, shear heating model for leucogranite generation, metamorphism, and deformation during the Proterozoic Trans-Hudson orogeny, Black Hills, South Dakota. *Tectonophysics* **342**, 371–388.
- Nelson, B. K. & DePaolo, D. J. (1985). Rapid production of continental crust 1.7 to 1.9 by ago: Nd isotopic evidence from the basement of the North American mid-continent. *Geological Society of America Bulletin* **96**, 746–754.
- Nicoli, G., Stevens, G., Moyen, J. F. & Frei, D. (2015). Rapid evolution from sediment to anatectic granulite in an Archean continental collision zone: the example of the Bandelierkop Formation metapelites, South Marginal Zone, Limpopo Belt, South Africa. *Journal of Metamorphic Geology* **33**, 177–202.
- Nicoli, G., Stevens, G., Moyen, J. F., Vezinet, A. & Mayne, M. (2017). Insights into the complexity of crustal differentiation: K<sub>2</sub>O-poor leucosomes within metasedimentary migmatites from the Southern Marginal Zone of the Limpopo Belt, South Africa. *Journal of Metamorphic Geology* **35**, 999–1022.
- Nironen, M. (1997). The Svecofennian Orogen: a tectonic model. *Precambrian Research* **86**, 21–44.
- Nutman, A. P. & Cordani, U. G. (1993). SHRIMP U–Pb zircon geochronology of Archean granitoids from the Contendas–Mirante area of the São Francisco Craton, Bahia, Brazil. *Precambrian Research* **63**, 179–188.
- Nutman, A. P., Cordani, U. G. & Sabaté, P. (1994). SHRIMP U–Pb ages of detrital zircons from the Early Proterozoic Contendas–Mirante supracrustal belt, São Francisco Craton, Bahia, Brazil. *Journal of South American Earth Science* **7**, 109–114.
- Nyman, M. W. & Karlstrom, K. E. (1997). Pluton emplacement processes and tectonic setting of the 1.42 Ga Signal batholith, SW USA: important role of crustal anisotropy during regional shortening. *Precambrian Research* **82**, 237–263.
- Nyman, M. W., Karlstrom, K. E., Kirby, E. & Graubard, C. M. (1994). Mesoproterozoic contractional orogeny in western North America: Evidence from ca. 1.4 Ga plutons. *Geology* **22**, 901–904.
- Och, L. M. & Shields-Zhou, G. A. (2012). The Neoproterozoic oxygenation event: environmental perturbations and biogeochemical cycling. *Earth-Science Reviews* **110**, 26–57.
- Palmer, E. M. (2018). Petrogenesis of the Archean Prestige leucogranites and spatially associated LCT pegmatites, NWT: Insights from whole-rock and muscovite trace element geochemistry and apatite U–Pb geochronology. MSc thesis, University of New Brunswick, Fredericton, NB.
- Palmer, E. M., Lentz, D. R. & Falck, H. (2016). *Field and lithogeochemical data for the Prestige pluton and surrounding pegmatites, NWT, Canada. Northwest Territories Geological Survey, Yellowknife, NWT Open Report 2016-003*, 16 pp.
- Pan, Y. & Breaks, F. W. (1997). Rare-earth elements in fluorapatite, Separation Lake area, Ontario: Evidence for S-type granite-rare-element pegmatite linkage. *Canadian Mineralogist* **35**, 659–671.
- Pan, Y., Therens, C. & Breaks, F. (1997). Geochemistry of granitoids in the English River Subprovince, Separation Lake area. 1997 Western Superior Transect Third Annual Workshop, April 11–12, 1997. *Lithoprobe Report* **63**, 55–61.
- Paris, G., Adkins, J. F., Sessions, A. L., Webb, S. M. & Fischer, W. W. (2014). Neoproterozoic carbonate-associated sulfate records positive  $\Delta^{33}\text{S}$  anomalies. *Science* **346**, 739–741.
- Patiño Douce, A. E. & Beard, J. S. (1995). Dehydration-melting of biotite gneiss and quartz amphibolite from 3 to 15 kbar. *Journal of Petrology* **36**, 707–738.
- Patiño Douce, A. E. & Harris, N. (1998). Experimental constraints on Himalayan anatexis. *Journal of Petrology* **39**, 689–710.
- Patiño Douce, A. E. & Johnston, A. D. (1991). Phase equilibria and melt productivity in the pelitic system: implications for the origin of peraluminous granitoids and aluminous granulites. *Contributions to Mineralogy and Petrology* **107**, 202–218.
- Partin, C. A., Bekker, A., Planavsky, N. J., Scott, C. T., Gill, B. C., Li, C., Podkovyrov, V., Maslov, A., Konhauser, K. O., Lalonde, S. V. & Love, G. D. (2013). Large-scale fluctuations in Precambrian atmospheric and oceanic oxygen levels from the record of U in shales. *Earth and Planetary Science Letters* **369**, 284–293.
- Payne, J. L., Hand, M., Pearson, N. J., Barovich, K. M. & McInerney, D. J. (2015). Crustal thickening and clay: Controls on O isotope variation in global magmatism and siliciclastic sedimentary rocks. *Earth and Planetary Science Letters* **412**, 70–76.
- Peng, P., Guo, J.-H., Zhai, M.-G. & Bleeker, W. (2010). Paleoproterozoic gabbro-noritic and granitic magmatism in the northern margin of the North China Craton: evidence of crust–mantle interaction. *Precambrian Research* **183**, 635–659.

- Peng, P., Guo, J. H., Windley, B. F., Liu, F., Chu, Z. & Zhai, M. G. (2012). Petrogenesis of Late Paleoproterozoic Liangcheng charnockites and S-type granites in the central–northern margin of the North China Craton: implications for ridge subduction. *Precambrian Research* **222**, 107–123.
- Percival, J. A. (1986). Metamorphism and plutonism in the Quetico Belt, Superior Province, NW Ontario. In: *Lunar and Planetary Institute Workshop of Early Crustal Genesis, The World's Oldest Rocks*, pp. 84–85.
- Percival, J. A. (1989). Granulite terranes and the lower crust of the Superior Province. In: Mereu, R. F., Mueller, S. & Fountain, D. M. (eds) *Properties and Processes of Earth's Lower Crust*, Washington, DC: American Geophysical Union, pp. 301–310.
- Percival, J. A. & Easton, R. M. (2007). *Geology of the Canadian Shield in Ontario: an update*. Ontario Geological Survey, Open File Report **6196**, 66 pp.
- Percival, J. A., Sanborn-Barrie, M., Skulski, T., Stott, G. M., Helmstaedt, H. & White, D. J. (2006). Tectonic evolution of the western Superior Province from NATMAP and Lithoprobe studies. *Canadian Journal of Earth Sciences* **43**, 1085–1117.
- Percival, J. A. & Williams, H. R. (1989). Late Archean Quetico accretionary complex, Superior Province, Canada. *Geology* **17**, 23–25.
- Percival, J. A., Stern, R. A. & Digel, M. R. (1985). *Regional geological synthesis of western Superior Province, Ontario*. Geological Survey of Canada Paper **85-1A**, 385–397.
- Peterman, Z. E., Hedge, C. E. & Braddock, W. A. (1968). Age of Precambrian events in the northeastern Front Range, Colorado. *Journal of Geophysical Research* **73**, 2277–2296.
- Petersson, A., Scherstén, A., Kemp, A. I. S., Kristinsdóttir, B., Kalvig, P. & Anum, S. (2016). Zircon U–Pb–Hf evidence for subduction related crustal growth and reworking of Archaean crust within the Palaeoproterozoic Birimian terrane, West African Craton, SE Ghana. *Precambrian Research* **275**, 286–309.
- Pichavant, M., Montel, J. M. & Richard, L. R. (1992). Apatite solubility in peraluminous liquids: Experimental data and an extension of the Harrison–Watson model. *Geochimica et Cosmochimica Acta* **56**, 3855–3861.
- Pickering, J. M. & Johnston, D. A. (1998). Fluid-absent melting behavior of a two-mica metapelite: experimental constraints on the origin of Black Hills granite. *Journal of Petrology* **39**, 1787–1804.
- Planavsky, N. J. (2014). The elements of marine life. *Nature Geoscience* **7**, 855.
- Planavsky, N. J., Asael, D., Hofmann, A., Reinhard, C. T., Lalonde, S. V., Knudsen, A., Wang, X., Ossa Ossa, F., Pecoits, E., Smith, A. J. B., Beukes, N. J., Bekker, A., Johnson, T. M., Konhauser, K. O., Lyons, T. W. & Rouxel, O. J. (2014). Evidence for oxygenic photosynthesis half a billion years before the Great Oxidation Event. *Nature Geoscience* **7**, 283.
- Poulet, A., Vidal, M., Delor, C., Simeon, Y. & Alric, G. (1996). Le volcanisme birimien du nord-est de la Côte-d'Ivoire, mise en évidence de deux phases volcano-tectoniques distinctes dans l'évolution géodynamique du Paleoproterozoïque. *Bulletin de la Société géologique de France* **167**, 529–541.
- Poujol, M. (2001). U–Pb isotopic evidence for episodic granulite emplacement in the Murchison greenstone belt, South Africa. *Journal of African Earth Sciences* **33**, 155–163.
- Poujol, M. & Robb, L. J. (1999). New U–Pb zircon ages on gneisses and pegmatite from south of the Murchison greenstone belt, South Africa. *South African Journal of Geology* **102**, 93–98.
- Poujol, M., Robb, L. J., Anhaeusser, C. R. & Gericke, B. (2003). A review of the geochronological constraints of the Kaapvaal Craton, South Africa. *Precambrian Research* **127**, 181–213.
- Qiao, H., Yin, C., Li, Q., He, X., Qian, J. & Li, W. (2016). Application of the revised Ti-in-zircon thermometer and SIMS zircon U–Pb dating of high-pressure pelitic granulites from the Qianlishan–Helanshan Complex of the Khondalite Belt, North China Craton. *Precambrian Research* **276**, 1–13.
- Qui, Y. & Groves, D. I. (1999). Late Archean collision and delamination in the Southwest Yilgarn Block: the driving force for Archean orogenic lode gold mineralization. *Economic Geology* **94**, 115–122.
- Qui, Y. M. (1997). Long-lived granulite magmatism in the Southern Cross province, Yilgarn craton, Western Australia, and its relationship with Archean gold mineralization. PhD thesis, University of Western Australia, Nedlands, WA, 298 pp.
- Rämö, O. T., McLemore, V. T., Hamilton, M. A., Kosunen, P. J., Heizler, M. & Haapala, I. (2003). Intermittent 1630–1220 Ma magmatism in central Mazatzal Province: New geochronologic piercing points and some tectonic implications. *Geology* **31**, 335–338.
- Rasmussen, B. & Buick, R. (1999). Redox state of the Archean atmosphere: evidence from detrital heavy minerals in ca. 3250–2750 Ma sandstones from the Pilbara Craton, Australia. *Geology* **27**, 115–118.
- Redden, J. A., Norton, J. J. & McLaughlin, R. J. (1982). *Geology of the Harney Peak Granite, Black Hills, South Dakota*. US Geological Survey, Professional Papers **82-481**.
- Redden, J. A., Peterman, Z. E., Zartman, R. E. & DeWitt, E. (1990). U–Th–Pb geochronology and preliminary interpretation of Precambrian tectonic events in the Black Hills, South Dakota. *Geological Association of Canada, Special Papers* **37**, 229–251.
- Reed, J. C. & Zartman, R. E. (1973). Geochronology of Precambrian rocks of the Teton Range, Wyoming. *Geological Society of America Bulletin* **84**, 561–582.
- Reinhard, C. T., Lalonde, S. V. & Lyons, T. W. (2013). Oxidative sulfide dissolution on the early Earth. *Chemical Geology* **362**, 44–55.
- Reinhard, C. T., Planavsky, N. J., Gill, B. C., Ozaki, K., Robbins, L. J., Lyons, T. W., Fischer, W. W., Wang, C., Cole, D. B. & Konhauser, K. O. (2017). Evolution of the global phosphorus cycle. *Nature* **541**, 386–389.
- Reis, N. J., de Faria, M. S. G., Fraga, L. M. B. & Haddad, R. C. (2000). Orosirian calc-alkaline volcanism and the Orocaina event in the Northern Amazonian Cráton, Eastern Roraima State. *Revista Brasileira de Geociências* **30**, 380–383.
- Robb, L. J., Brandl, G., Anhaeusser, C. R. & Poujol, M. (2006). Archaean granulite intrusions. In Johnson, M. R., Anhaeusser, C. R. & Thomas, R. J. (eds) *The Geology of South Africa*. Pretoria: Geological Society of South Africa: Johannesburg/Council of Geosciences, pp. 57–89.
- Rockhold, J. R., Nabelek, P. I. & Glascock, M. D. (1987). Origin of rhythmic layering in the Calamity Peak satellite pluton of the Harney Peak Granite, South Dakota: the role of boron. *Geochimica et Cosmochimica Acta* **51**, 487–496.
- Ronov, A. B. (1964). Common tendencies in the chemical evolution of the Earth's crust, ocean and atmosphere. *Geochemistry International* **1**, 713–737.
- Ross, G. M., Parrish, R. R., Villeneuve, M. E. & Bowring, S. A. (1991). Geophysics and geochronology of the crystalline basement of the Alberta Basin, western Canada. *Canadian Journal of Earth Sciences* **28**, 512–522.
- Rouxel, O. J., Bekker, A. & Edwards, K. J. (2005). Iron isotope constraints on the Archean and Paleoproterozoic ocean redox state. *Science* **307**, 1088–1091.

- Sabaté, P., Marinho, M. M., Vidal, P. & Caen-Vachette, M. (1990). The 2-Ga peraluminous magmatism of the Jacobina–Contendas Mirante belts (Bahia, Brazil): geologic and isotopic constraints on the sources. *Chemical Geology* **83**, 325–338.
- Santosh, M., Sajeev, K. & Li, J. H. (2006). Extreme crustal metamorphism during Columbia supercontinent assembly: evidence from North China Craton. *Gondwana Research* **10**, 256–266.
- Sasaki, A. & Ishihara, S. (1979). Sulfur isotopic composition of the magnetite-series and ilmenite-series granitoids in Japan. *Contributions to Mineralogy and Petrology* **68**, 107–115.
- Sawyer, E. W. & Barnes, S. J. (1988). Temporal and compositional differences between subsolidus and anatectic migmatite leucosomes from the Quetico metasedimentary belt, Canada. *Journal of Metamorphic Geology* **6**, 437–450.
- Scaillot, B., Pichavant, M. & Roux, J. (1991). Tourmaline, biotite and muscovite stability in felsic peraluminous liquids. *EOS Transactions, American Geophysical Union* **72**, 311.
- Schreurs, J. & Westra, L. (1986). The thermotectonic evolution of a Proterozoic, low pressure, granulite dome, West Uusimaa, SW Finland. *Contributions to Mineralogy and Petrology* **93**, 236–250.
- Scott, C., Lyons, T. W., Bekker, A., Shen, Y., Poulton, S. W., Chu, X. & Anbar, A. D. (2008). Tracing the stepwise oxygenation of the Proterozoic ocean. *Nature* **452**, 456–458.
- Sederholm, J. S. (1926). *On migmatites and associated Precambrian rocks of SW Finland: ii: the region around Barosundsfjord*. Bulletin de la Commission Géologique de Finlande **77**, 143.
- Sha, L. K. & Chappell, B. W. (1999). Apatite chemical composition, determined by electron microprobe and laser-ablation inductively coupled plasma mass spectrometry, as a probe into granite petrogenesis. *Geochimica et Cosmochimica Acta* **63**, 3861–3881.
- Shand, S. J. (1927). *Eruptive Rocks*. New York: John Wiley.
- Shearer, C. K., Papike, J. J. & Laul, J. C. (1987). Mineralogical and chemical evolution of a rare-element granite–pegmatite system: Harney Peak Granite, Black Hills, South Dakota. *Geochimica et Cosmochimica Acta* **51**, 473–486.
- Shearer, C. K., Papike, J. J. & Jolliff, B. L. (1992). Petrogenetic links among granites and pegmatites in the Harney Peak rare-element granite–pegmatite system, Black Hills, South Dakota. *Canadian Mineralogist* **30**, 785–809.
- Sheppard, S., Occhipinti, S. A. & Nelson, D. R. (2005). Intracontinental reworking in the Capricorn Orogen, Western Australia: the 1680–1620 Ma Mangaroon Orogeny. *Australian Journal of Earth Sciences* **52**, 443–460.
- Shieh, Y. N. & Schwarcz, H. P. (1978). The oxygen isotope composition of the surface crystalline rocks of the Canadian Shield. *Canadian Journal of Earth Sciences* **15**, 1773–1782.
- Silver, L. T., Williams, I. S. & Woodhead, J. A. (1981). *Uranium in granites from the southwestern United States: actinide parent–daughter system, sites, and mobilization*. US Department of Energy, Open-File Report **GJBX-45**, 315 pp.
- Smit, K. V., Shirey, S. B., Hauri, E. H. & Stern, R. A. (2019). Sulfur isotopes in diamonds reveal differences in continent construction. *Science* **364**, 383–385.
- Smith, P. M. & Asimow, P. D. (2005). Adibat\_1ph: a new public front-end to the MELTS, pMELTS, and pHMELTS models. *Geochemistry, Geophysics, Geosystems* **6**, Q02004.
- Smithies, R. H. & Champion, D. C. (2000). The Archaean high-Mg diorite suite: links to tonalite–trondhjemite–granodiorite magmatism and implications for early Archaean crustal growth. *Journal of Petrology* **41**, 1653–1671.
- Souders, A. K. & Frost, C. D. (2006). In suspect terrane? Provenance of the late Archean Phantom Lake metamorphic suite, Sierra Madre, Wyoming. *Canadian Journal of Earth Sciences* **43**, 1557–1577.
- Southwick, D. L. (1991). On the genesis of Archean granite through two-stage melting of the Quetico accretionary prism at a transpressional plate boundary. *Geological Society of America Bulletin* **103**, 1385–1394.
- Southwick, D. L. & Sims, P. K. (1979). *The Vermilion Granitic Complex—A new name for old rocks in northern Minnesota*. US Geological Survey, Professional Papers **1124A**, A1–A11.
- Spear, F. S., Kohn, M. J. & Cheney, J. T. (1999). *P–T* paths from anatectic pelites. *Contributions to Mineralogy and Petrology* **134**, 17–32.
- Spencer, C. J., Cawood, P. A., Hawkesworth, C. J., Raub, T. D., Prave, A. R. & Roberts, N. M. (2014). Proterozoic onset of crustal reworking and collisional tectonics: Reappraisal of the zircon oxygen isotope record. *Geology* **42**, 451–454.
- Spencer, C. J., Roberts, N. M. W. & Santosh, M. (2017). Growth, destruction, and preservation of Earth's continental crust. *Earth-Science Reviews* **172**, 87–106.
- Spencer, C. J., Murphy, J. B., Kirkland, C. L., Liu, Y. & Mitchell, R. N. (2018). A Palaeoproterozoic tectono-magmatic lull as a potential trigger for the supercontinent cycle. *Nature Geoscience* **11**, 97–101.
- Spencer, C. J., Partin, C. A., Kirkland, C. L., Raub, T. D., Liebmann, J. & Stern, R. A. (2019). Paleoproterozoic increase in zircon  $\delta^{18}\text{O}$  driven by rapid emergence of continental crust. *Geochimica et Cosmochimica Acta* **257**, 16–25.
- Stevens, G., Clemens, J. D. & Droop, G. T. (1997). Melt production during granulite-facies anatexis: experimental data from 'primitive' metasedimentary protoliths. *Contributions to Mineralogy and Petrology* **128**, 352–370.
- Stevens, G., Villaros, A. & Moyen, J. F. (2007). Selective peritectic garnet entrainment as the origin of geochemical diversity in S-type granites. *Geology* **35**, 9–12.
- St-Onge, M. R. & Davis, W. J. (2018). Wopmay orogen revisited: Phase equilibria modeling, detrital zircon geochronology, and U–Pb monazite dating of a regional Buchan-type metamorphic sequence. *Geological Society of America Bulletin* **130**, 678–704.
- Stott, G. M. (1996). *The geology and tectonic history of the central Uchi Subprovince*. Ontario Geological Survey, Open File Report **5952**, 178 pp.
- Stott, G. M., Corkery, J. A., Percival, M., Simard, M. & Goutier, J. (2010). *A revised terrane subdivision of the Superior Province of Ontario*. Ontario Geological Survey, Open File Report **6260**, 20–1–20–10.
- Stuckless, J. S. (1989). *Petrogenesis of Two Contrasting, Late Archean Granitoids, Wind River Range, Wyoming*. US Geological Survey, Professional Papers **1491**.
- Stuckless, J. S. & Miesch, A. T. (1981). *Petrogenetic modeling of a potential uranium source rock, Granite Mountains, Wyoming*. US Geological Survey, Professional Papers **1225**.
- Stuckless, J. S., Hedge, C. E., Worl, R. G., Simmons, K. R., Nkomo, I. T. & Wenner, D. B. (1985). Isotopic studies of the late Archean plutonic rocks of the Wind River Range, Wyoming. *Geological Society of America Bulletin* **96**, 850–860.
- Suominen, V. (1991). *The chronostratigraphy of southwestern Finland with special reference to Postjotnian and Subjotnian diabases*. Geological Survey of Finland Bulletin **356**, 100 pp.
- Sverjensky, D. A. & Lee, N. (2010). The great oxidation event and mineral diversification. *Elements* **6**, 31–36.
- Sweetapple, M. T. & Collins, P. L. (2002). Genetic framework for the classification and distribution of Archean rare metal

- pegmatites in the North Pilbara Craton, Western Australia. *Economic Geology* **97**, 873–895.
- Sylvester, P. J. (1994). Archean granite plutons. In: Condie, K. C. (ed.) *Archean Crustal Evolution, Developments in Precambrian Geology*, **11**. Amsterdam: Elsevier, pp. 261–314.
- Sylvester, P. J. (1998). Post-collisional strongly peraluminous granites. *Lithos* **45**, 29–44.
- Tang, M., Wang, X. L., Shu, X. J., Wang, D., Yang, T. & Gopon, P. (2014). Hafnium isotopic heterogeneity in zircons from granitic rocks: Geochemical evaluation and modeling of 'zircon effect' in crustal anatexis. *Earth and Planetary Science Letters* **389**, 188–199.
- Taylor, J. & Stevens, G. (2010). Selective entrainment of peritectic garnet into S-type granitic magmas: evidence from Archean mid-crustal anatexites. *Lithos* **120**, 277–292.
- Taylor, P. N., Moorbath, S., Leube, A. & Hirdes, W. (1992). Early Proterozoic crustal evolution in the Birimian of Ghana: constraints from geochronology and isotope geochemistry. *Precambrian Research* **56**, 97–111.
- Taylor, S. R. & McLennan, S. M. (1995). The geochemical evolution of the continental crust. *Reviews of Geophysics* **33**, 241–265.
- Thériault, R. J. (1992). Nd isotopic evolution of the Taltson Magmatic Zone, Northwest Territories, Canada: insights into early Proterozoic accretion along the Western margin of the Churchill Province. *Journal of Geology* **100**, 465–475.
- Thomassot, E., Cartigny, P., Harris, J. W., Lorand, J. P., Rollion-Bard, C. & Chaussidon, M. (2009). Metasomatic diamond growth: A multi-isotope study ( $^{13}\text{C}$ ,  $^{15}\text{N}$ ,  $^{33}\text{S}$ ,  $^{34}\text{S}$ ) of sulphide inclusions and their host diamonds from Jwaneng (Botswana). *Earth and Planetary Science Letters* **282**, 79–90.
- Thurston, P. C. (1990). Early Precambrian basic rocks of the Canadian shield. In: Hall, R. P. & Hughes E. J. (ed.) *Early Precambrian Basic Magmatism*. Glasgow: Blackie, pp. 221–247.
- Tindle, A. G., Selway, J. B. & Breaks, F. W. (2002). *Electron microprobe and bulk analyses of fertile peraluminous granites and related rare-element pegmatites, Superior Province, northwest and northeast Ontario, Operation Treasure Hunt*. Ontario Geological Survey, Miscellaneous Release Data, 111 pp.
- Trumbull, R. B. (1993). A petrological and Rb–Sr isotopic study of an early Archean fertile granite–pegmatite system: the Sinceni pluton in Swaziland. *Precambrian Research* **61**, 89–116.
- Tweto, O. & Schoenfeld, R. E. (1979). *Geologic Map of Colorado*. Reston, VA: US Geological Survey.
- Vaasjoki, M. & Sakko, M. (1988). The evolution of the Raahe–Ladoga zone in Finland: isotopic constraints. *Geological Survey of Finland Bulletin* **343**, 7–32.
- Väisänen, M. & Hölttä, P. (1999). Structural and metamorphic evolution of the Turku migmatite complex, southwestern Finland. *Geological Survey of Finland Bulletin* **71**, 177–218.
- Väisänen, M., Manttari, I., Kriegsman, L. M. & Hölttä, P. (2000). Tectonic setting of post-collisional magmatism in the Palaeoproterozoic Svecofennian Orogen, SW Finland. *Lithos* **54**, 63–81.
- Valley, J. W. (2003). Oxygen isotopes in zircon. In: Valley, J. W. (ed.) *Oxygen Isotopes in Zircon*. Mineralogical Society of America and Geochemical Society, Reviews in Mineralogy and Geochemistry **53**, 343–385.
- Valley, J. W., Lackey, J. S., Cavosie, A. J., Clechenko, C. C., Spicuzza, M. J., Basei, M. A. S., Bindeman, I. N., Ferreira, V. P., Sial, A. N., King, E. M., Peck, W. H., Sinha, A. K. & Wei, C. S. (2005). 4.4 billion years of crustal maturation: oxygen isotope ratios of magmatic zircon. *Contributions to Mineralogy and Petrology* **150**, 561–580.
- van Breemen, O., Davis, W. J. & King, J. E. (1992a). Temporal distribution of granitoid plutonic rocks in the Archean Slave Province, northwest Canadian Shield. *Canadian Journal of Earth Sciences* **29**, 2186–2199.
- van Breemen, O., Bostock, H. H. & Loveridge, W. D. (1992b). Geochronology of granites along the margin of the northern Taltson magmatic zone and western Rae Province, Northwest Territories. *Radiogenic age and isotopic studies: report 5, Geological Survey of Canada, Paper* **91-2**, 17–24.
- Van Duin, J. A. & Nieman, C. P. (1993). Pressure and temperature history of a low-pressure transitional granulite area, Turku, SW Finland. *Geologie en Mijnbouw* **71**, 259–280.
- Vearncombe, J. R. (1988). Structure and metamorphism of the Archean Murchison belt, Kaapvaal craton, South Africa. *Tectonics* **7**, 761–774.
- Vearncombe, J. R., Barton, J. M., Jr, Cheshire, P. E., De Beer, J. H., Stettler, E. H. & Brandl, G. (1992). *Geology, Geophysics and Mineralization of the Murchison Schist Belt, Rooiwater Complex and Surrounding Granitoids*. Memoirs of the Geological Survey of South Africa, 139.
- Veizer, J. & Mackenzie, F. T. (2003). Evolution of sedimentary rocks. In: Mackenzie, F. T. (ed.) *Treatise on Geochemistry* **7**, Pergamon, pp. 369–407.
- Vidal, M. & Alric, G. (1994). The Paleoproterozoic (Birimian) of Haute-Comoé in the West African Craton, Ivory Coast: a transtensional back-arc basin. *Precambrian Research* **65**, 207–229.
- Vielzeuf, D. & Holloway, J. R. (1988). Experimental determination of the fluid-absent melting relations in the pelitic system. *Contributions to Mineralogy and Petrology* **98**, 257–276.
- Vielzeuf, D. & Montel, J. M. (1994). Partial melting of metagreywackes. Part I. Fluid-absent experiments and phase relationships. *Contributions to Mineralogy and Petrology* **117**, 375–393.
- Villaros, A., Stevens, G. & Buick, I. S. (2009). Tracking S-type granite from source to emplacement: clues from garnet in the Cape Granite Suite. *Lithos* **112**, 217–235.
- Walker, R. J., Hanson, G. N., Papike, J. J. & O'Neil, J. R. (1986). Nd, O and Sr isotopic constraints on the origin of Precambrian rocks, southern Black Hills, South Dakota. *Geochimica et Cosmochimica Acta* **50**, 2833–2846.
- Wall, E. N. (2004). Petrologic, geochemical, and isotopic constraints on the origin of 2.6 Ga post-tectonic granitoids of the central Wyoming province. MSc thesis, University of Wyoming, Laramie, WY.
- Wall, V. J., Clemens, J. D. & Clarke, D. B. (1987). Models for granitoid evolution and source compositions. *Journal of Geology* **95**, 731–750.
- Wang, F., Li, X.-P., Chu, H. & Zhao, G.-C. (2011). Petrology and metamorphism of khondalites from the Jining complex, North China craton. *International Geology Review* **53**, 212–229.
- Wang, L. J., Guo, J. H., Yin, C. & Peng, P. (2017). Petrogenesis of ca. 1.95 Ga meta-leucogranites from the Jining Complex in the Khondalite Belt, North China Craton: Water-fluxed melting of metasedimentary rocks. *Precambrian Research* **303**, 355–371.
- Wang, L. J., Guo, J. H., Yin, C., Peng, P., Zhang, J., Spencer, C. J. & Qian, J. H. (2018). High-temperature S-type granitoids (charnockites) in the Jining complex, North China Craton: Restite entrainment and hybridization with mafic magma. *Lithos* **320**, 435–453.
- Watson, E. B. & Capobianco, C. J. (1981). Phosphorus and the rare earth elements in felsic magmas: an assessment of the

- role of apatite. *Geochimica et Cosmochimica Acta* **45**, 2349–2358.
- Watson, E. B. & Harrison, T. M. (1983). Zircon saturation revisited: temperature and composition effects in a variety of crustal magma types. *Earth and Planetary Science Letters* **64**, 295–304.
- Whalen, J. B. & Chappell, B. W. (1988). Opaque mineralogy and mafic mineral chemistry of I- and S-type granites of the Lachlan fold belt, Southeast Australia. *American Mineralogist* **73**, 281–296.
- White, A. J. & Chappell, B. W. (1977). Ultrametamorphism and granitoid genesis. *Tectonophysics* **43**, 7–22.
- Wilde, S. A., Zhao, G.-C. & Sun, M. (2002). Development of the North China Craton during the Late Archean and its final amalgamation at 1.8 Ga: some speculation on its position within a global Paleoproterozoic Supercontinent. *Gondwana Research* **5**, 85–94.
- Windley, B. F. (1977). Timing of continental growth and emergence. *Nature* **270**, 426.
- Wones, D. R. & Eugster, H. P. (1965). Stability of biotite: experiment, theory, and application. *American Mineralogist* **50**, 1228–1272.
- Yin, C., Zhao, G., Guo, J., Sun, M., Xia, X., Zhou, X. & Liu, C. (2011). U–Pb and Hf isotopic study of zircons of the Helanshan Complex: constraints on the evolution of the Khondalite Belt in the Western Block of the North China Craton. *Lithos* **122**, 25–38.
- Yin, C. Q., Zhao, G. C., Sun, M., Xia, X. P., Wei, C. J., Zhou, X. W. & Leung, W. H. (2009). LA- ICP-MS U–Pb zircon ages of the Qianlishan Complex: constraints on the evolution of the Khondalite Belt in the Western Block of the North China Craton. *Precambrian Research* **174**, 78–94.
- Zartman, R. E. & Reed, J. C., Jr (1998). Zircon geochronology of the Webb Canyon Gneiss and the Mount Owen Quartz Monzonite, Teton Range, Wyoming: significance to dating Late Archean metamorphism in the Wyoming craton. *Mountain Geologist* **35**, 71–77.
- Zeh, A., Gerdes, A. & Barton, J. M. (2009). Archean accretion and crustal evolution of the Kalahari Craton—the zircon age and Hf isotope record of granitic rocks from Barberton/Swaziland to the Francistown Arc. *Journal of Petrology* **50**, 933–966.
- Zen, E. A. (1988). Phase relations of peraluminous granitic rocks and their petrogenetic implications. *Annual Review of Earth and Planetary Sciences* **16**, 21–51.
- Zeng, L., Asimow, P. D. & Saleeby, J. B. (2005a). Coupling of anatectic reactions and dissolution of accessory phases and the Sr and Nd isotope systematics of anatectic melts from a metasedimentary source. *Geochimica et Cosmochimica Acta* **69**, 3671–3682.
- Zeng, L., Saleeby, J. B. & Asimow, P. (2005b). Nd isotope disequilibrium during crustal anatexis: A record from the Goat Ranch migmatite complex, southern Sierra Nevada batholith, California. *Geology* **33**, 53–56.
- Zhai, M., Guo, J., Li, Y., Liu, W., Peng, P. & Shi, X. (2003). Two linear granite belts in the central–western North China Craton and their implication for Late Neoarchaean–Palaeoproterozoic continental evolution. *Precambrian Research* **127**, 267–283.
- Zhang, D. H., Wei, J. H., Fu, L. B., Schmitt, A. K., Wang, D. Z., Tan, J. & Liu, J. K. (2017). Petrogenesis and thermal overprint of S-type granites in Helanshan region, North China Craton: Constraints on the 1.90 Ga khondalites decompression melting and 1.32 Ga tectono-thermal event. *Precambrian Research* **303**, 660–672.
- Zhang, X., Zhang, Y., Zhai, M., Wu, F., Hou, Q. & Yuan, L. (2017). Decoding Neoarchaean to Palaeoproterozoic tectonothermal events in the Rangnim Massif, North Korea: regional correlation and broader implications. *International Geology Review* **59**, 16–28.
- Zhao, G. & Zhai, M. (2013). Lithotectonic elements of Precambrian basement in the North China Craton: review and tectonic implications. *Gondwana Research* **23**, 1207–1240.
- Zhao, G., Wilde, S. A., Cawood, P. A. & Sun, M. (2001). Archean blocks and their boundaries in the North China Craton: lithological, geochemical, structural and *P–T* path constraints and tectonic evolution. *Precambrian Research* **107**, 45–73.
- Zhao, G., Sun, M., Wilde, S. A. & Sanzhong, L. (2005). Late Archean to Palaeoproterozoic evolution of the North China Craton: key issues revisited. *Precambrian Research* **136**, 177–202.
- Zhao, G., Cao, L., Wilde, S. A., Sun, M., Choe, W. J. & Li, S. (2006). Implications based on the first SHRIMP U–Pb zircon dating on Precambrian granitoid rocks in North Korea. *Earth and Planetary Science Letters* **251**, 365–379.
- Zhong, C.-T., Deng, J.-F., Wan, Y.-S., Mao, D.-B. & Li, H.-M. (2007). Magma recording of Paleoproterozoic orogeny in central segment of northern margin of North China craton: geochemical characteristics and zircon SHRIMP dating of S-type granitoids. *Geochimica* **36**, 633–637 [in Chinese with English abstract].



